Order Number 8820887

Coupled thermoelastic crack problems

Phurkhao, Pichaya, Ph.D.

City University of New York, 1988

U·M·I

300 N. Zeeb Rd.
Ann Arbor, MI 48106

PLEASE NOTE:

In all cases this material has been filmed in the best possible way from the available copy. Problems encountered with this document have been identified here with a check mark __✓__.

1. Glossy photographs or pages _____
2. Colored illustrations, paper or print _____
3. Photographs with dark background _____
4. Illustrations are poor copy _____
5. Pages with black marks, not original copy __✓__
6. Print shows through as there is text on both sides of page _____
7. Indistinct, broken or small print on several pages __✓__
8. Print exceeds margin requirements _____
9. Tightly bound copy with print lost in spine _____
10. Computer printout pages with indistinct print _____
11. Page(s) _____ lacking when material received, and not available from school or author.
12. Page(s) _____ seem to be missing in numbering only as text follows.
13. Two pages numbered _____. Text follows.
14. Curling and wrinkled pages _____
15. Dissertation contains pages with print at a slant, filmed as received _____
16. Other _____

_____

_____

COUPLED THERMOELASTIC CRACK PROBLEMS

by

PICHAYA PHURKHAO

A dissertation submitted to the Graduate Faculty in Engineering in partial fulfillment of the requirements for the degree of Doctor of Philosophy, The City University of New York.

1988

This manuscript has been read and accepted for the Graduate Faculty in Engineering in satisfaction of the dissertation requirement for the degree of Doctor of Philosophy.

December 21, 1987 — Mumtaz K. Kassir

date — Chair of Examining Committee

12/21/87 — Jacques E. Benveniste

date — Executive Officer

Prof. Jacques E. Benveniste

Prof. Charles A. Miller

Prof. Carl. J Costantino

Prof. Mumtaz K. Kassir

Supervisory Committee

The City University of New York

Abstract

COUPLED THERMOELASTIC CRACK PROBLEMS

by

Pichaya Phurkhao

Advisor: Prof. Mumtaz K. Kassir

In this research, coupled thermoelastic problems of stationary cracks are discussed. It is assumed that the crack is disturbed by thermal and/or elastic waves generated by external thermal and/or mechanical excitations. Two classes of problems of particular interest are investigated in detail. These are the scattering of plane harmonic thermoelastic waves and the sudden application of thermal and/or mechanical loadings to the crack surfaces (transient problems). Integral transform techniques are employed to formulate the problems and reduce them to Fredholm integral equations of the second kind and/or to a system of simultaneous algebraic equations. The resulting equations are then solved numerically and the singular stress field near the crack tip, which is of paramount importance in

determining crack propagation, is determined in explicit form. Also, the magnitude of this stress field, which is conveniently described by a parameter k_1' (stress-intensity factor), is calculated.

The effect of the frequency of the input thermal and/or elastic waves as well as the influence of coupling upon the dynamic stress-intensity factor for few materials are determined and displayed graphically. In the transient problems, a numerical Laplace inversion technique is used to convert the values of k_1' in the Laplace plane to the regular time domain, and the results are compared to the corresponding steady-state values to reveal the influence of inertia and coupling on the dynamic stress-intensity factor.

For both problems, the important results are; (1) the stresses are singular of order $r_1^{-\frac{1}{2}}$ as $r_1 \to 0$ at the crack tip, (2) the inertia effect upon the variation of k_1' with frequency and time is found to be significant while the coupling effect is negligibly small, and (3) k_1' is proportional to material constants and crack size. It is also observed that there is a peak in k_1' in both problems. The corresponding values of time and frequency vary depending upon material properties and crack size.

In applying the methodology of Linear Elastic Fracture Mechanics (LEFM), the information gained is essential to determine the conditions of crack propagation under thermal loading.

To my Mom, Boonta, and

my Dad, Jane.

ACKNOWLEDGEMENT

I would like to take this opportunity to express my sincere thanks to Professor Mumtaz Kassir, my thesis advisor, for his constant guidance, insight, and encouragement that make this thesis possible.

I am also thankful to Professor Jacques E. Benveniste for kindly providing useful informations on IMSL Subroutines and all the valuable discussions I have had with him.

Special thanks to Professor G. Donald Brandt, Head of Civil Engineering Department, for giving me opportunity to teach while I was doing research.

I gratefully acknowledge the financial help received from The Research Foundation of the City University of New York.

Finally, I would like to thank my parents, my lovely sister and my brothers, to whom this thesis is dedicated, for their financial and moral encouragement to pursue doctoral degree.

TABLE OF CONTENTS

LIST OF FIGURES

LIST OF TABLES

NOMENCLATURE

$A(s,p)$, $A_1(s,p)$, $A_{11}(s,p)$, $A_{12}(s,p)$	Arbitrary functions of s and p
a	Half of the crack width
$a_{ij}(s,p)$, $(i,j=1,2)$	Functions defined in Appendix C
$B(p,q)$	Beta function
$B_{i,r}(p)$, $(i=1,2)$, $(r=1,3,5,.....)$	Functions defined by Eq. (4.66)
$B(s,p)$, $B_1(s,p)$, $B_{11}(s,p)$, $B_{12}(s,p)$	Arbitrary functions of s and p
b_{ij}, $(i,j=1,2)$	Functions defined in Appendix C
b	Constant $(= \gamma T_0/\mu)$
$C(s,p)$, $C_1(s,p)$, $C_{11}(s,p)$, $C_{12}(s,p)$	Arbitrary functions of s and p
c_{ij}, $(i,j=1,2)$	Functions defined in Appendix C
c_1	Velocity of dilatational wave $(\lambda+2\mu/\rho)^{\frac{1}{2}}$, cm/s
c_2	Velocity of transverse wave $(\mu/\rho)^{\frac{1}{2}}$, cm/s
c	Function defined in Appendix B
c_E	Specific heat at constant strain, cal/gm^{o}C

$\bar{c}$	Function defined in Appendix C
$D(\wp,p)$	Function defined by Eq. (4.52)
$E(s)$	Function defined by Eq. (3.62)
$E_1(s)$, $E_2(s)$	Functions defined in Appendix C
e	Dilatation in dimensionless units
$e(s,p)$	Function defined by Eq. (4.49)
$F(s,p)$	Function defined by Eq. (4.32)
$\bar{F}(s,p)$	Function defined by Eq. (4.36)
f_{ij}, $(i,j=1,2)$	Functions defined in Appendix C
$f_r(t)$, $(r=1,2,3)$	Functions of t
$G_i(\eta_i)$, $(i=1,2)$	Functions defined by Eq. (5.2)
g	Constant $(= \frac{\gamma}{\rho c_E})$
g_{ij}, $(i,j=1,2)$	Functions defined in Appendix C
g_j, $(j=1,2,3)$	Functions defined in Appendix B
H	Outer or surface conductivity in conventional units, $Cal/cm^2 s^oC$
$H(t)$	Heaviside unit step function
h	Outer or surface conductivity in dimensionless units
h_j, $(j=1,2,3)$	Functions defined in Appendix B
I_j, $(j=1,2,3)$	Imaginary part of $(s^2-\xi_i^2)^{\frac{1}{2}}$
$I(x,p)$	Function defined by Eq. (4.48)
I_0	Modified Bessel function of the first kind of order zero

J_p	Bessel function of the first kind of order p
K_1	Kernel function defined by Eqs. (4.35), (4.38)
K_0	Modified Bessel function of the second kind of order zero
$k_1(t)$	Dynamic stress-intensity factor in dimensionless units
k	Thermal conductivity, Cal/s.cm.^oK
k_j, (j=1,2)	Real numbers (=0 or 1)
$L(\tau,\eta)$	Complex kernel defined by Eq. (3.66)
$L_j(\tau,\eta)$, (j=1,2)	Real kernels defined by Eqs. (3.68), (3.69)
l_j, (j=1,2)	Functions defined in Appendix C
$M_1(p)$, $M_2(p)$	Functions defined in Appendix B
m_j, (j=1,2,3)	Functions defined by Eqs. (3.44), (3.52)
N	Even number of sub-interval between 0 to 1
n	Function defined in Appendix B
$\bar{n}$	Function defined in Appendix C
n_j, (j=1,2,3)	Functions defined by Eqs. (3.45), (3.52)

$P(x)$	Function of x
$\bar{P}(x)$	Function of x
p	Laplace transform parameter
p_j, (j=1,2,3,4,5,6)	Functions defined in Appendix C
$Q(\eta)$	Function defined in Appendix A
Q_0	Non-dimensional magnitude of specified thermal flux
$q(s)$	Function defined in Appendix A
q_j, (j=1,2)	Attenuation coefficients in dimensionless units
R_j, (j=1,2,3)	Real part of $(s^2-\xi_j^2)^{\frac{1}{2}}$
r, $\bar{\theta}$ r_1, $\bar{\theta}_1$ r_2, $\bar{\theta}_2$	Polar coordinates in dimensionless units
$S_1(s,p)$, $S_2(s,p)$	Functions defined in Appendix E
s	Fourier sine and cosine transform parameter
T	Temperature, ^oK
T_0	Reference temperature (absolute) for which the material is stress-free, ^oK
t	Dimensionless time variable

U, V	Displacement components in conventional units, cm
u, v	Displacement components in dimensionless units
$V_1(s,p)$, $V_2(s,p)$	Unknown functions
v_j, $(j=1,2)$	Phase velocities
w^*	Characteristic frequency $(=\rho c_E c_1^2/k)$
$W_1(s,p)$, $W_2(s,p)$	Unknown complex functions
x,y,z	Rectangular coordinates in dimensionless units
$Y_1(s)$, $Y_2(s)$	Functions defined in Appendix C
$Z(x)$	Complex function defined by Eq. (3.63)
$\bar{Z}(x)$	Complex function defined by Eq. (3.78)
$Z_1(x)$, $Z_2(x)$	Functions defined in Appendix C

Greek Symbols:

ϕ, ψ	Potential functions
θ	Temperature in dimensionless units, $(= \frac{T-T_0}{T_0})$
Φ_i, $(i=1,2,3)$	Auxiliary functions
$\Lambda(s)$, $\Lambda_1(s)$, $\Lambda_2(s)$	Unknown functions
$\chi_{i,1}(p)$, $(i=1,2)$	Auxiliary functions
ϕ^o, ϕ_i^o	Arbitrary constants
θ^o, θ_i^o, $(i=1,2)$	
Ψ, Ψ_1, Ψ_2	Auxiliary functions
Υ	
Ω_ϕ, Ω_T	Complex quantities defined by Eq. (3.19)
$\Omega_{\phi r}$, $\Omega_{\phi i}$, Ω_{Tr}, Ω_{Ti}	Real quantities defined by Eq. (3.20)
σ_0	Non-dimensional magnitude of applied normal stress
σ_q	Constant $(= \gamma \kappa Q_0'/c_1)$
σ_r	Constant $(= \sqrt{\frac{2}{\pi}}\, h(\beta^2-1)\theta_0'\gamma/\beta^2)$
θ_0	Dimensionless magnitude of temperature

σ	Magnitude of static stress ($=-\mu\phi^{o}\xi_3^2$), dyn/cm^2
σ_θ	Constant ($= -\mu\theta^{o}$), dyn/cm^2
ϕ^t, τ^t, ϕ^e, σ^e	Functions in Appendix C
$\gamma_i(s,p)$, (i=1,2,3)	Functions defined by Eq. (4.24)
ζ_i, (i=1,2,3)	Roots of characteristic equations (4.22), (4.23)
ξ_i, (i=1,2,3)	Roots of characteristic equations (3.43), (3.52)
α_i, (i=1,2)	Roots of characteristic equation (3.11)
	Complex quantity
$\Delta(s,p)$, $\Delta_1(s,p)$	Functions defined in Appendix C
β_i, (i=1,2)	Constants
$\bar{\beta}$	Incident angle, radian
α_T	Coefficient of linear thermal expansion, cm/cm^{o}C
ρ	Mass density, gm/cm^3
γ	Constant $=(3\lambda+2\mu)\alpha_T$
λ, μ	Lame' constants
κ	Diffusitivity ($=k/\rho c_E$), cm^2/s

ε	Coupling constant (= bg/β^2)
β	Constant (= c_1/c_2)
δ	Phase angle (= $\tan^{-1} I/R$), radian
Ω	Dimensionless frequency (=Ω'/w^*)
ε_x, ε_y, ε_{xy}	Non-dimensional strain components
σ_x, σ_y, τ_{xy}	Non-dimensional stress components
$\mathcal{F}_k$	Jacobi polynomial
Γ	Gamma function
τ, η	Dummy variables
η_j, (j=1,2,3)	Functions defined by Eqs. (3.46), (3.51)
θ_{pj}, (j=1,2)	Arguments
∇	Del operator
∇^2	Laplacian operator
$f^{(i)}$	Function associated with incident waves
$f^{(s)}$	Function associated with scattered waves
f'	Function in conventional units
ν	Poisson ratio

CHAPTER 1

Introduction

More than a century ago, Duhamel [9] * and Neumann [18] formulated a theory of thermoelasticity of elastic solids subject to temperature variation. The governing equations of the theory consist of the Navier equations of motion coupled with the Fourier heat conduction equation. This theory takes into account the interaction effect of straining upon the temperature field and temperature distribution upon the strains in the body. Moreover, unlike the conventional thermoelasticity theory, which ignores the inertia terms in the governing equations and is concerned with solving the heat conduction equation and the equations of motion separately, this theory allows the dynamic response to be determined by solving the coupled set of governing equations simultaneously. Despite its mathematical complexity, coupled thermoelasticity gives a deeper insight into the mechanism of deformation

---

* Number in brackets designate reference given on pages 160-163

process connected with thermal phenomena in elastic solids. Utilizing this theory, Biot [2], Chadwich [5], Boley and Weiner [3], Nowacki [20], and others obtained solutions to some thermal stress problems.

Concern over thermal effects in the design of structural components has caused investigators to consider the implications, theoretical as well as practical, of the thermal stresses and strains in the vicinity of cracks in structural members. However, because of the complexity of the field equations, most of the previous investigations were carried out under certain simplifying assumptions. Usually the inertia terms in the equations of motion and/or the coupling term in the heat conduction equation are neglected. Thus, upon omission of the coupling term in the heat conduction equation, the equations become uncoupled and there results what is often termed as the Uncoupled Theory. Further omission of the inertia terms in the equations of motion results in Uncoupled Quasi-Static Theory of Thermoelasticity (or, more simply, Thermoelasticity). When there is no time involved in the equations the steady-state condition is reached.

Cracking of brittle solids due to thermal stress

is a well-known phenomenon. When a steady heat flow is disturbed by the presence of a crack, there is local intensification of temperature field accompanied by singular thermal stress which may cause crack propagation resulting in serious damage to structural members. Sufficiently rapid local heating or cooling of solids (thermal shock) can also lead to serious catastrophe. This could occur, for example, in cracked structural components under the influence of laser beams or electrical (spark) discharges, in pressurized water reactor (PWR) and its piping system experiencing a thermal transient during a loss of coolant accident (LOCA), in space crafts and jet engines, etc.. Furthermore, when the thermal loading is fluctuating and periodic with time it gives rise to the fluctuating and periodic stresses and displacements propagating through the medium in the form of waves. It would be expected that, near the crack tips, these waves will cause high local stress intensification causing the propagation of the crack. Since in the current technology of Linear Elastic Fracture Mechanics (LEFM), the critical value of the intensity of the local stress field can be associated with the fracture toughness of the material, it follows that by knowing the stress

intensity factors as functions of the temperature field, material properties, and flaw size, it is possible to predict a critical thermal loading which will not result in failure of the material.

Up until now most of the analysis efforts developed in the area of fracture mechanics due to thermal stress have been confined to either steady-state or quasi-static problems. None of the investigations available in the literature have utilized the coupled theory. It is expected that when the temperature field exhibits sufficiently steep time-gradients or fluctuates and varies harmonically with time, the dynamic effects disregarded in the traditional treatment of the problems may become significant. Summaries of some solutions to steady-state thermal crack problems are given by Sneddon and Lowengrub [22] and by Kassir and Sih [15]. While some solutions to quasi-static crack problems can be found in recent book by Cherepanov [7] .

Elastodynamic crack problems have been investigated. Thorough summaries of the methods of analyses in dynamic elastic fracture mechanics have been given by Chen and Sih [6], Achenbach [1], and Freund [12]. It is often found that inertia effects have significant influence on the response of structural components. At specific locations in a body, namely, in the vicinity of crack

tips, the stresses and displacements and, in turn, the dynamic stress-intensity factors are higher than those encountered under static loadings. This stress 'overshoot' in the vicinity of a crack tip may be as high as 30% above the corresponding static value. In view of the dynamic amplification of the stress level it is conceivable that there are cases for which fracture does not occur under a gradually applied system of loads, but does indeed take place when the same system of loads is applied rapidly or when it is flutuating periodically with time giving rise to propagating mechanical disturbances. Even though elastodynamic theory takes inertia effects into consideration, however, in order to study the influence of thermal waves, one needs to include the mechanical coupling term in the heat conduction equation as well as to consider the inertia effects.

In this dissertation, it is intended to investigate the nature of thermal waves generated by thermal disturbances in a two-dimensional medium containing a central crack when the general theory of coupled thermoelasticity is employed. Special emphasis is focused on finding the stress-intensity factors, the critical values of which govern the condition of crack propagation.

The fracture of solids under elastic waves will also be studied so that the salient feature of the influence of the mechanical coupling term upon the stress-intensity factor can be brought out when the corresponding results are compared with the known static solution. It will be assumed that initially the medium is at rest, stress-free, at absolute temperature (T_o) everywhere and the deformations are small relative to the dimension of the body. Furthermore, all thermoelastic material properties are assumed to be independent of temperature. With these assumptions, the governing equations are greatly simplified, become linear and amenable to analytical treatment, namely, by means of integral transform techniques. Every variation of strains will be accompanied by variations in temperature and vice versa. Two classes of problems of particular interest are considered separately. These are the problem of scattering of plane harmonic thermoelastic waves by a stationary crack and transient problems in which the crack surfaces experience sudden application of thermal disturbances and/or mechanical loadings. Figure 1 shows a sketch of the geometry of the problems. In terms of the co-ordinate system (x',y',z') the crack occupies the region $|x'|<a'$, $|z'|<\infty$

of the mid-plane y'=0. The stresses in the medium are produced by either a passage of incoming thermal and/or mechanical waves (thermoelastic waves), or by the application of an instantaneous uniform change of thermal disturbances and/or stresses across the crack surfaces.

The basic governing equations of coupled thermoelasticity are presented in chapter 2. The general equations consist of one displacement equation of motion (Navier Equation) written in vector form and one equation of heat conduction coupled with change of strain. For plane-strain problem, the dependent variables are two components of displacement and temperature. The stress components are related to the strain components and temperature through the Duhamel-Neumann relations while the strains are connected to displacements by the strain-displacement relationships. The equations stated above are based upon the assumption of small variation of temperature due to change of strain and small displacements. In addition it is necessary to specify initial and boundary conditions in order to describe fully the transient problems in which the crack surfaces experience sudden variation of thermal and/or mechanical disturbances. However when the

disturbance is in the form of wave (thermoelastic wave), which is harmonic in time, only boundary conditions are necessary.

Chapter 3 is devoted to the problem of diffraction of thermoelastic waves around a stationary crack. The equations of chapter 2 are first non-dimensionalized into a form which is convenient for subsequent analyses, and the theory of plane harmonic thermoelastic waves is then developed and appropriate solutions are derived to investigate the diffraction of these waves around a crack embedded in structural members. In this analysis, it is assumed that the crack is insulated and traction-free (see Fig. 2). Making use of linearity, the analysis can be divided into two parts; one is concerned with impinging of thermal wave with accompanying elastic wave while the other deals with an elastic wave accompanied by thermal wave. The two input waves may be viewed as waves arising from thermal and mechanical excitation in the members, respectively. The complete solution will then be taken as the sum of the two solutions. For the mere purpose of finding the dynamic stress-intensity factor, it is sufficient to focus attention on the scattered wave field. The solution is then conveniently solved

by considering a symmetric and a skew symmetric problem which are even and odd in y, respectively. Furthermore, each problem is divided into two parts, one is even in x and the other is odd in x. Since both parts can be solved in the same manner, only the symmetric and even problem in x will be studied in detail. Integral transform techniques are used to reduce the problem to a pair of dual integral equations in a complex variable domain which can be further reduced to a system of coupled, real, Fredholm integral equations of the second kind. The system of integral equations is solved numerically and the dynamic stress-intensity factor is then determined in term of the solutions of these equations. The singularity is found to retain its classical order $O(r^{-\frac{1}{2}})$, but the stress field is greatly influenced by the frequency of the thermoelastic waves.

In chapter 4, the problems dealing with the applications of thermal and/or mechanical impact loading on the crack surfaces are discussed. In particular, three specific examples are considered in detail; namely 1) crack problem under sudden application of uniform normal stress on insulated crack surfaces, 2) crack problem under sudden variation of thermal flux

on crack surfaces, and 3) crack problem under sudden variation of thermal radiation on crack surfaces. Again, the governing equations are non-dimensionalized and solved. The use of potential functions in conjunction with Laplace and Fourier integral transforms reduce the problems of the first two categories to the solutions of standard pair of dual integral equations in the Laplace transform plane. The solution of the dual integral equations is reduced to the determination of an auxiliary function governed by a Fredholm integral equation of the second kind which is amenable to numerical treatment. The dynamic stress-intensity factor is then determined in term of the auxiliary function evaluated at the crack tip in the Laplace transform plane. A numerical inversion of the Laplace transform is then employed to invert the dynamic stress-intensity factor into regular time domain. Similarly, the mixed-boundary conditions of the third example reduce the problem to a system of dual integral equations which can be further reduced to a system of simultaneous algebraic equations having infinite unknown functions. The dynamic stress-intensity factor in Laplace transform domain is again found to be directly

proportional to the sum of these unknown functions. The unknown functions can be determined effectively by truncating the equations to finite numbers. Upon application of the numerical inversion of Laplace transform, the dynamic stress-intensity factor in the real time domain is obtained. For the three examples considered the stress singularities are found to retain their classical order $O(r^{-\frac{1}{2}})$.

In chapter 5, the procedure for the solutions of Fredholm integral equations and numerical inversion of Laplace transforms are presented. This part of analysis comprises most of computer effort and, consequently, deserves a great deal of attention, especially, when dealing with slowly convergent integrals having an infinite interval of integration and with integrals having singularities within the limits of integration. Therefore, special techniques are developed and employed. The method of solving Fredholm integral equation is based on the replacement of the equation by a finite system of linear algebraic equations which is outlined by Kantorovich and Krylov [14] . The integral terms are approximately replaced by a finite sum using Simpson formula. The accuracy is achieved by increasing

number of terms in the summations. The numerical inversion of the Laplace transform technique which is employed in chapter 4 is based on the method outlined by Miller and Guy [17]. It utilizes the properties of Jacobi polynomials. This technique is found to be useful and suitable for the problems considered in this research.

To illustrate the applicability of the solutions developed, numerical results are obtained and displayed graphically in chapter 6 for two materials, lead and copper, having relatively high and low values of the coupling constant, respectively. For the problem of scattering of thermal wave accompanied by elastic wave, the variations of the dynamic stress intensity factors with the non-dimensional frequency $\Omega = \omega'/w^*$ for crack length $2a' = 1$ cm. and 2 cm. and incident angle $\bar{\beta} = 90^{\circ}$ are shown on semi-log scale. It is observed that the stress-intensity factor k_1' rises sharply at first, reaches the peak and then decreases rapidly with increasing values of Ω. The peaks of the k_1' occur at different frequencies depending upon material properties and crack size. Increasing crack length tends to induce the peak in k_1' to occur at lower frequency. As an example, for copper

with crack lengths of 1 cm. and 2 cm., the peaks occur at frequencies $\Omega' = 4.25$ rad/s and $\Omega' = 1.67$ rad/s, respectively. As the frequency approaches zero, the stress intensity factor, k_1', tends to zero value. A similar feature is also observed when the input waves consist of an elastic wave accompanied by a thermal wave. The peak in the dynamic stress-intensity factors as compared to the analogous statical value are about 30% - 40% higher. In both cases, the coupling effect is found to be negligibly small. In particular case of isotropic material (coefficient of thermal expansion $\alpha_T = 0$), the solutions associated with elastic wave accompanied by thermal wave reduce to known solutions obtained by Chen and Sih [6]. It should also be mentioned that when the medium is disturbed by both thermal and mechanical excitations simultaneously, the solution can be obtained by superposition of the two solutions. For the transient problems, the results are calculated and the dynamic stress intensity factors (k_1') for the three categories mentioned previously are displayed graphically. A crack length $2a' = 2\kappa/c_1$ (or non-dimensional crack length $2a = 2$) is taken for numerical calculation purpose.

In all cases, the curves are observed to exhibit the usual dynamic effect. The overshoot in the values of k_1' as compared to the analogous steady-state one is about 11% - 30%. The effect of the mechanical coupling term in the heat conduction equation is brought out by letting the coupling constant $\varepsilon = 0$ in the numerical calculation. The results are then plotted and compared with those obtained from the coupled theory. It is found that the coupling effect is minimal and may be neglected.

In conclusion, integral transform solutions have been developed to study the nature of thermal waves in cracked structural components. In each case the problem is reduced to a pair (or a system) of dual integral equations which in turn can be further reduced to an integral equation (or a system of algebraic equations) suitable for numerical solutions. Reduction of a pair of dual integral equations to Fredholm integral equation of the second kind is well known. The validity of the method is dictated by the nature of the weight functions, kernels and the input functions. Elegant summary of the development of the theory of dual integral equations can

be found in the book written by Sneddon [23]. On the other hand, it can be shown that reduction of the system of dual integral equations to simultaneous Fredholm integral equations for the transient problem associated with the thermal radiation boundary condition on the crack surfaces considered in this dissertation is hopeless. The reason for this is due to the nature of the functions stated above. Therefore a more general and straight forward procedure discussed by Erdogan and Bahar [11], which is the generalization of the method developed by Tranter [24], is employed. This method which is based on the properties of some definite integrals of Weber-Sonine-Schafheitlin type involving Bessel functions reduces the problem to an infinite set of linear algebraic equations. Its solution can be obtained by cutting off the computation of the infinite number of linear algebraic equations after n equations for large n. It should be noted that it is very difficult to investigate the regularity of this system of equations but numerical experiments show that the approximate solutions obtained by considering only the first few terms (e.g. 6 terms)

exhibit good behaviour. To this end, it should be pointed out that the procedure developed in this dissertation can be equally well applied to various other problems having different kind of boundary conditions.

The results obtained in this study play a key role in the methods of Linear Elastic Fracture Mechanics (LEFM) with regard to fracture initiation and propagation in structural components. These methods have been demonstrated to be adequate and have been verified by various experiments and have a wide range of practical applications. The knowledge of the stress distribution in the neighbourhood of a crack tip in a structure subjected to temperature that varies periodically with time, to fluctuating loads, thermal shock and/or impact loadings is imperative for a safe prediction of the strength of, especially, modern structures. It is known that the stress-intensity factor is a prime parameter characterizing crack propagation. Having performed the appropriate stress analysis and obtained the stress intensity factor for the problem under consideration, it is then possible to estimate

the maximum allowable load and/or thermal disturbances a machine or structural component can tolelate for a given defect size or the maximum defect size that is permitted to exist in a given material.

CHAPTER 2

Statement of the Problems and Basic Equations

In this dissertation, it is intended to study, within the framework of the linear coupled thermoelastic theory, the nature of the propagation of thermal and elastic waves in an infinite, homogeneous, isotropic elastic solid containing a finite crack. In particular, attention is focused on the distribution of the singular stress field in the vicinity of the crack tips and to what degree it is influenced by the frequencies of the input waves, inertia effects and the mutual dependence of temperature and displacement fields inherent in the theory of coupled thermoelasticity. It is assumed that the temperature has no effects upon thermoelastic constants and, furthermore, the temperature changes and deformations are small relative to the dimension of the body. In view of this, and assuming there are no heat sources and body forces in the medium, the governing equations are [5]

$$\mu \nabla^2 \vec{U} + (\lambda+\mu) \nabla e' - \gamma \nabla (T-T_0) = \rho \frac{\partial^2 \vec{U}}{\partial t'^2} \qquad (2.1a)$$

$$k \nabla^2 T - \rho c_E \frac{\partial T}{\partial t'} - \gamma T_0 \frac{\partial e'}{\partial t'} = 0 \qquad (2.1b)$$

Eqs.(2.1a) and (2.1b) relate the displacement vector $\vec{U} = U\vec{i}+V\vec{j}$ and the (small) deviation $T-T_0$ from the equilibrium temperature (absolute), T_0, for which the material is stress-free. Moreover, e' is the dilatation, t' is the usual time variable and the constants k, ρ and c_E denote, respectively, the thermal conductivity, the density and the specific heat at constant strain of the material. The constant γ stands for

$$\gamma = (3\lambda+2\mu)\alpha_T \tag{2.2}$$

where λ and μ are Lame's elastic constants and α_T is the coefficient of linear thermal expansion.

For plane strain problem, the strain-displacement relations are

$$\epsilon_{x'} = \frac{\partial U}{\partial x'}$$

$$\epsilon_{y'} = \frac{\partial V}{\partial y'} \tag{2.3}$$

$$\epsilon_{x'y'} = \frac{1}{2}\left(\frac{\partial U}{\partial y'} + \frac{\partial V}{\partial x'} \right).$$

While the stress-strain relations are

$$\sigma_{x'} = 2\mu\varepsilon_{x'} + \lambda e' - \gamma(T-T_0)$$

$$\sigma_{y'} = 2\mu\varepsilon_{y'} + \lambda e' - \gamma(T-T_0) \qquad (2.4)$$

$$\tau_{x'y'} = \tau_{y'x'} = 2\mu\varepsilon_{x'y'}$$

where $\varepsilon_{x'}$, $\varepsilon_{y'}$ and $\varepsilon_{x'y'}$ are the strain components and $\sigma_{x'}$, $\sigma_{y'}$ and $\tau_{x'y'}$ are the stress components. In addition, appropriate boundary conditions and regularity requirements must be satisfied.

Two classes of problems of particular interest are considered separately. One is concerned with the effect of thermoelastic waves (thermal and/or mechanical waves) impinging on a stationary crack of finite length and the other one deals with the sudden application of thermal disturbances and/or uniform normal stress on the crack surfaces (transient problem). The geometry of the problems is shown in Fig. 1 with the center of crack coinciding with the origin of the coodinates. For the former problems, the effect of a thermal wave (accompanied by an associated mechanical wave) impinging on the crack surfaces is studied in details while for the latter problems the following

cases are considered to illustrate the procedure:

1. Sudden application of uniform normal stress on insulated crack surfaces.
2. Sudden variation of thermal flux on crack surfaces
3. Sudden variation of radiation thermal conditions on crack surfaces.

In each case attention is focused on finding the stress field in the vicinity of the crack tips and the relevant results, from the practical view point, are pointed out.

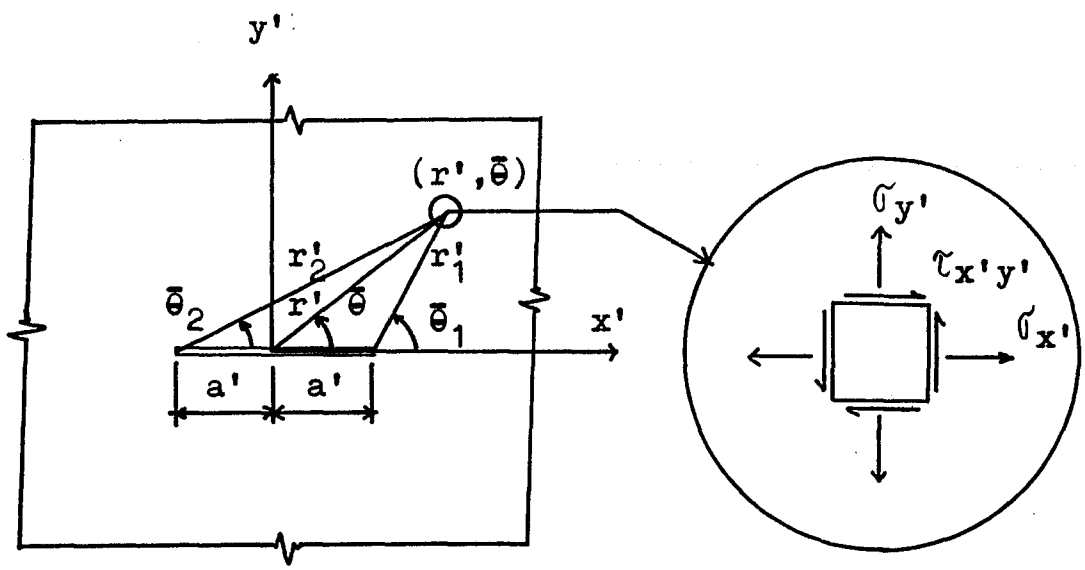

Figure 1

Geometry of a Finite Crack

CHAPTER 3

Diffraction of Thermoelastic Waves Around Crack

3.1 Plane Harmonic Thermoelastic Waves

In this chapter, the expression of thermoelastic waves are derived first and subsequently used to generate the stresses obtained from diffraction of such waves around cracks of finite length embedded in structural components. For this purpose it is found convenient to introduce the following dimensionless quantities:

$$w^* = \frac{c_1^2}{\kappa} \quad \text{(characteristic frequency)}$$

$$t = w^* t'$$

$$x = \frac{w^* x'}{c_1}, \qquad y = \frac{w^* y'}{c_1} \tag{3.1}$$

$$\vec{u} = \frac{w^* \vec{U}}{c_1}$$

$$\theta = \frac{T - T_0}{T_0}$$

$$\sigma_x = \frac{\sigma_{x'}}{\mu}, \quad \sigma_y = \frac{\sigma_{y'}}{\mu}, \quad \tau_{xy} = \frac{\tau_{x'y'}}{\mu}$$

Moreover, introducing the dimensionless abbreviations

$$\beta^2 = \frac{\lambda+2\mu}{\mu} = \frac{c_1^2}{c_2^2}$$

$$b = \frac{\gamma T_0}{\mu} \qquad (3.2)$$

$$g = \frac{\gamma}{\rho c_E}$$

and making use of Eqs.(3.1), Eqs. (2.1) may be written in the concise form:

$$\nabla^2 \vec{u} + (\beta^2 - 1)\nabla e - b\nabla\theta = \beta^2 \frac{\partial^2 \vec{u}}{\partial t^2} \qquad (3.3a)$$

$$\nabla^2 \theta - \frac{\partial \theta}{\partial t} - g \frac{\partial e}{\partial t} = 0 \qquad (3.3b)$$

where ∇ is the del operator, e is the dilatation in dimensionless units, $c_1 = \sqrt{\frac{\lambda+2\mu}{\rho}}$ is the velocity of longitudinal elastic waves in a medium with zero coefficient of expansion (isothermal velocity), $c_2 = \sqrt{\frac{\mu}{\rho}}$ is the velocity of distortional waves and $\kappa = \frac{k}{\rho c_E}$ is the diffusitivity of the material.

Similarly for plane-strain problem, the strain-displacement relations are

$$\varepsilon_x = \frac{\partial u}{\partial x}$$

$$\varepsilon_y = \frac{\partial v}{\partial y} \qquad (3.4)$$

$$\varepsilon_{xy} = \frac{1}{2}\left(\frac{\partial u}{\partial y} + \frac{\partial v}{\partial x} \right)$$

and the stress-strain relations become

$$\sigma_x = 2\varepsilon_x + (\beta^2 - 2)e - b\theta$$

$$\sigma_y = 2\varepsilon_y + (\beta^2 - 2)e - b\theta \qquad (3.5)$$

$$\tau_{xy} = \tau_{yx} = 2\varepsilon_{xy}.$$

According to Helmholtz theorem, the displacement vector field can be expressed as the sum of the gradient of a scalar field ϕ and the curl of a vector field $\vec{\psi}$:

$$\vec{u} = \nabla\phi + \operatorname{curl}\vec{\psi} \; . \qquad (3.6)$$

Applying relation (3.6), Eqs. (3.3) assume the form

$$\beta^2 \nabla^2 \phi - b\theta = \beta^2 \frac{\partial^2 \phi}{\partial t^2} \qquad (3.7a)$$

$$\nabla^2 \theta - \frac{\partial \theta}{\partial t} - g \frac{\partial}{\partial t} \nabla^2 \phi = 0 \qquad (3.7b)$$

$$\nabla^2 \psi = \beta^2 \frac{\partial^2 \psi}{\partial t^2} \qquad (3.7c)$$

Eqs. (3.7) show that the compressional wave (P-wave) and the thermal wave are coupled while the shear wave (S-wave) is independent of thermal straining. This cross-coupling vanishes when the coefficient of thermal expansion α_T is zero and equations (3.7a) and (3.7b) then reduce respectively to the wave equations and heat conduction equation.

Some of the stress-strain relations become

$$\sigma_y = 2\left[\frac{\partial^2 \phi}{\partial y^2} - \frac{\partial^2 \psi}{\partial y \partial x}\right] + (\beta^2 - 2)\nabla^2 \phi - b\theta$$

$$\tau_{xy} = 2\frac{\partial^2 \phi}{\partial x \partial y} + \frac{\partial^2 \psi}{\partial y^2} - \frac{\partial^2 \psi}{\partial x^2}. \qquad (3.8)$$

Seeking solutions of Eqs. (3.7a,b) of the forms

$$\phi = \phi^0 e^{-i\left\{\alpha(x\cos\bar{\beta} + y\sin\bar{\beta}) + \Omega t\right\}} \qquad (3.9a)$$

$$\theta = \theta^0 e^{-i\left\{\alpha(x\cos\bar{\beta} + y\sin\bar{\beta}) + \Omega t\right\}}. \qquad (3.9b)$$

Upon substituting Eqs. (3.9a,b) into Eqs. (3.7a,b), one can readily shows that

$$b\theta^0 = \rho^2(\Omega^2 - \alpha^2)\phi^0 \qquad (3.10a)$$

$$ig\alpha^2\Omega\phi^0 = (i\Omega - \alpha^2)\theta^0. \qquad (3.10b)$$

Elimination of ϕ^0/θ^0 results in the characteristic equation

$$(\alpha^2 - \Omega^2)(\Omega + i\alpha^2) + \varepsilon\alpha^2\Omega = 0. \qquad (3.11)$$

Here, $\varepsilon = \frac{bg}{\rho^2}$ is the coupling constant, $\bar{\beta}$ is the incident angle, ϕ^0 and θ^0 are constant magnitudes, α and Ω are ,in general, complex quantities so that the wave length is $2\pi/\mathrm{Re}(\alpha)$ and the period$=2\pi/\mathrm{Re}(\Omega)$. It is usual to regard either α or Ω as a real constant so that waves of a given wavelength (α regarded as a constant) or of a specified frequency Ω may be studied. However when α = constant,

one of the solutions associated with temperature θ is standing wave, the wave pattern does not advance, causing no wave diffraction at the cracks and, consequently, giving no rise to high stress intensification around the crack tips. Thus,only waves of assigned frequency Ω is considered.

Assuming Ω is a real constant (specified frequency), Eq. (3.11) gives 4 roots $\pm\alpha_1$, $\pm\alpha_2$, where

$$\begin{aligned}
\alpha_1 &= \frac{1}{2}\sqrt{\Omega}\left\{\left[\Omega+(1+i)\sqrt{2\Omega}+i(1+\varepsilon)\right]^{\frac{1}{2}} + \right. \\
&\qquad \left. \left[\Omega-(1+i)\sqrt{2\Omega}+i(1+\varepsilon)\right]^{\frac{1}{2}}\right\} \\
\alpha_2 &= \frac{1}{2}\sqrt{\Omega}\left\{\left[\Omega+(1+i)\sqrt{2\Omega}+i(1+\varepsilon)\right]^{\frac{1}{2}} - \right. \\
&\qquad \left. \left[\Omega-(1+i)\sqrt{2\Omega}+i(1+\varepsilon)\right]^{\frac{1}{2}}\right\}
\end{aligned} \tag{3.12}$$

Upon putting $\alpha_T = 0$ in Eqs. (3.12), it follows that

$$\alpha_1^2 = \Omega^2$$

$$\alpha_2^2 = i\Omega$$

and comparing with the corresponding results from Eqs. (3.10a,b), it is seen that $\pm \alpha_1$ represent modified elastic waves while $\pm \alpha_2$ represent modified thermal waves. Introducing

$$\alpha_j = \frac{\Omega}{v_j} + iq_j \ , \quad j=1,2 \tag{3.13}$$

where v_j, q_j and Ω are the phase velocities, the attenuation coefficients and frequency in dimensionless units respectively which in conventional units take the form

$$v_j' = c_1 v_j \tag{3.14}$$

$$q_j' = \frac{w^*}{c_1} q_j \tag{3.15}$$

$$\Omega' = w^* \Omega \ . \tag{3.16}$$

Then, the plane wave solution of the thermoelastic equations (3.7a,b) can be expressed as

$$\left\{\phi,\theta\right\} = \left\{\phi_1^0,\theta_1^0\right\} e^{q_1(x\cos\bar{\beta}+y\sin\bar{\beta})-i\Omega\left[t+\frac{1}{v_1}(x\cos\bar{\beta}+y\sin\bar{\beta})\right]}$$

$$+\left\{\phi_2^0,\theta_2^0\right\} e^{q_2(x\cos\bar{\beta}+y\sin\bar{\beta})-i\Omega\left[t+\frac{1}{v_2}(x\cos\bar{\beta}+y\sin\bar{\beta})\right]}$$

$$+\left\{\phi_3^0,\theta_3^0\right\} e^{-q_1(x\cos\bar{\beta}+y\sin\bar{\beta})-i\Omega\left[t-\frac{1}{v_1}(x\cos\bar{\beta}+y\sin\bar{\beta})\right]}$$

$$+\left\{\phi_4^0,\theta_4^0\right\} e^{-q_2(x\cos\bar{\beta}+y\sin\bar{\beta})-i\Omega\left[t-\frac{1}{v_2}(x\cos\bar{\beta}+y\sin\bar{\beta})\right]} \qquad (3.17)$$

In Eqs. (3.17), the waves associated with the exponents $t+\frac{1}{v_j}(x\cos\bar{\beta}+y\sin\bar{\beta})$ and $t-\frac{1}{v_j}(x\cos\bar{\beta}+y\sin\bar{\beta})$ are the incoming and outgoing waves, respectively.

Considering only the incoming waves and making use of Eqs. (3.10), Eqs. (3.17) become

$$\phi = \phi_1^0 e^{q_1(x\cos\bar{\beta}+y\sin\bar{\beta})-i\Omega\left[t+\frac{1}{v_1}(x\cos\bar{\beta}+y\sin\bar{\beta})\right]} +$$

$$\Omega_{\phi\theta}\theta_2^0 e^{q_2(x\cos\bar{\beta}+y\sin\bar{\beta})-i\Omega\left[t+\frac{1}{v_2}(x\cos\bar{\beta}+y\sin\bar{\beta})\right]}$$

$$\theta = \theta_2^0 e^{q_2(x\cos\bar{\beta}+y\sin\bar{\beta})-i\Omega\left[t+\frac{1}{v_2}(x\cos\bar{\beta}+y\sin\bar{\beta})\right]} +$$

$$\Omega_T\phi_1^0 e^{q_1(x\cos\bar{\beta}+y\sin\bar{\beta})-i\Omega\left[t+\frac{1}{v_1}(x\cos\bar{\beta}+y\sin\bar{\beta})\right]} \qquad (3.18)$$

where

$$\Omega_{\phi} = \Omega_{\phi r} + i\,\Omega_{\phi i}$$

$$\Omega_{T} = \Omega_{Tr} + i\,\Omega_{Ti} \tag{3.19}$$

in which

$$\Omega_{\phi r} = \frac{b}{\beta^2} \cdot \frac{\Omega^2 - \Omega^2/v_2^2 + q_2^2}{(\Omega^2 - \Omega^2/v_2^2 + q_2^2)^2 + 4\,\Omega^2 q_2^2/v_2^2}$$

$$\Omega_{\phi i} = \frac{b}{\beta^2} \cdot \frac{2\,\Omega q_2/v_2}{(\Omega^2 - \Omega^2/v_2^2 + q_2^2)^2 + 4\,\Omega^2 q_2^2/v_2^2} \tag{3.20}$$

$$\Omega_{Tr} = g \cdot \frac{\Omega^2(\Omega^2/v_1^2 - q_1^2)}{(\Omega^2/v_1^2 - q_1^2)^2 + (\Omega - 2\Omega q_1/v_1)^2}$$

$$\Omega_{Ti} = g \cdot \frac{\Omega\left[2\Omega q_1(\Omega - 2\Omega q_1/v_1)/v_1 - (\Omega^2/v_1^2 - q_1^2)\right]}{(\Omega^2/v_1^2 - q_1^2)^2 + (\Omega - 2\Omega q_1/v_1)^2}$$

Eqs. (3.18), being known as incoming thermoelastic waves, consist of an elastic wave and a thermal wave. Neither component can exist without the other. In general, the elastic wave contains both quasi-elastic and quasi-thermal modes associated respectively with the exponents $t+\frac{1}{v_1}(x\cos\bar{\beta}+y\sin\bar{\beta})$ and $t+\frac{1}{v_2}(x\cos\bar{\beta}+y\sin\bar{\beta})$. Similarly, both modes are represented in the thermal wave. The presence of the mode of opposite type in each constituent of the thermoelastic waves represent a coupling of elastic and thermal effects, the strength of which depends upon the frequency Ω and the coupling constant ε . The quasi-elastic mode, in contradistinction to purely elastic waves, is subjected to damping and dispersion, the attenuation coefficient q_1 and the phase velocity v_1 both being functions of Ω . Both the purely thermal wave and its modification, the quasi-thermal mode, also exhibit damping and dispersion.

Explicit formulas for the phase velocities v_1, v_2 and the attenuation coefficients q_1, q_2 can be derived directly from Eqs. (3.12), but the results are more informative when expressed as series expansions in either of the parameters ε or Ω . In

most applications of the theory, the coupling constant ε and Ω are small numbers compared with unity as shown in table 1, chapter 6. Therefore expanding Eqs. (3.12) in Taylor series of powers of ε and Ω and making use of Eq. (3.13), the following formulas for v_j and q_j are obtained [5].

Expansions in powers of ε gives

$$v_1 = 1 + \frac{\varepsilon}{2(1+\Omega^2)} - \frac{\varepsilon^2(1-14\Omega^2+\Omega^4)}{8(1+\Omega^2)^3} + \frac{\varepsilon^3(1-79\Omega^2+159\Omega^4-17\Omega^6)}{16(1+\Omega^2)^5} + O(\varepsilon^4) \qquad (3.21)$$

$$q_1 = \frac{\varepsilon\Omega^2}{2(1+\Omega^2)} - \frac{\varepsilon^2\Omega^2(5-3\Omega^2)}{4(1+\Omega^2)^3} + \frac{\varepsilon^3\Omega^2(35-155\Omega^2+65\Omega^4-\Omega^6)}{16(1+\Omega^2)^5} + O(\varepsilon^4) \qquad (3.22)$$

$$v_2 = \sqrt{2\Omega}\left[1 - \frac{\varepsilon(1+\Omega)}{2(1+\Omega^2)} + \frac{\varepsilon^2(3+10\Omega-8\Omega^2-6\Omega^3+5\Omega^4)}{8(1+\Omega^2)^3} - \frac{\varepsilon^3(5+35\Omega-65\Omega^2-151\Omega^3+143\Omega^4+73\Omega^5-43\Omega^6+3\Omega^7)}{16(1+\Omega^2)^5} + O(\varepsilon^4)\right] \qquad (3.23)$$

$$q_2 = \sqrt{\frac{\Omega}{2}}\left[1 + \frac{\varepsilon(1-\Omega)}{2(1+\Omega^2)} - \frac{\varepsilon^2(1-6\Omega-12\Omega^2+10\Omega^3+3\Omega^4)}{8(1+\Omega^2)^3}\right.$$

$$+ \frac{\varepsilon^3(1-15\Omega-65\Omega^2+135\Omega^3+155\Omega^4-101\Omega^5-35\Omega^6+5\Omega^7)}{16(1+\Omega^2)^5}$$

$$\left. + O(\varepsilon^4)\right] \qquad (3.24)$$

While expansions in powers of Ω yield

$$v_1 = \sqrt{1+\varepsilon}\left[1 - \frac{\Omega^2\varepsilon(4-3\varepsilon)}{8(1+\varepsilon)^4} + \right.$$

$$\left.\frac{\Omega^4\varepsilon(64-304\varepsilon+232\varepsilon^2-17\varepsilon^3)}{128(1+\varepsilon)^8} + O(\Omega^6)\right] \qquad (3.25)$$

$$q_1 = \frac{1}{\sqrt{1+\varepsilon}}\left[\frac{\Omega^2\varepsilon}{2(1+\varepsilon)^2} - \frac{\Omega^4\varepsilon(8-20\varepsilon+5\varepsilon^2)}{16(1+\varepsilon)^6} + O(\Omega^6)\right] \qquad (3.26)$$

$$v_2 = \sqrt{\frac{2\Omega}{1+\varepsilon}}\left[1 - \frac{\Omega\varepsilon}{2(1+\varepsilon)^2} + \frac{\Omega^2\varepsilon(4+\varepsilon)}{8(1+\varepsilon)^4} + \right.$$

$$\frac{\Omega^3\varepsilon(8-20\varepsilon+\varepsilon^2)}{16(1+\varepsilon)^6} - \frac{\Omega^4\varepsilon(64-208\varepsilon-8\varepsilon^2+5\varepsilon^3)}{128(1+\varepsilon)^8} +$$

$$\left. O(\Omega^5)\right] \qquad (3.27)$$

$$q_2 = \sqrt{\frac{\Omega(1+\varepsilon)}{2}}\left[1 - \frac{\Omega\varepsilon}{2(1+\varepsilon)^2} - \frac{\Omega^2\varepsilon(4-\varepsilon)}{8(1+\varepsilon)^4} + \right.$$

$$\left. + \frac{\Omega^3\varepsilon(8-12\varepsilon+\varepsilon^2)}{16(1+\varepsilon)^6} + \frac{\Omega^4\varepsilon(64-240\varepsilon+120\varepsilon^2-5\varepsilon^3)}{128(1+\varepsilon)^8} + O(\Omega^5)\right.$$

(3.28)

3.2 Boundary Conditions and Formulations

When a medium is subjected to an external thermal and mechanical disturbances at some points, a form of wave is created and it propagates through the medium. In using coupled theory this wave will consist of two types of waves, one is elastic wave the other one is thermal wave. Each wave consists of quasi-elastic and quasi-thermal mode. The coupling between the two waves is characterized by the factors Ω_T and Ω_ϕ which depend upon the coupling constant ε and frequency Ω . Because of the fact that Ω_T and Ω_ϕ are complex, it is clear from Eq. (3.18) that the quasi-elastic components of the two constituents of thermoelastic waves differ in phase and that the two quasi-thermal modes also have this property. Thus in this case it is to be assumed that the input waves will be of the form

$$\begin{aligned} \phi^{(i)} &= \phi_1^{(i)} + \phi_2^{(i)} \\ \theta^{(i)} &= \theta_1^{(i)} + \theta_2^{(i)} \\ \psi^{(i)} &= 0 \end{aligned} \tag{3.29}$$

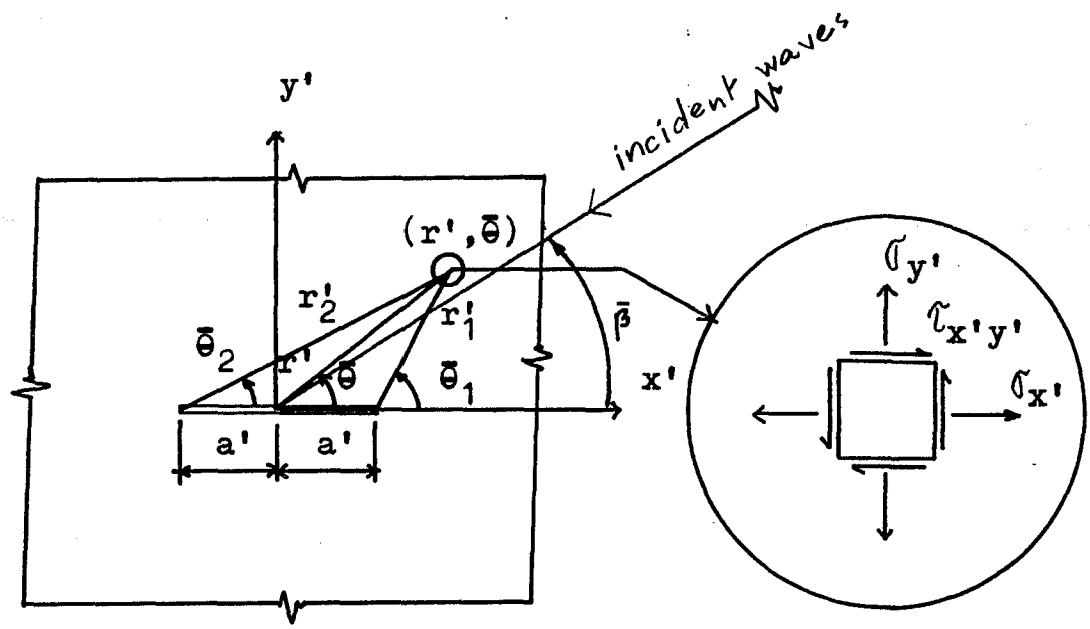

Figure 2

A Finite Crack Subjected to Incident Waves

in which

$$\phi_1^{(i)} = \phi^0 \, e^{q_1(x\cos\bar{\beta}+y\sin\bar{\beta})-i\Omega\left[t+\frac{1}{v_1}(x\cos\bar{\beta}+y\sin\bar{\beta})\right]}$$

$$\phi_2^{(i)} = \Omega_{\phi\theta}\theta^0 e^{q_2(x\cos\bar{\beta}+y\sin\bar{\beta})-i\Omega\left[t+\frac{1}{v_2}(x\cos\bar{\beta}+y\sin\bar{\beta})\right]}$$

$$\theta_1^{(i)} = \Omega_T\phi^0 e^{q_1(x\cos\bar{\beta}+y\sin\bar{\beta})-i\Omega\left[t+\frac{1}{v_1}(x\cos\bar{\beta}+y\sin\bar{\beta})\right]}$$

$$\theta_2^{(i)} = \theta^0 \, e^{q_2(x\cos\bar{\beta}+y\sin\bar{\beta})-i\Omega\left[t+\frac{1}{v_2}(x\cos\bar{\beta}+y\sin\bar{\beta})\right]} \tag{3.30}$$

However, it is more informative to study the effects of the thermal wave with an accompanying elastic wave (θ^0=constant, ϕ^0=0) and the elastic wave with an accompanying thermal wave (ϕ^0=constant, θ^0=0) upon the stability of the crack separately. The solution for the incoming thermoelastic waves of the forms Eqs. (3.29), therefore, may be taken as the linear sum of their solutions (refer to Fig. 2 for geometrical parameters and direction of the incident waves).

Some of the corresponding stress components are

$$\sigma_y^{(i)} = 2\frac{\partial^2 \phi^{(i)}}{\partial y^2} + (\beta^2-2)\nabla^2\phi^{(i)} - b\theta^{(i)}$$

$$\tau_{xy}^{(i)} = 2\frac{\partial^2 \phi^{(i)}}{\partial x \partial y} . \qquad (3.31)$$

The resulting wave fields, ϕ, ψ and θ may be taken as the linear sum of the incident wave fields and scattered wave fields as follows:

$$\phi = \phi^{(i)} + \phi^{(s)}$$

$$\psi = \psi^{(i)} + \psi^{(s)} \qquad (3.32)$$

$$\theta = \theta^{(i)} + \theta^{(s)}$$

where the scattered wave fields must satisfy the conditions

$$\phi^{(s)}, \psi^{(s)}, \theta^{(s)} \longrightarrow 0 \quad \text{as} \quad (x^2+y^2)^{\frac{1}{2}} \longrightarrow \infty$$

and be governed by the following equations

$$\beta^2 \nabla^2 \phi^{(s)} - b\theta^{(s)} = \beta^2 \frac{\partial^2 \phi^{(s)}}{\partial t^2} \qquad (3.33a)$$

$$\nabla^2 \theta^{(s)} - \frac{\partial \theta^{(s)}}{\partial t} - g \frac{\partial}{\partial t} \nabla^2 \phi^{(s)} = 0 \qquad (3.33b)$$

$$\nabla^2 \psi^{(s)} = \beta^2 \frac{\partial^2 \psi^{(s)}}{\partial t^2} \qquad (3.33c)$$

and subjected to specified conditions on the crack surfaces. For traction-free insulated crack surfaces, the total normal, shear stress and heat flux on y=0 plane and $|x|<a$ must vanish, i.e.,

$$\sigma_y(x,0,t) = \sigma_y^{(i)}(x,0,t) + \sigma_y^{(s)}(x,0,t) = 0, \quad |x|<a$$

$$\tau_{xy}(x,0,t) = \tau_{xy}^{(i)}(x,0,t) + \tau_{xy}^{(s)}(x,0,t) = 0, \quad |x|<a$$

$$\frac{\partial \theta}{\partial y}(x,0,t) = \frac{\partial \theta^{(i)}}{\partial y}(x,0,t) + \frac{\partial \theta^{(s)}}{\partial y}(x,0,t) = 0, \quad |x|<a \qquad (3.34)$$

from which the boundary conditions of the scattered wave problem may be established. For convenience, the problem will be divided into a symmetric and skew

symmetric part being even and odd in y respectively. The corresponding mixed-boundary conditions on y=0 plane are

Symmetric Problem

$$\begin{aligned}
\tau_{xy}^{(s)} &= 0 && \text{for all } x \\
\sigma_{y}^{(s)} &= -\sigma_{y}^{(i)} && \text{for } |x|<a \\
\frac{\partial \theta}{\partial y}^{(s)} &= -\frac{\partial \theta}{\partial y}^{(i)} && \text{for } |x|<a \qquad (3.35) \\
v^{(s)} &= 0 && \text{for } |x|>a \\
\frac{\partial \theta}{\partial y}^{(s)} &= 0 && \text{for } |x|>a
\end{aligned}$$

Skew-Symmetric Problem

$$\begin{aligned}
\sigma_{y}^{(s)} &= 0 && \text{for all } x \\
\tau_{xy}^{(s)} &= -\tau_{xy}^{(i)} && \text{for } |x|<a \\
\frac{\partial \theta}{\partial y}^{(s)} &= 0 && \text{for } |x|<a \qquad (3.36) \\
u^{(s)} &= 0 && \text{for } |x|>a \\
\theta^{(s)} &= 0 && \text{for } |x|>a
\end{aligned}$$

The complete solution of the original problem can be obtained by adding the solutions found from the

conditions (3.35) and (3.36). Furthermore, each of the previous parts can be subdivided into systems even or odd in x. In this dissertation, only the symmetric problem even in x will be studied in detail.

Combination of Eqs. (3.33a) and (3.33b) leads to equation having only $\phi^{(s)}$ as the dependent variable.

$$\left[\nabla^2 - \frac{\partial^2}{\partial t^2}\right]\left[\nabla^2 - \frac{\partial}{\partial t}\right] \phi^{(s)} - \varepsilon \frac{\partial}{\partial t} \nabla^2 \phi^{(s)} = 0 \tag{3.37}$$

In view of the problem being even in x it is seen that $\phi^{(s)}$ and $\theta^{(s)}$ are even functions in x while $\psi^{(s)}$ is an odd function in x. Thus it is appropriate to apply the Fourier Cosine transform with respect to x to Eq. (3.37). This can be accomplished by setting

$$\phi^{(s)} = f(x,y)\, e^{-i\Omega t}. \tag{3.38}$$

Substitution of Eq. (3.38) into Eq. (3.37) and making use of the Fourier Cosine theorem, namely

$$f_c(s,y) = \int_0^\infty f(x,y)\cos(sx)dx, \quad 0 < s < \infty$$

$$f(x,y) = \frac{2}{\pi}\int_0^\infty f_c(s,y)\cos(sx)ds, \quad 0 < x < \infty, \tag{3.39}$$

leads to

$$\frac{d^4 f_c}{dy^4} + \left[\Omega^2 + i\Omega(1+\varepsilon) - 2s^2\right]\frac{d^2 f_c}{dy^2} +$$

$$\left\{s^4 - s^2\left[\Omega^2 + i\Omega(1+\varepsilon)\right] + i\Omega^3\right\} f_c = 0 \tag{3.40}$$

For solutions to be bounded at the remote distances, Eq. (3.40) admits the form

$$f_c(s,y) \sim e^{-(s^2 - \xi^2)^{\frac{1}{2}} y} \tag{3.41}$$

Substitution of Eq. (3.41) into Eq. (3.40) yields the characteristic equation

$$\xi^4 - \left[\Omega^2 + i\Omega(1+\varepsilon)\right]\xi^2 + i\Omega^3 = 0 \tag{3.42}$$

which is identical with Eq. (3.11). Eq. (3.42) has

four roots $\pm\xi_1$ and $\pm\xi_2$ where

$$\xi_j^2 = m_j + in_j, \quad j=1,2 \tag{3.43}$$

in which

$$m_j = \frac{\Omega^2}{v_j^2} - q_j^2, \quad j=1,2 \tag{3.44}$$

and

$$n_j = \frac{2\Omega}{v_j} q_j, \quad j=1,2. \tag{3.45}$$

Letting

$$\eta_j \equiv \eta_j(s) = (s^2 - \xi_j^2)^{\frac{1}{2}}, \quad j=1,2 \tag{3.46}$$

and making use of Eqs. (3.38) and (3.39), the solution $\phi^{(s)}$ is obtained

$$\phi^{(s)} = \frac{2}{\pi} \int_0^\infty \left\{ A_1(s)e^{-\eta_1 y} + B_1(s)e^{-\eta_2 y} \right\} \cos(sx)e^{-i\Omega t} ds. \tag{3.47}$$

The solution $\theta^{(s)}$ may be obtained by substituting Eq. (3.47) into Eq. (3.33a). Thus

$$\theta^{(s)} = \frac{2\beta^2}{\pi b}\int_0^{\infty}\left\{(\Omega^2 - \xi_1^2)A_1(s)e^{-\eta_1 y} + (\Omega^2 - \xi_2^2)B_1(s)e^{-\eta_2 y}\right\}\cos(sx)e^{-i\Omega t}ds \tag{3.48}$$

Application of the Fourier Sine transform theorem, namely

$$\begin{aligned} f_s(s,y) &= \int_0^{\infty} f(x,y)\sin(sx)dx, \quad 0 < s < \infty \\ f(x,y) &= \frac{2}{\pi}\int_0^{\infty} f_s(s,y)\sin(sx)ds, \quad 0 < x < \infty \end{aligned} \tag{3.49}$$

to Eq. (3.33c) leads to

$$\psi^{(s)} = \frac{2}{\pi}\int_0^{\infty} C_1(s)e^{-\eta_3 y}\sin(sx)e^{-i\Omega t}ds \tag{3.50}$$

where

$$\eta_3 = (s^2 - \xi_3^2)^{\frac{1}{2}} \tag{3.51}$$

$$\xi_3^2 \equiv m_3 = \Omega^2\beta^2 \text{ and } n_3 = 0 \tag{3.52}$$

It should be noted that in evaluating the quantities $(s^2-\xi_j^2)^{\frac{1}{2}}$ the root with positive real part must be taken in each case to ensure boundedness at the remote distances from the origin.

Utilizing the theory of complex variables, the quantities $(s^2-\xi_j^2)^{\frac{1}{2}}$ may be written as

$$\eta_j = (s^2-\xi_j^2)^{\frac{1}{2}} = R_j+iI_j \ , \quad j=1,2,3 \tag{3.53}$$

where

$$\begin{aligned} R_j &= \left[(s^2-m_j)^2+n_j^2\right]^{\frac{1}{4}} \cos\frac{\theta_{pj}+2k_j\pi}{2} \\ I_j &= \left[(s^2-m_j)^2+n_j^2\right]^{\frac{1}{4}} \sin\frac{\theta_{pj}+2k_j\pi}{2} \end{aligned} \tag{3.54}$$

in which the argument

$$0 \leqslant \theta_{pj} < 2\pi$$

and $k_j = 0$ or 1 whichever gives the value of $R_j > 0$. When $n_j=0$ and $s^2-m_j < 0$, R_j becomes zero and

$$(s^2-\xi_j^2)^{\frac{1}{2}} = -i(m_j-s^2)^{\frac{1}{2}}, \quad j=1,2,3$$

where the branch cuts of the function have been discussed in [19].

3.3 Thermal Wave with Accompanying Elastic Wave Impinging on Crack

In this case the input waves are assumed to be in the forms

$$\theta^{(i)} = \theta^0 e^{q_2(x\cos\bar{\beta}+y\sin\bar{\beta})-i\Omega\left[t+\frac{1}{v_2}(x\cos\bar{\beta}+y\sin\bar{\beta})\right]}$$

$$\phi^{(i)} = \Omega_\phi \theta^0 e^{q_2(x\cos\bar{\beta}+y\sin\bar{\beta})-i\Omega\left[t+\frac{1}{v_2}(x\cos\bar{\beta}+y\sin\bar{\beta})\right]}$$

$$\psi^{(i)} = 0 \qquad (3.55)$$

The associated scattered wave solutions $\phi^{(s)}$, $\theta^{(s)}$ and $\psi^{(s)}$ are as follows:

$$\phi^{(s)} = \frac{2}{\pi}\int_0^\infty \left[A_{11}(s)e^{-\eta_1 y} + B_{11}(s)e^{-\eta_2 y}\right]\cos(sx)e^{-i\Omega t}\,ds$$

$$\theta^{(s)} = \frac{2\beta^2}{\pi b}\int_0^\infty \Big[(\Omega^2 - \xi_1^2)A_{11}(s)e^{-\eta_1 y} + (\Omega^2 - \xi_2^2)B_{11}(s)e^{-\eta_2 y} \Big]\cos(sx)e^{-i\Omega t}\,ds$$

$$\psi^{(s)} = \frac{2}{\pi} \int_0^\infty C_{11}(s) e^{-\eta_3 y} \sin(sx) e^{-i\Omega t} ds \qquad (3.56)$$

where η_i (i=1,2,3) are given by Eq. (3.53)

Applying the boundary conditions Eqs. (3.35) to the appropriate expressions of displacement, stress and temperature obtained from putting Eqs. (3.56) into Eqs. (3.6) and (3.8), the results may be written as:

$$\int_0^\infty \left[f_{11}(s)A_{11}(s)+f_{12}(s)B_{11}(s) \right] \cos(sx) ds = -\frac{\pi}{2} \sigma^t, \quad 0 < x < a \qquad (3.57a)$$

$$\int_0^\infty \left[f_{21}(s)A_{11}(s)+f_{22}(s)B_{11}(s) \right] \cos(sx) ds = \frac{\pi b \tau^t}{2 \beta^2}, \quad 0 < x < a \qquad (3.57b)$$

$$\int_c^\infty \left[g_{11}(s)A_{11}(s)+g_{12}(s)B_{11}(s) \right] \cos(sx) ds = 0, \quad x > a \qquad (3.57c)$$

$$\int_0^\infty \left[f_{21}(s)A_{11}(s)+f_{22}(s)B_{11}(s) \right] \cos(sx) ds = 0, \quad x > 0 \qquad (3.57d)$$

where f_{ij}, g_{ij} (i,j=1,2), σ^t and τ^t are abbreviations

given in Appendix C.

Application of Inversion of Cosine Transform theorem to Eqs. (3.57b) and (3.57d) yields

$$f_{21}(s)A_{11}(s)+f_{22}(s)B_{11}(s) = \frac{b}{\beta^2}\int_0^a \tau^t \cos(sx)ds, \qquad 0<x<\infty \tag{3.58}$$

Now let

$$W_1(s) = g_{11}(s)A_{11}(s)+g_{12}(s)B_{11}(s) \tag{3.59}$$

and solve for $A_{11}(s)$ and $B_{11}(s)$. Thus

$$A_{11}(s) = \frac{1}{\Delta_1(s)}\left\{ g_{12}(s)\frac{b}{\beta^2}\int_0^a \tau^t \cos(sx)dx - f_{22}(s)W_1(s)\right\} \tag{3.60}$$

$$B_{11}(s) = \frac{1}{\Delta_1(s)}\left\{-g_{11}(s)\frac{b}{\beta^2}\int_0^a \tau^t \cos(sx)dx + f_{21}(s)W_1(s)\right\}$$

where $\Delta_1(s)$ is given in Appendix C.

Substitution of $A_{11}(s)$ and $B_{11}(s)$ from Eqs. (3.60) into Eq. (3.57a) and $W_1(s)$ from Eq. (3.59) into Eq. (3.57c) leads to a pair of dual integral equations

$$\int_0^\infty sE(s)W_1(s)\cos(sx)ds = Z(x), \quad 0<x<a$$

$$\int_0^\infty W_1(s)\cos(sx)ds = 0 , \quad x>a \tag{3.61}$$

in which E(s) and Z(x) are defined as

$$sE(s) = \frac{\beta^2}{(\beta^2-1)\,\Delta_1(s)} \left\{ -f_{11}f_{22}+f_{12}f_{21} \right\} \tag{3.62}$$

and

$$Z(x) = \frac{\beta^2}{(\beta^2-1)} \int_0^\infty \frac{1}{\Delta_1(s)} \left[f_{12}g_{11}-f_{11}g_{12} \right]$$

$$\frac{b}{\beta 2} \int_0^a \tau^t \cos(sx)dx.\cos(sx)ds - \frac{\pi\beta^2\sigma^t}{2(\beta^2-1)} \tag{3.63}$$

The solution of the dual integral equations (3.61) is (for detail, see Appendix A)

$$W_1(s) = \frac{-\pi\beta^2\theta^0a^2}{2(\beta^2-1)} \int_0^1 \sqrt{\eta}\Psi(\eta)J_0(sa\eta)d\eta \tag{3.64}$$

where J_0 is the zero order Bessel function of the first kind. The unknown $\Psi(\eta)$ is governed by a standard Fredholm integral equation of the second kind

$$\Psi(\eta) - \int_0^1 \Psi(\tau) L(\tau,\eta) d\tau = \frac{4(\beta^2-1)\sqrt{\eta}}{\pi^2\beta^2\theta_0} \int_0^{\eta} \frac{Z(ax)dx}{(\eta^2-x^2)^{\frac{1}{2}}}, \quad 0<\eta\leq 1 \qquad (3.65)$$

where L is the symmetric kernel

$$L(\tau,\eta) = (\eta\tau)^{\frac{1}{2}} \int_0^{\infty} s\left[E(s/a)+1\right] J_0(s\tau)J_0(s\eta)ds, \qquad (3.66)$$

$$0<\eta\leq 1$$

$$0<\tau\leq 1$$

in which $E(s/a)+1 = O(s^{-2})$ as $s \longrightarrow \infty$.

Because of $\eta_i = (s^2-\xi_i^2)$ $(i=1,2)$ being complex, $\Psi(\eta)$, $L(\tau,\eta)$, $E(s/a)$ and $Z(ax)$ in Eq. (3.65) are, therefore, complex functions. Separating these functions into their real and imaginary parts in accordance with

$$\Psi(\eta) = \Psi_1(\eta) + i\Psi_2(\eta)$$

$$E(s/a) = E_1(s/a) + iE_2(s/a)$$

$$L(\tau,\eta) = L_1(\tau,\eta) + iL_2(\tau,\eta)$$

$$Z(ax) = Z_1(ax) + iZ_2(ax)$$

the following system of coupled Fredholm integral equations are obtained:

$$\Psi_1(\eta) - \int_0^1 \Psi_1(\tau)L_1(\tau,\eta)d\tau + \int_0^1 \Psi_2(\tau)L_2(\tau,\eta)d\tau = \frac{4(\beta^2-1)\sqrt{\eta}}{\pi^2\beta^2\theta^0}\int_0^\eta \frac{Z_1(ax)dx}{(\eta^2-x^2)^{\frac{1}{2}}}$$

$$\Psi_2(\eta) - \int_0^1 \Psi_1(\tau)L_2(\tau,\eta)d\tau - \int_0^1 \Psi_2(\tau)L_1(\tau,\eta)d\tau = \frac{4(\beta^2-1)\sqrt{\eta}}{\pi^2\beta^2\theta^0}\int_0^\eta \frac{Z_2(ax)dx}{(\eta^2-x^2)^{\frac{1}{2}}}. \quad (3.67)$$

Here, the function Z_1 and Z_2 are given in Appendix C.

The kernels $L_j(\tau,\eta)$ $(j=1,2)$ are given by

$$L_1(\tau,\eta) = (\tau\eta)^{\frac{1}{2}}\int_0^\infty s\left[E_1(s/a+1)\right]J_0(s\tau)J_0(s\eta)ds \quad (3.68)$$

$$L_2(\tau,\eta) = (\tau\eta)^{\frac{1}{2}} \int_0^\infty sE_2(s/a)J_0(s\tau)J_0(s\eta)ds \qquad (3.69)$$

in which $E_1(s/a)$ and $E_2(s/a)$ are given in Appendix C and J_0 stands for the usual Bessel function of the first kind of order zero.

The kernel L_1 given by Eq. (3.68) may be replaced by

$$L_1(\tau,\eta) = (\tau\eta)^{\frac{1}{2}}\bar{C}a^2 I_0(a\tau\bar{n})K_0(a\eta\bar{n}) +$$

$$(\tau\eta)^{\frac{1}{2}} \int_0^\infty s\left[E_1(s/a)+1-\frac{\bar{C}}{(s/a)^2+\bar{n}^2}\right]J_0(s\eta)J_0(s\tau).ds \qquad (3.70)$$

where $\bar{C}$ and $\bar{n}$ are given in Appendix C, I_0 and K_0 are the usual modified Bessel function of the first and second kind of order zero respectively.

The alternate kernel L_1 given by Eq. (3.70) converges faster than Eq. (3.68) as can be observed from

$$E_1(s) + 1 - \frac{\bar{C}}{s^2+\bar{n}^2} \longrightarrow O(s^{-6}) \text{ as } s \longrightarrow \infty$$

Thus, it poses no difficulties in numerical works.

In view of the kernels L_i (i=1,2) and forcing terms (right hand side terms) in Eqs. (3.67) being complicated, the system of coupled Fredholm equations must be solved numerically, the detail of which is discussed in chapter 5. It should also be noted that the forcing terms contain singularities at $x=\eta$. Thus certain technique must be developed before evaluating these functions numerically. This technique will be discused in detail in Appendix F.

Stress-Intensity Factor:

In fracture mechanics, much of the interest is centered on the near-field solution, in particular, the stress-intensity factor, a parameter characterizing the stability of crack propagation. To find the stress intensity factor for symmetric problem with system being even in x only $\beta = 90^{o}$ will be considered. Thus by following the same procedure as outlined in Appendix E, the singular stress σ_y, in the neighbourhood of the crack tips on the y=0 plane is

$$\sigma_{y'} = \frac{k_1'}{(2r_1')^{\frac{1}{2}}} + O(r_1^0) \qquad (3.71)$$

Here, k_1' is the dynamic stress-intensity factor which in conventional units takes the form

$$k_1' = \sigma_\theta \sqrt{a'}\, \Psi(1)\, e^{-i\Omega' t'} \qquad (3.72)$$

where $\sigma_\theta = -\mu\theta^o$ and θ^o is a constant specified by the incoming wave.

To illustrate the influence of frequency over the stress-intensity factor, the system of Fredholm integral equations (3.67) are solved numerically. The procedures discussed in Chapter 5 are used and the results for lead and copper are displayed graphically on the semi-log scale, for frequency range $\Omega = \Omega'/w^* = 1\text{x}10^{-12}$ to $1\text{x}10^{-6}$ as shown in Fig. 3. It is observed that the stress-intensity factors k_1' rise at first, reach the peak at relatively low frequency and then decay as the frequency increases.

3.4 Elastic Wave with Accompanying Thermal Wave Impinging on Crack

In this case the input waves are assumed as follows

$$\phi^{(i)} = \phi^0 e^{q_1(x\cos\bar{\beta}+y\sin\bar{\beta})-i\Omega\left[t+\frac{1}{v_1}(x\cos\bar{\beta}+y\sin\bar{\beta})\right]}$$

$$\theta^{(i)} = \Omega_T \phi^0 e^{q_1(x\cos\bar{\beta}+y\sin\bar{\beta})-i\Omega\left[t+\frac{1}{v_1}(x\cos\bar{\beta}+y\sin\bar{\beta})\right]}$$

$$\psi^{(i)} = 0 \qquad (3.73)$$

The proper expressions of the associated scattered solutions $\phi^{(s)}$, $\theta^{(s)}$ and $\psi^{(s)}$ are determined in the forms

$$\phi^{(s)} = \frac{2}{\pi}\int_0^\infty \left\{A_{12}(s)e^{-\eta_1 y} + B_{12}(s)e^{-\eta_2 y}\right\}\cos(sx)e^{-i\Omega t}\,ds$$

$$\theta^{(s)} = \frac{2\beta^2}{\pi b}\int_0^\infty \left\{(\Omega^2 - \xi_1^2)A_{12}(s)e^{-\eta_1 y} + (\Omega^2 - \xi_2^2)B_{12}(s)e^{-\eta_2 y}\right\}\cos(sx)e^{-i\Omega t}\,ds$$

$$\psi^{(s)} = \frac{2}{\pi} \int_0^\infty C_{12}(s) e^{-\eta_3 y} \sin(sx) e^{-i\omega t} ds \tag{3.74}$$

where η_i (i=1,2,3) are given by Eq. (3.53).

Application of the boundary conditions Eqs. (3.35) leads to

$$\begin{aligned}
&\int_0^\infty \left[f_{11}(s)A_{12}(s)+f_{12}(s)B_{12}(s)\right] \cos(sx)ds = -\frac{\pi}{2}\sigma^e && 0<x<a\\
&\int_0^\infty \left[f_{21}(s)A_{12}(s)+f_{22}(s)B_{12}(s)\right] \cos(sx)ds = \frac{\pi b}{2\beta^2}\tau^e && 0<x<a\\
&\int_0^\infty \left[g_{11}(s)A_{12}(s)+g_{12}(s)B_{12}(s)\right] \cos(sx)ds = 0 && x>a\\
&\int_0^\infty \left[f_{21}(s)A_{12}(s)+f_{22}(s)B_{12}(s)\right] \cos(sx)ds = 0 && x>a
\end{aligned} \tag{3.75}$$

where f_{ij}, g_{ij} (i,j=1,2), σ^e and τ^e are abbreviations given in Appendix C.

Application of the Inversion of Cosine Transform theorem and defining

$$W_2(s) = g_{11}(s)A_{12}(s)+g_{12}(s)B_{12}(s) \tag{3.76}$$

the Eqs. (3.75) may be reduced to a pair of dual integral equations

$$\begin{aligned} \int_0^\infty sE(s)W_2(s)\cos(sx)ds &= \bar{Z}(x), \quad 0<x<a \\ \int_0^\infty W_2(s)\cos(sx)ds &= 0, \quad x>a \end{aligned} \tag{3.77}$$

in which E(s) is defined by Eq. (3.62) and $\bar{Z}(x)$ by

$$\bar{Z}(x) = \frac{\beta^2}{(\beta^2-1)} \int_0^\infty \frac{1}{\Delta_1(s)} \left[f_{12}g_{11}-f_{11}g_{12}\right] \frac{b}{\beta 2} \int_0^a \tau^e \cos(sx)dx.$$

$$.\cos(sx)ds - \frac{\pi \beta^2 \tau^e}{2(\beta^2-1)} \tag{3.78}$$

Following a procedure similar to that used in the previous case, the solution of the dual integral

equations (3.77) is (for detail, see Appendix A)

$$W_2(s) = \frac{-\pi \phi^0 \xi_3^2(\beta^2-2\cos^2\bar{\beta})a^2}{2(\beta^2-1)} \int_0^1 \sqrt{\eta}\,\Upsilon(\eta)J_0(sa\eta)d\eta \quad (3.79)$$

where J_0 is the zero order Bessel function of the first kind. The unknown $\Upsilon(\eta)$ is governed by a standard Fredholm integral equation of the second kind

$$\Upsilon(\eta) - \int_0^1 \Upsilon(\tau)L(\tau,\eta)d\tau = \frac{4(\beta^2-1)\sqrt{\eta}}{\pi\xi_3^2(\beta^2-2\cos^2\bar{\beta})\phi^0} \int_0^\eta \frac{\bar{Z}(ax)dx}{(\eta^2-x^2)^{\frac{1}{2}}} \quad (3.80)$$

where L is the symmetric kernel given by Eq. (3.66).

An inspection of Eq. (3.80) reveals that when $\varepsilon = 0$, $g=0$ the equation reduces to the known solutions in [6,21].

Stress-Intensity Factor

It can be shown that for symmetric problem with system being even in x and $\bar{\beta} = 90^\circ$ the stress σ_y in the neighbourhood of the crack tips on the y=0 plane is

$$\sigma_{y'} = \frac{k_1'}{(2r_1')^{\frac{1}{2}}} + O(r_1'^{0}) \qquad (3.81)$$

where k_1', the dynamic stress-intensity factor in conventional units, is given as

$$k_1' = \sigma\sqrt{a'}\, Y(1)\, e^{-i\Omega' t'} \qquad (3.82)$$

in which $\sigma = -\mu\phi^0 \xi_3^2$ is the magnitude of static stress associated with $\alpha_T=0$ and applied in the direction normal to the crack plane. In experimental investigations using ultrasonics it is determined that the characteristic frequency, w*, is bounded by the relation

$$\Omega' \ll w^* < w_c$$

where $$w_c = 2\pi(c_1)_s\left(\frac{3\rho}{4\pi M}\right)^{\frac{1}{2}}$$

is the cut-off frequency obtained from the Debye spectrum for longitudinal waves, M being the atomic mass of elastic material and $(c_1)_s$ is the velocity of longitudinal wave measured under adiabatic conditions, and consequently, for mechanical vibrations occuring in

practice it may be assumed that $\Omega = \Omega'/w^* \ll 1$. The variations of the stress-intensity factors k_1' with the non-dimensional frequency Ω in the range $1x10^{-10}$-$1x10^{-5}$ ($1.8x10^{1}$rad/s $< \Omega' < 1.8x10^{6}$rad/s for lead; and $1.7x10^{1}$ rad/s$< \Omega' < 1.7x10^{6}$rad/s for copper) are displayed graphically on the semi-log scale as indicated in Fig. 4. The variation is observed to exhibit the usual feature, i.e., the stress-intensity factors increase with frequency, reaching maximum and then monotonically decreasing.

CHAPTER 4

Transient Thermoelastic Crack Problems

4.1 Basic Equations, Boundary Conditions and Formulations

Consider an infinite medium containing a through finite crack located along the x'-axis from -a' to +a' and the z'-axis coincides with the center line of the crack as shown in Fig. 1. Stresses in the medium are produced by an instantaneous uniform change of stress and/or thermal disturbances applied across the crack surfaces.

The governing equations are given by Eqs. (2.1). For the analysis in subsequent sections, it is convenient to introduce the dimensionless variables

$$x = \frac{c_1 x'}{\kappa} \tag{4.1}$$

$$y = \frac{c_1 y'}{\kappa}$$

$$t = \frac{c_1^2 t'}{\kappa} \tag{4.2}$$

Similarly, the components of displacements and stresses are made dimensionless by setting

$$u = \frac{\rho c_1^3 U}{\gamma T_0 k}$$
$$v = \frac{\rho c_1^3 V}{\gamma T_0 k} \tag{4.3}$$

and

$$\sigma_x = \frac{\sigma_{x'}}{\gamma T_0}$$
$$\sigma_y = \frac{\sigma_{y'}}{\gamma T_0} \tag{4.4}$$
$$\tau_{xy} = \frac{\tau_{x'y'}}{\gamma T_0}$$

In this manner, the governing equations assume the form

$$\nabla^2 \vec{u} + (\beta^2 - 1) \nabla e - \beta^2 \nabla \theta = \beta^2 \frac{\partial^2 \vec{u}}{\partial t^2} \tag{4.5a}$$

$$\nabla^2 \theta - \frac{\partial \theta}{\partial t} - \varepsilon \frac{\partial e}{\partial t} = 0 \tag{4.5b}$$

where e is the dilatation in dimensionless units, ε is the coupling constant and θ is dimensionless

temperature defined in Eq. (3.1).

Expressing the displacement vector $\vec{u}$ as the sum of irrotational and rotational components as before

$$\vec{u} = \nabla\phi + \text{Curl}\,\vec{\psi} \tag{4.6}$$

where ϕ and $\vec{\psi}$ are the scalar and equivoluminal vector potentials, respectively. It can be seen that Eqs. (4.5a,b) are satisfied provided that ϕ, ψ and θ are solutions of the following equations

$$\nabla^2\phi - \theta = \frac{\partial^2\phi}{\partial t^2} \tag{4.7a}$$

$$\nabla^2\theta - \frac{\partial\theta}{\partial t} - \varepsilon\nabla^2\left\{\frac{\partial\phi}{\partial t}\right\} = 0 \tag{4.7b}$$

$$\nabla^2\psi = \rho^2\frac{\partial^2\psi}{\partial t^2} \tag{4.7c}$$

Similarly, some of the stress components can be expressed in terms of the potential functions as

$$\sigma_y = \frac{2}{\beta^2}\left[\frac{\partial^2\phi}{\partial y^2} - \frac{\partial^2\psi}{\partial x\partial y}\right] + \frac{(\beta^2-2)}{\beta^2}\nabla^2\phi - \theta \qquad (4.8a)$$

$$\tau_{xy} = \frac{1}{\beta^2}\left[2\frac{\partial^2\phi}{\partial x\partial y} + \frac{\partial^2\psi}{\partial y^2} - \frac{\partial^2\psi}{\partial x^2}\right] \qquad (4.8b)$$

From Eqs. (4.7) it is easily seen that only the compressional wave is influenced by the temperature distribution and vice versa.

Assuming the problems possess symmetry with respect to y=0 plane, several examples can be formulated for $y \gtrless 0$ where the stress field due to the presence of the crack is obtained by specifying appropriate boundary conditions on the plane of symmetry and at infinity. To illustrate the applications, the following examples are considered.

1. Sudden Application of Normal Stress on Insulated Crack Surfaces: Here the relevant boundary conditions are

$$\tau_{xy}(x,0,t) = 0 \quad \text{for all } x \qquad (4.9a)$$

$$\sigma_y(x,0,t) = -\sigma_0 H(t) \quad \text{for } |x| < a \qquad (4.9b)$$

$$v(x,0,t) = 0 \quad \text{for } |x| > a \qquad (4.9c)$$

$$\frac{\partial\theta}{\partial y}(x,0,t) = 0 \quad \text{for all } x\,. \qquad (4.9d)$$

2. Sudden Variation of Thermal Flux on Crack Surfaces: The applicable boundary conditions are

$$\tau_{xy}(x,0,t) = 0 \qquad \text{for all } x \qquad (4.10a)$$

$$\sigma_y(x,0,t) = 0 \qquad \text{for } |x| < a \qquad (4.10b)$$

$$v(x,0,t) = 0 \qquad \text{for } |x| > a \qquad (4.10c)$$

$$\frac{\partial \theta}{\partial y}(x,0,t) = Q_0 H(t) \qquad \text{for } |x| < a \qquad (4.10d)$$

$$\frac{\partial \theta}{\partial y}(x,0,t) = 0 \qquad \text{for } |x| > a\,. \qquad (4.10e)$$

3. Sudden Variation of Thermal Radiation Conditions on Crack Surfaces: In this case the thermal disturbances are specified as

$$\frac{\partial \theta}{\partial t}(x,0,t) + h\left[\theta(x,0,t) - \theta_0 H(t)\right] = 0, \text{ for } |x| < a \qquad (4.11a)$$

$$\frac{\partial \theta}{\partial y}(x,0,t) = 0 \quad \text{for } |x| > a \qquad (4.11b)$$

and Eqs. (4.10a) to (4.10c) confirm the presence of a

symmetric stress-free crack in the medium.

In addition, the regularity conditions

$$u(x,y,t) = v(x,y,t) = \theta(x,y,t) = 0 \text{ for } (x^2+y^2)^{\frac{1}{2}} \longrightarrow \infty \tag{4.12}$$

must be satisfied in all cases.

In Eqs. (4.9b),(4.10d) and (4.11a), H(t) is the Heaviside unit step function, σ_0, Q_0 and θ_0 are the non-dimensional magnitude of the applied normal stress, heat flux and temperature, respectively, which,in conventional units,are

$$\sigma_0' = \gamma T_0 \sigma_0 \tag{4.13}$$

$$Q_0' = \frac{c_1 T_0 Q_0}{\kappa} \tag{4.14}$$

$$\theta_0' = \theta_0 T_0 \tag{4.15}$$

The dimensionless quantity h in Eq. (4.11a) relates to H, the outer or surface conductivity [4] through

$$h = \frac{\kappa H}{c_1 k} \tag{4.16}$$

Elimination of Θ from Eqs. (4.7a,b), noticing that ϕ and Θ are even functions of x and ψ is an odd function of x, and applying Fourier Sine and Cosine transforms to remove the variable x and Laplace transform to freeze the time variable, i.e.

$$f^*(p) = \int_0^\infty f(t)e^{-pt}dt$$
$$f(t) = \frac{1}{2\pi i}\int_{Br} f^*(p)e^{pt}dp \qquad (4.17)$$

the following ordinary differential equations with y being the independent variable are readily obtained

$$\frac{d^4\phi_c^*}{dy^4} - \left\{2s^2+\left[p^2+(1+\epsilon)p\right]\right\}\frac{d^2\phi_c^*}{dy^2} + \left\{s^4+s^2\left[p^2+(1+\ )p\right]+p^3\right\}\phi_c^* = 0 \qquad (4.18)$$

$$\frac{d^2\psi_s^*}{dy^2} - (s^2+p^2\beta^2)\,\psi_s^* = 0\,. \qquad (4.19)$$

Eqs. (4.19) admit the following solutions which give

rise to bounded displacements and stresses for large y

$$\phi_c^* \sim e^{-(s^2+\zeta^2)^{\frac{1}{2}}y}$$

and

$$\psi_s^* \sim e^{-(s^2+\zeta^2)^{\frac{1}{2}}y},$$

substituting ϕ_c^* and ψ_s^* into Eqs. (4.18) and (4.19) and making use of Eqs. (3.39), (3.49) and (4.17) the following results are obtained.

$$\phi^*(x,y,p) = \frac{2}{\pi}\int_0^\infty \left[A(s,p)e^{-\gamma_1 y} + B(s,p)e^{-\gamma_2 y}\right] \cos(sx)ds \tag{4.20a}$$

$$\theta^*(x,y,p) = \frac{2}{\pi}\int_0^\infty \left[(\zeta_1^2-p^2)A(s,p)e^{-\gamma_1 y} + (\zeta_2^2-p^2)B(s,p)e^{-\gamma_2 y}\right] \cos(sx)ds \tag{4.20b}$$

$$\psi^*(x,y,p) = \frac{2}{\pi}\int_0^\infty C(s,p)e^{-\gamma_3 y}\sin(sx)ds \tag{4.20c}$$

where ζ_1^2 and ζ_2^2 are the roots of the equation

$$\zeta^4 - \zeta^2\left[p^2+(1+\varepsilon)p\right] + p^3 = 0 \tag{4.21}$$

that is

$$\zeta_{1,2}^2 = \left[p+1+\varepsilon \pm \sqrt{(p+1+\varepsilon)^2-4p} \right] p/2 \qquad (4.22)$$

and

$$\zeta_3^2 = \beta^2 p^2 \qquad (4.23)$$

In addition, the following abbreviations have been used

$$\gamma_i = \gamma_i(s,p) = (s^2+\zeta_i^2)^{\frac{1}{2}}, \quad i=1,2,3 \qquad (4.24)$$

In the above equations the function f^* is the Laplace transform of the function f with p being the transform parameter and Br stands for the Bromwich path, an infinite line parallel to and to the right of imaginary axis.

It should be noted that in Eqs. (4.20), the s-plane has been cut in such a way that $(s^2+\zeta_i^2)^{\frac{1}{2}} \geq 0$, $(i=1,2,3)$ for $0 < s < \infty$, and the requirement that the displacement and temperature fields vanish at infinity is satisfied. $A(s,p)$, $B(s,p)$ and $C(s,p)$ are the unknown functions to be determined from the set of boundary conditions in Laplace domain, which may be written for the three examples mentioned earlier as

Example 1:

$$\begin{aligned}
\tau^*_{xy}(x,0,p) &= 0 && \text{for all } x \\
\sigma^*_y(x,0,p) &= -\sigma_0/p && \text{for } |x| < a \\
v^*(x,0,p) &= 0 && \text{for } |x| > a \\
\frac{\partial \theta^*}{\partial y}(x,0,p) &= 0 && \text{for all } x
\end{aligned} \tag{4.25}$$

Example 2:

$$\begin{aligned}
\tau^*_{xy}(x,0,p) &= 0 && \text{for all } x \\
\sigma^*_y(x,0,p) &= 0 && \text{for } |x| < a \\
v^*(x,0,p) &= 0 && \text{for } |x| > a \\
\frac{\partial \theta^*}{\partial y}(x,0,p) &= Q_0/p && \text{for } |x| < a \\
\frac{\partial \theta^*}{\partial y}(x,0,p) &= 0 && \text{for } |x| > a
\end{aligned} \tag{4.26}$$

Example 3:

$$\tau^*_{xy}(x,0,p) = 0 \quad \text{for all } x$$

$$\sigma^*_y(x,0,p) = 0 \quad \text{for } |x| < a$$

$$v^*(x,0,p) = 0 \quad \text{for } |x| > a \qquad (4.27)$$

$$\frac{\partial \theta^*}{\partial y}(x,0,p) + h\left[\theta^*(x,0,p) - \theta/p\right] = 0 \quad \text{for } |x| < a$$

$$\frac{\partial \theta^*}{\partial y}(x,0,p) = 0 \quad \text{for } |x| > a$$

4.2 Example 1: Sudden Application of Normal Stress on Insulated Crack Surfaces

For the determination of the unknown functions, A(s,p), B(s,p) and C(s,p), the boundary conditions Eqs. (4.25a,d) give the following linear algebraic equations

$$C(s,p) = -\frac{2s\left[\gamma_1(s,p)A(s,p)+\gamma_2(s,p)B(s,p)\right]}{2s^2+\zeta_3^2} \tag{4.28}$$

$$B(s,p) = -\frac{(\zeta_1^2-p^2)\,\gamma_1(s,p)}{(\zeta_2^2-p^2)\,\gamma_2(s,p)}A(s,p) \tag{4.29}$$

and the mixed-boundary conditions Eqs. (4.25b,c) with the aid of Eqs. (4.28) and (4.29) give a pair of dual integral equations

$$\begin{aligned}
&\int_0^\infty sF(s,p)\,\Lambda_1(s,p)\cos(sx)ds = \frac{\pi\sigma_0\beta^2}{2p^3(\beta^2-1)}, && 0<x<a \\
&\int_0^\infty \Lambda_1(s,p)\cos(sx)ds = 0, && x>a
\end{aligned} \tag{4.30}$$

where $\Lambda_1(s,p)$ is new unknown function which relates to A(s,p) through

$$\Lambda_1(s,p) = \frac{-2(\zeta_2^2-\zeta_1^2)\gamma_1(s,p)}{(\zeta_2^2-p^2)(2s^2+\zeta_3^2)} A(s,p) \qquad (4.31)$$

and F(s,p) is defined as

$$F(s,p) = \frac{2s^2+\zeta_3^2}{2(\zeta_2^2-\zeta_1^2)s\gamma_1\gamma_2} \left[a_{11}(s,p)\gamma_2(\zeta_2^2-p^2) - a_{12}(s,p)\gamma_1(\zeta_1^2-p^2) \right] \frac{\beta^2}{p^2(\beta^2-1)} \qquad (4.32)$$

in which a_{ij} (j=1,2) are given in Appendix C.

The solution of the dual integral equations (4.30) is (for detail, see Appendix A)

$$\Lambda_1(s,p) = \frac{\pi\sigma_0 a^2 \beta^2}{2p^3(\beta^2-1)} \int_0^1 \sqrt{\beta}\,\Phi_1(\beta,p) J_0(sa\beta) d\beta \qquad (4.33)$$

The unknown $\Phi_1(\beta,p)$ in Eq. (4.33) is governed by a

standard Fredholm equation of the second kind.

$$\bar{\Phi}_1(\eta,p) + \int_0^1 \bar{\Phi}_1(\tau,p)K_1(\eta,\tau,p)d\tau = \sqrt{\eta} \quad , \quad 0<\eta<1 \quad (4.34)$$

where the kernel K_1 is symmetric in τ and η, i.e.,

$$K_1(\eta,\tau,p) = (\eta\tau)^{\frac{1}{2}} \int_0^\infty s \left[F(s/a,p)-1 \right] J_0(s\eta)J_0(s\tau)ds \quad (4.35)$$

The standard Fredholm integral equation (4.34) can be solved numerically for the unknown $\bar{\Phi}_1$, the detail is given in Chapter 5, and subsequently the dynamic stress-intensity factor can be obtained. It can be observed that $F(s,p)-1 = O(s^{-1})$ as $s \to 0$, therefore, the integrand in Eq. (4.35) is $O(s^0)$ as $s \to 0$ and thus the integral converges at the lower limit. Furthermore at the upper limit, the integral converges since $F(s,p)-1 = O(s^{-2})$ as $s \to \infty$.

To evaluate the integral in Eq. (4.35) numerically, the integrand must be replaced such that there is a rapid decay when s becomes large. For this purpose by introducing the function

$$\bar{F}(s/a,p) = F(s/a,p) - 1 - \frac{c}{(s/a)^2+n^2} = O(s^{-6}),\ s\to\infty \tag{4.36}$$

and making use of the identity [10]

$$\int_0^\infty \frac{s}{(s/a)^2+n^2} J_0(s\eta)J_0(s\tau)ds = a^2 I_0(a\eta n)K_0(a\tau n),\quad 0\leq\eta\leq\tau \tag{4.37}$$

the kernel K_1 may be written as

$$K_1(\eta,\tau,p) = (\eta\tau)^{\frac{1}{2}} c a^2 I_0(a\eta n)K_0(a\tau n) + (\eta\tau)^{\frac{1}{2}}\int_0^\infty s\bar{F}(s/a,p)J_0(s\eta)J_0(s\tau)ds,\ 0\leq\eta\leq 1 \tag{4.38}$$

where c, n are given in Appendix B, I_0 and K_0 are modified zero order Bessel functions of the first and second kind respectively. The alternate kernel given

by Eq. (4.38) converges more rapidly than the one given by Eq. (4.35), thus, it poses no difficulties in numerically work.

Stress-Intensity Factor

By using the procedure outlined in Appendix E, it can be shown that the stress σ_y in the neighbourhood of the crack tips on the y=0 plane is

$$\sigma_y = \frac{k_1(t)}{(2r_1)^{\frac{1}{2}}} + O(r_1^0) \tag{4.39}$$

In the above equation, $k_1(t)$ is the dynamic stress-intensity factor which in dimensionless units assumes the form

$$k_1(t) = \mathcal{L}^{-1}\{k_1(p)\} = \sigma_0 \sqrt{a}\, \mathcal{L}^{-1}\{\Phi_1(1,p)/p\} \tag{4.40}$$

The corresponding dynamic stress-intensity factor in the conventional units is

$$k_1'(t') = \sigma_0' \sqrt{a'}\, \mathcal{L}^{-1}\{\Phi_1(1,p)/p\} \tag{4.41}$$

where σ_0' is defined by Eq. (4.13) and a', being half of the crack width, is defined by

$$a' = \frac{a\kappa}{c_1} \tag{4.42}$$

Numerical calculations have been carried out for two typical materials, lead and copper, one with high coupling constant and the other with low coupling constant. The results shown in Fig.5 show that the rise in stress-intensity factor is about 25% and occurs at time $t'=5\times10^{-11}$ sec. for lead and for copper the peak is lower about 21% and occurs at shorter time $t'=3\times10^{-11}$ sec.. The coupling effect is observed to be small which may be considered negligible.

4.3 Example 2: Sudden Variation of Thermal Flux on Crack Surfaces

Substitution of Eqs. (4.20) into Eq. (4.26a) yields an algebraic equation (4.28). With the help of Eqs. (4.28) and (4.20) it can be shown that the boundary conditions Eqs. (4.26b) to (4.26e) give the following simultaneous dual integral equations

$$\int_0^\infty \left[a_{11}(s,p)A(s,p)+a_{12}(s,p)B(s,p)\right] \cos(sx)ds = 0 \qquad 0<x<a \qquad (4.43a)$$

$$\int_0^\infty \left[b_{21}(s,p)A(s,p)+b_{22}(s,p)B(s,p)\right] \cos(sx)ds = \frac{\pi Q_0}{2p} \qquad 0<x<a \qquad (4.43b)$$

$$\int_0^\infty \left[b_{11}(s,p)A(s,p)+b_{12}(s,p)B(s,p)\right] \cos(sx)ds = 0 \qquad x>a \qquad (4.43c)$$

$$\int_0^\infty \left[b_{21}(s,p)A(s,p)+b_{22}(s,p)B(s,p)\right] \cos(sx)ds = 0 \qquad x>a \qquad (4.43d)$$

where a_{ij} and b_{ij} $(i,j=1,2)$ are given in Appendix C.

Now application of the Inversion Theorem of the Cosine Transform to Eqs. (4.43b,d) leads to

$$b_{21}(s,p)A(s,p)+b_{22}(s,p)B(s,p) = Q_0\sin(sa)/ps \qquad 0<s<\infty \quad (4.44)$$

Then let

$$\Lambda_2(s,p) = b_{11}(s,p)A(s,p)+b_{12}(s,p)B(s,p) \quad (4.45)$$

and solve for A(s,p) and B(s,p) from Eqs. (4.44) and (4.45)

$$A(s,p) = \frac{1}{\Delta(s,p)}\left[b_{22}(s,p)\Lambda_2(s,p)-b_{12}(s,p)Q_0\frac{\sin(sa)}{ps}\right]$$

$$B(s,p) = \frac{1}{\Delta(s,p)}\left[-b_{21}(s,p)\Lambda_2(s,p)+b_{11}(s,p)Q_0\frac{\sin(sa)}{ps}\right] \quad (4.46)$$

where $\Delta(s,p)$ is given in Appendix C.

Substitution of Eqs. (4.46) into Eq. (4.43a) and (4.45) into Eq. (4.43c) yields the following set

of dual integral equations

$$\int_0^\infty sF(s,p)\,\Lambda_2(s,p)\cos(sx)ds = I(x,p),\quad 0<x<a$$

$$\int_0^\infty \Lambda_2(s,p)\cos(sx)ds = 0,\quad x>a \tag{4.47}$$

where $F(s,p)$ is given by Eq. (4.32) and $\Lambda_2(s,p)$ is a new unknown function. In addition, the following contraction have been introduced

$$I(x,p) = \frac{Q_0\beta^2}{p^3(\beta^2-1)}\int_0^\infty e(s,p)\sin(sa)\cos(sx)ds \tag{4.48}$$

in which

$$e(s,p) = \frac{1}{s\Delta(s,p)}\left[-a_{11}(s,p)b_{12}(s,p)+ +a_{12}(s,p)b_{11}(s,p)\right] \tag{4.49}$$

It is not difficult to see that $e(s,p) = O(s^{-2})$ for $s \to \infty$ and for small $s, e(s,p) = O(s^{-1})$. Thus the integral in Eq. (4.48) converges rapidly at upper limit. At lower limit the integrand has a removable singularity which can be removed by using L'hospital rule.

Since the dual integral equations (4.47) are in the same form as Eqs. (4.30) except the forcing term (right hand side term of the equations), thus, the solution of Eqs. (4.47) may be given as

$$A_2(s,p) = \frac{-\pi Q_0 a^2 \beta^2}{2p^3(\beta^2-1)} \int_0^1 \sqrt{\eta}\, \Phi_2(\eta,p) J_0(sa\eta)\, d\eta \qquad (4.50)$$

where Φ_2 is governed by a standard Fredholm integral equation of the first kind.

$$\Phi_2(\eta,p) + \int_0^1 \Phi_2(\tau,p) K_1(\eta,\tau,p)\, d\tau = D(\eta,p), \qquad 0<\eta<1 \qquad (4.51)$$

in which the kernel K_1 is given by Eq. (4.35) or (4.38) and $D(\eta,p)$ is given by

$$D(\eta,p) = \frac{-2\sqrt{\eta}}{\pi a} \int_0^\infty e(s/a,p)\sin(s)J_0(s\eta)ds \qquad (4.52)$$

The integral equation (4.51) can be solved numerically as outlined in Chapter 5.

Stress-Intensity Factor

Following the same procedure as in example 1, the dynamic stress-intensity factor in dimensionless units is

$$k_1(t) = -Q_0 \sqrt{a}\, \mathcal{L}^{-1}\left\{\bar{\Phi}_2(1,p)/p\right\} \qquad (4.53)$$

Making use of Eqs. (4.4) and (4.14), the dynamic stress intensity factor in conventional units is obtained.

$$k_1'(t') = -\sigma_q \sqrt{a'}\, \mathcal{L}^{-1}\left\{\bar{\Phi}_2(1,p)/p\right\} \qquad (4.54)$$

where

$$\sigma_q = \frac{\gamma\kappa}{c_1} Q_0' \qquad (4.55)$$

in which $Q_0' = \dfrac{\kappa Q_0}{c_1 T_0}$

Graphical representation of the results for lead and copper are shown in Fig. 6,7. Again it exhibits the inertia effect. The overshoot in stress-intensity factor is about 30% for lead and 11% for copper. The corresponding elaspsed time for both materials occurs at $t' = 3 \times 10^{-11}$, 2.75×10^{-11} sec. for copper and lead respectively. The coupling effect is found to be small and may be negligible.

4.4 Example 3: Sudden Variation of Thermal Radiation on Crack Surfaces

Following the same procedure as in the previous examples and for the sake of simplicity, taking a=1, the boundary conditions (4.27) give the following system of simultaneous dual integral equations

$$\int_0^\infty \left[a_{11}(s,p)A(s,p)+a_{12}(s,p)B(s,p)\right] \cos(sx)ds = 0 \qquad 0<x<1 \qquad (4.56a)$$

$$\int_0^\infty \left[a_{21}(s,p)A(s,p)+a_{22}(s,p)B(s,p)\right] \cos(sx)ds = \frac{\pi h\Theta_0}{2p} \qquad 0<x<1 \qquad (4.56b)$$

$$\int_0^\infty \left[b_{11}(s,p)A(s,p)+b_{12}(s,p)B(s,p)\right] \cos(sx)ds = 0 \qquad x>1 \qquad (4.56c)$$

$$\int_0^\infty \left[b_{21}(s,p)A(s,p)+b_{22}(s,p)B(s,p)\right] \cos(sx)ds = 0 \qquad x>1 \qquad (4.56d)$$

where a_{ij} and b_{ij} (i,j=1,2) are given in Appendix C.

Now let

$$V_1(s,p) = s^{\frac{1}{2}} \left[b_{11}(s,p)A(s,p)+b_{12}(s,p)B(s,p) \right]$$

$$V_2(s,p) = s^{\frac{1}{2}} \left[b_{21}(s,p)A(s,p)+b_{22}(s,p)B(s,p) \right] \tag{4.57}$$

Solving for A(s,p) and B(s,p) from Eqs. (4.57) yields

$$A(s,p) = \frac{s^{-\frac{1}{2}}}{\Delta(s,p)} \left[b_{22}(s,p)V_1(s,p)-b_{12}(s,p)V_2(s,p) \right]$$

$$B(s,p) = \frac{s^{-\frac{1}{2}}}{\Delta(s,p)} \left[-b_{21}(s,p)V_1(s,p)+b_{11}(s,p)V_2(s,p) \right] \tag{4.58}$$

where $\Delta(s,p)$ is given in Appendix C.

Substitution of Eqs. (4.57) and (4.58) into Eq. (4.56) and making use of the identity [16] .

$$\cos(sx) = \left(\frac{\pi sx}{2}\right)^{\frac{1}{2}} J_{-\frac{1}{2}}(sx) \tag{4.59}$$

the Eqs. (4.56) can be put in a standard form as follow

$$\int_0^\infty \left[c_{11}(s,p)V_1(s,p)+c_{12}(s,p)V_2(s,p)\right] J_{-\frac{1}{2}}(sx)ds = 0 \qquad 0 < x < 1 \qquad (4.60a)$$

$$\int_0^\infty \left[c_{21}(s,p)V_1(s,p)+c_{22}(s,p)V_2(s,p)\right] J_{-\frac{1}{2}}(sx)ds = \sqrt{\frac{\pi}{2}}\, h\theta_0 x^{-\frac{1}{2}}/p, \quad 0 < x < 1 \qquad (4.60b)$$

$$\int_0^\infty V_1(s,p)J_{-\frac{1}{2}}(sx)ds = 0, \quad x > 1 \qquad (4.60c)$$

$$\int_0^\infty V_2(s,p)\, J_{-\frac{1}{2}}(sx)ds = 0, \quad x > 1 \qquad (4.60d)$$

where c_{ij} $(i,j=1,2)$ are given in Appendix C.

It is not difficult to show that reduction of a system of simultaneous dual integral equations to a system of Fredholm integral equations is hopeless because it will lead to divergent kernels. An alternate method is to adopt the method outlined by Erdogan and Bahar [11] which is an extension to the method developed by Tranter [24] , that is by defining

$$V_1(s,p) = \sqrt{\frac{\pi}{2}} \frac{h\theta_0 s^{1-\beta_1}}{p^3} \sum_{m=0}^{\infty} \chi_{1,1}(p) J_{-\frac{1}{2}+2m+\beta_1}(s) \qquad (4.61a)$$

$$V_2(s,p) = \sqrt{\frac{\pi}{2}} \frac{h\theta_0 s^{1-\beta_2}}{p^3} \sum_{m=0}^{\infty} \chi_{2,1}(p) J_{-\frac{1}{2}+2m+\beta_2}(s) \qquad (4.61b)$$

$$l=2m+1$$

where $\chi_{i,l}$ are the unknown coefficients to be determined and β_i are the parameters to be chosen so as to make the subsequent integrals convergent.

It can be seen that with the choice of $V_i(s,p)$ as given by Eq. (4.61), the Eqs. (4.60c,d) will be automatically satisfied because of the properties of the following Sonine-Schafheitlin integrals [16]

$$\int_0^{\infty} s^{1-\beta_i} J_{-\frac{1}{2}+2m+\beta_i}(s) J_{-\frac{1}{2}}(sx)ds = 0, \quad x > 1 \qquad (4.62)$$

$$\mathrm{Re}2(m+\tfrac{1}{2}) > 0, \ \beta_i > 0$$

Substituting Eq. (4.61) into Eqs. (4.60a,b) and interchanging the order of summation and integrations, the following equations are obtained

$$\sum_{m=0}^{\infty} \chi_{1,1}(p) \int_0^{\infty} s^{1-\beta_1} c_{11}(s,p) J_{-\frac{1}{2}+2m+\beta_1}(s) J_{-\frac{1}{2}}(sx)ds +$$

$$\sum_{m=0}^{\infty} \chi_{2,1}(p) \int_0^{\infty} s^{1-\beta_2} c_{12}(s,p) J_{-\frac{1}{2}+2m+\beta_2}(s) J_{-\frac{1}{2}}(sx)ds = 0,$$

$$0 < x < 1 \qquad (4.63a)$$

$$\sum_{m=0}^{\infty} \chi_{1,1}(p) \int_0^{\infty} s^{1-\beta_1} c_{21}(s,p) J_{-\frac{1}{2}+2m+\beta_1}(s) J_{-\frac{1}{2}}(sx)ds +$$

$$\sum_{m=0}^{\infty} \chi_{2,1}(p) \int_0^{\infty} s^{1-\beta_2} c_{22}(s,p) J_{-\frac{1}{2}+2m+\beta_2}(s) J_{-\frac{1}{2}}(sx)ds = p^2 x^{-\frac{1}{2}},$$

$$0 < x < 1 \qquad (4.63b)$$

Multiplying both sides of Eq. (4.63a) by

$$x^{\frac{1}{2}}(1-x^2)^{\beta_1-1} \mathcal{F}_k(-\tfrac{1}{2}+\beta_1, \tfrac{1}{2}, x^2)$$

and Eq. (4.63b) by

$$x^{\frac{1}{2}}(1-x^2)^{\beta_2-1} \mathcal{F}_k(-\tfrac{1}{2}+\beta_2, \tfrac{1}{2}, x^2)$$

$$k=0,1,2,3,....$$

integrating in x from 0 to 1, using the following integrals [24]

$$s^{-\beta_i} J_{-\frac{1}{2}+2k+\beta_i}(s) = \frac{\Gamma(k+\frac{1}{2})}{2^{\beta_i-1}\Gamma(\frac{1}{2})\Gamma(k+\beta_i)} \cdot$$

$$\cdot \int_0^\infty x^{\frac{1}{2}}(1-x^2)^{\beta_i-1} \tilde{\mathcal{F}}_k(-\tfrac{1}{2}+\beta_i, \tfrac{1}{2}, x^2) J_{-\frac{1}{2}}(sx)dx \qquad (4.64)$$

and defining $\beta_1 = 3/2$, $\beta_2 = 1$, the following equations are obtained

$$\sum_{m=0}^{\infty} \chi_{1,l}(p) \int_0^\infty s^{-2} c_{11}(s,p) J_l(s) J_r(s) ds +$$

$$\sum_{m=0}^{\infty} \chi_{2,l}(p) \int_0^\infty s^{-3/2} c_{12}(s,p) J_{l-\frac{1}{2}}(s) J_r(s) ds = B_{1,r}(p) \qquad (4.65a)$$

$$\sum_{m=0}^{\infty} \chi_{1,l}(p) \int_0^\infty s^{-3/2} c_{21}(s,p) J_l(s) J_{r-\frac{1}{2}}(s) ds +$$

$$\sum_{m=0}^{\infty} \chi_{2,l}(p) \int_0^\infty s^{-1} c_{22}(s,p) J_{l-\frac{1}{2}}(s) J_{r-\frac{1}{2}}(s) ds = B_{2,r}(p) \qquad (4.65b)$$

$k=0,1,2..,\ r=2k+1,\ l=2m+1$

where [see Appendix D]

$$B_{1,r}(p) = 0 \quad \text{for } r=1,3,5,.....$$

$$B_{2,r}(p) = \frac{\Gamma(\frac{1}{2}+k)p^2}{\Gamma(\frac{1}{2})\Gamma(k+1)} \int_0^1 \tilde{\mathcal{J}}_k(\tfrac{1}{2},\tfrac{1}{2},x^2)dx, \quad k=0,1,2,..$$

$$= \begin{cases} 0 & \text{for } r > 1 \\ p^2 & \text{for } r = 1 \end{cases} \tag{4.66}$$

in which $\mathcal{J}_k$ is the Jacobi polynomial.

Eqs. (4.65) can be put in a more convenient form for numerical purpose by adding and subtracting the following sum of integrals to and from the left hand sides [16]

$$\sum_{m=0}^{\infty} \chi_{1,1}(p) \int_0^{\infty} J_r(s) J_1(s) \frac{ds}{s} = \frac{\chi_{1,r}(p)}{2r}$$

$$\sum_{m=0}^{\infty} \chi_{2,1}(p) \int_0^{\infty} J_{1-\frac{1}{2}}(s) J_{r-\frac{1}{2}}(s) \frac{ds}{s} = \frac{\chi_{2,r}(p)}{2r-1} \tag{4.67}$$

giving

$$\chi_{1,r}(p)/2r + \sum_{m=0}^{\infty} \chi_{1,1}(p) \int_0^{\infty} \left[s^{-1} c_{11}(s,p) - 1 \right] J_{l}(s) J_{r}(s) \frac{ds}{s}$$

$$+ \sum_{m=0}^{\infty} \chi_{2,1}(p) \int_0^{\infty} s^{-3/2} c_{12}(s,p) J_{l-\frac{1}{2}}(s) J_{r}(s) ds = B_{1,r}(p)$$

$$\chi_{2,r}(p)/(2r-1) + \sum_{m=0}^{\infty} \chi_{1,1}(p) \int_0^{\infty} s^{-3/2} c_{21}(s,p) J_{l}(s) J_{r-\frac{1}{2}}(s) ds$$

$$+ \sum_{m=0}^{\infty} \chi_{2,1}(p) \int_0^{\infty} \left[c_{22}(s,p) - 1 \right] J_{l-\frac{1}{2}}(s) J_{r-\frac{1}{2}}(s) \frac{ds}{s} = B_{2,r}(p)$$

(4.68b)

It should be noted that

$$s^{-1} c_{11}(s,p) - 1 = O(s^{-2})$$

$$c_{12}(s,p) = O(s^{-1})$$

$$c_{21}(s,p) = O(s^{-1})$$

$$c_{22}(s,p) - 1 = O(s^{-1})$$

for $s \to \infty$, and for $s \to 0$ all the integrands in Eqs. (4.68) are order O(1). Thus all the integrals in Eqs. (4.68) exist. Eqs. (4.68) are infinite system of equations in $\chi_{i,r}$, i=1,2; r=1,3,5,..... which can be solved by truncating the equations to finite numbers.

Stress-Intensity Factor

It can be shown that the dynamic stress-intensity factor in conventional units is [see Appendix E]

$$k_1'(t') = \sigma_r \mathcal{L}^{-1}\left\{\Phi_3(p)/p\right\} \tag{4.69}$$

where

$$\Phi_3(p) = \sum_{m=1}^{\infty} (-1)^{m+1} \chi_{1,2m-1}(p) \tag{4.70}$$

and

$$\sigma_r = \sqrt{\frac{2}{\pi}}\, h(\beta^2-1)\theta_0' \gamma/\beta^2 \tag{4.71}$$

The results for lead and copper for different

values of H (outer or surface conductivity) are shown graphically in Fig. 8-13. It still reveals the dynamic effect but small coupling effect. For lead, the overshoot in stress-intensity factor is approximately 30% and for copper about 15%. The corresponding elaspsed time $t'=3.3\times10^{-11}$s and 3×10^{-11} s for lead and copper respectively.

CHAPTER 5

Numerical Techniques

This chapter discusses the numerical solutions of Fredholm integral equations and numerical inversion of the Laplace transform technique for the problems formulated in Chapter 3 and 4. Special techniques concerning the accuracy of numerical integrations of slow convergent integrals and of the integrals possessing singularities are also discused in some detail .

5.1 Numerical Solutions of System of Fredholm Integral Equations

To solve the system of Fredholm integral equations (3.67) the method outlined by Kantorovich and krylov [14] will be followed. Simpson's rule for approximate integration is used and Eqs. (3.67) are approximately replaced by the algebraic relations

$$\Psi_1(\eta_i) - \sum_{j=1}^{N+1} A_j L_1(\eta_i, \eta_j)\Psi_1(\eta_j) +$$

$$\sum_{J=1}^{N+1} A_j L_2(\eta_i, \eta_j)\Psi_2(\eta_j) = G_1(\eta_i) + \varepsilon_i$$

$$\Psi_2(\eta_i) - \sum_{j=1}^{N+1} A_j L_2(\eta_i, \eta_j)\Psi_1(\eta_j) -$$

$$\sum_{j=1}^{N+1} A_j L_1(\eta_i, \eta_j)\Psi_2(\eta_j) = G_2(\eta_i) + \varepsilon_i \qquad (5.1)$$

where

$$G_1(\eta_i) = \frac{4(\beta^2-1)\sqrt{\eta_i}}{\pi^2\beta^2\theta_0}\int_0^{\eta_i}\frac{Z_1(ax)dx}{(\eta_i^2-x^2)^{\frac{1}{2}}}$$

$$G_2(\eta_i) = \frac{4(\beta^2-1)\sqrt{\eta_i}}{\pi^2\beta^2\theta_0}\int_0^{\eta_i}\frac{Z_2(ax)dx}{(\eta_i^2-x^2)^{\frac{1}{2}}} \qquad (5.2)$$

in which Z_1 and Z_2 are given in Appendix C, and

N = even number of sub-intervals between 0 to 1

$A_1 = A_{N+1} = 1/3N$

$A_2 = A_4 = A_6 = \ldots\ldots\ldots\ldots = A_N = 4/3N$

$A_3 = A_5 = A_7 = \ldots\ldots\ldots\ldots = A_{N-1} = 2/3N$

ε_i = error which can be made to a small value if number of equations are increased, therefore, can be neglected.

$\eta_i = (i-1)/N, \quad i=1,2,3,\ldots. N+1$

Eqs. (5.1) are simultaneous linear algebraic equations in N+1 equations having $\Psi_1(\eta_i)$ and $\Psi_2(\eta_i)$

$(i=1,2,\ldots,N+1)$ as unknowns which can be solved by any conventional method. Thus to find the stress-intensity factor

$$k_1' = \sigma_\theta \sqrt{a'}\, \Psi_1(1)\, e^{-i\Omega' t'}$$

only Ψ_1 and Ψ_2 evaluated at $\eta_i = 1$ are necessary.

The main difficulties encountered in solving this set of equations are basically due to two factors. One is the slow convergence of the kernel $L_1(\tau,\eta)$, as can be observed from the order of magnitude of the integrand

$$f(s) = s\left[E_1(s/a)+1\right] J_0(s\eta)J_0(s\tau) = O(s^{-2})$$

for $s \to \infty$. This troublesome can be overcome by subtracting and adding the integrand f(s) a certain function

$$g(s) = \frac{s\bar{C}}{(s/a)^2+\bar{n}^2} J_0(s\eta)J_0(s\tau)$$

which has the same order of magnitude $O(s^{-2})$ as f(s)

for large s and whose solution is known in elementary form. In this manner, the resulting integrand becomes $O(s^{-6})$ for large s, consequently, the corresponding integral converges faster than the original one and requires computer time only a fraction of second. Another difficulty is due to the presence of singularities at upper limit $x=\eta$ in the forcing terms (right hand side terms). This type of singularity, being known as a weak singularity, can be effectively dealt with by the method outlined in Appendix F.

One more point which care must be taken properly is when dealing with the quantities

$$\eta_j = (s^2-\xi_j^2)^{\frac{1}{2}} = R_j+iI_j, \quad j=1,2,3 \tag{5.3}$$

It is noted that the function defined by Eq. (5.3) has 2 branches, one having positive R_j and the other one having negative R_j. The geometry of the problems suggests the branch having $R_j > 0$ so that far away from the crack, temperature, stresses and displacements become zero. However question arises as to how to select the branches of the function when $R_j = 0$ which

is the situation when $\eta_j = 0$ and $s^2 - m_j < 0$. In this case, without getting into any further discussion since it has already been discussed in great detail by Noble [19], the branch with negative imaginary part must be chosen

$$\eta_j = (s^2 - \xi_j^2)^{\frac{1}{2}} = -iI_j = -i(m_j - s^2)^{\frac{1}{2}}, \quad j=1,2,3$$

Similarly, the same technique can also be applied to the solutions of Eq. (3.80).

Eqs. (4.34) and (4.51) are Fredholm integral equations of the second kind which again can be solved numerically by the method of Kantorovich and Krylov [14]. Thus, for example, Eq. (4.34) may be replaced by

$$\Phi_1(\beta_i, p) + \sum_{j=1}^{N+1} A_j K_1(\beta_i, \beta_j, p)\Phi_1(\beta_j, p) = \sqrt{\beta_i} + \varepsilon_i \qquad i,j=1,2,..N+1 \quad (5.4)$$

where A_j, N and ε_i are defined as before and $\beta_j = (i-1)/N$.

Again Eq. (5.4) is the simultaneous algebraic equations in N+1 equations having $\bar{\Phi}_1(\zeta_i,p)$ $(i=1,2,..N+1)$ as unknowns. Thus upon solving Eq. (5.4), in particular for $\bar{\Phi}_1(1,p)$, the stress-intensity factor

$$k_1'(t') = \sigma_o' \sqrt{a'} \mathcal{L}^{-1}\left\{\bar{\Phi}_1(1,p)/p\right\}$$

is obtained.

Similarly, the numerical value of $\bar{\Phi}_2(1,p)$ in Eq. (4.51) can be obtained in the same manner as outlined above.

The coefficients $\chi_{1,2m-1}(p)$, $(m=1,2,3,....)$ in the series (4.70) is determined by the infinite set of linear algebraic equations given by Eq. (4.68). This system of equations having infinite variables is well-known. The solution of this type of equations can be found effectively by truncating the infinite equations to finite numbers and , therefore, any iterative algorithm such as the Gauss-Seidel procedure can be applied. It should be noted that the proof of the regularity of the Eqs. (4.68) is impossible because of the complexity of the kernels but it is confirmed by numerical results. In this problem, retaining 6 terms

in the infinite series (4.61) is found to give a good approximation (3 significant digits).

5.2 Numerical Inversion of the Laplace Transforms

The main difficulty in applying the Laplace transform technique is the inversion or determination of the original function from its transform

$$\bar{\Phi}_r(1,p)/p = \int_0^\infty e^{-pt} f_r(t)dt, \quad r=1,2,3 \tag{5.5}$$

i,e to find $f_r(t)$ from the known function $\bar{\Phi}_r(1,p)/p$. In many applications analytical methods are not possible, e.g., when $\bar{\Phi}_r(1,p)$ is the numerical solution of an integral equation. Therefore numerical methods must be used. One of the successful methods is given by Miller and Guy [17] . This method is based on the values of the functions $\bar{\Phi}_r(1,p)/p$ evaluated at discrete points along the real axis, $p = (\beta+1+k)\,\delta$, $k=0,1,2,3,\ldots\ldots$, β and δ are real numbers.

Suitably changing of variable of integration and expanding $f_r(t)$ in terms of Jacobi polynomials

$$f_r(t) = \sum_{N=0}^{\infty} C_n P_n^{(0,\beta)}(2e^{-\delta t}-1), \quad r=1,2,3 \tag{5.6}$$

leads to

$$\frac{\Phi_r[1,(\beta+1+k)]}{(\beta+1+k)} = \frac{2}{\delta}^{-(\beta+1+k)} \int_{-1}^{1} (1-x)^{\beta} \sum_{m=0}^{\infty} a_m P_m^{(0,\beta)}(x) \left[\sum_{n=0}^{\infty} C_n P_n^{(0,\beta)}(x) \right] dx \qquad (5.7)$$

where a_m are known coefficients and C_n are to be determined from orthogonality of Jacobi polynomial which leads to n system of simultaneous algebraic equations.

$$\begin{aligned}
\frac{\Phi_r[1,(\beta+1)]}{\beta+1} &= \frac{C_0}{\beta+1} \\
\frac{\Phi_r[1,(\beta+2)]}{\beta+2} &= \frac{C_0}{\beta+2} + \frac{1!C_1}{(\beta+2)(\beta+3)} \qquad (5.8) \\
\frac{\Phi_r[1,(\beta+3)]}{\beta+3} &= \frac{C_0}{\beta+3} + \frac{2C_1}{(\beta+3)(\beta+4)} + \frac{2!C_2}{(\beta+3)(\beta+4)(\beta+5)} \\
. &= \ldots\ldots\ldots\ldots\ldots\ldots\ldots\ldots\ldots\ldots \\
. &= \ldots\ldots\ldots\ldots\ldots\ldots\ldots\ldots\ldots\ldots
\end{aligned}$$

In this manner the inverse Laplace transform assumes the form

$$f_r(t) = \mathcal{L}^{-1}\left\{\Phi_r(1,p)/p\right\} \approx \sum_{n=0}^{N}{}' C_n P_n^{(0,\beta)}(2e^{-\delta t}-1) \quad (5.9)$$

where $P_n^{(0,\beta)}$ is the Jacobi polynomial of degree n.

In using this method, it is suggested that, according to ref. [17], $-.5 \leq \beta \leq 5.0$ and $.05 \leq \delta \leq 2.0$. Thus the required computer time is only a fraction of a second. It is also noted that the following set of values $\beta = 0$, $\delta = .125$; $\beta = 0$, $\delta = .275$ and $\beta = 0$, $\delta = .35$ have been found useful.

CHAPTER 6

Numerical Results, Conclusions and Suggestions for Future Researchs

6.1 Numerical Results

Two typical materials, copper and lead, one with low coupling constant and the other with high coupling constant, were selected for numerical computation and application of the solution presented. The numerical values of the materials are found in ref. [8] and are reproduced here in Table 1.

The plane harmonic thermoelastic waves, the simplest type of thermoelastic disturbances, were chosen to study the problem of diffraction of thermoelastic waves around crack so that the salient features of utilizing the coupled thermoelastic theory can be brought out. In case of transient problem, three examples were chosen to illustrate the results.

The Fredholm integral equations (3.67), (3.80), (4.34) and (4.51) were solved numerically by the

method described in Chapter 5 to yield the values of the functions $\Psi(1)$, $\Upsilon(1)$, $\Phi_1(1,p)$ and $\Phi_2(1,p)$. The accuracy of the results was achieved by choosing large value of N in approximation of integrals in Fredholm integral equations. The number of terms N = 21 was observed to give a reasonable accurate results. The function $\Phi_3(p)$ was obtained by taking a few terms of $\chi_{1,2m-1}(p)$ in the series Eq. (4.70). The functions $\chi_{1,2m-1}(p)$, m=1,2,3,.... are the solutions of the system of algebraic equations (4.68) which were solved numerically by truncating the infinite series to a finite number of terms. Six terms in the series were observed to give good results. In all cases examined the numerical computation converged smoothly and no unusual difficulties were encountered. These values were then inserted into Eqs. (3.72), (3.82) (4.41), (4.54) and (4.69) to determine the corresponding stress-intensity factors. The inversion of the Laplace transforms were accomplished through the numerical method described in Chapter 5 or ref. [17] .

For convenience, the stress-intensity factors given by Eqs. (3.72) and (3.82) may be rewritten in the form

$$k_1' = (R+iI)e^{-i\Omega' t'} = |k_1'|\, e^{-i(\Omega' t' - \delta)} \qquad (6.1)$$

where $\delta = \tan^{-1}\frac{I}{R}$ is the phases angle, and $|k_1'|$ is the max. stress-intensity factor.

Shown graphically on semi-log scale in Fig. 3 is the behaviour of the normalized max. stress-intensity factor $|k_1'|/\sigma_\Theta\sqrt{a'}$ as function of frequency $\Omega = \Omega'/w^*$ when a crack of length $2a' = 1.0$ cm. and 2.0 cm. is impinged upon by a thermal wave accompanied by an elastic wave at an incident angle $\bar{\phi} = 90^\circ$. Since $\Omega = \Omega'/w^*$, the normalized stress-intensity factor will depend upon the circular frequency of incident thermal wave and characteristic frequency w^*. The time t' at which it occurs depends upon the phase angle $\delta = \tan^{-1}\frac{\mathrm{Im}\Psi(1)}{\mathrm{Re}\Psi(1)}$. Examination of the results in Fig. 3 shows that the max. stress-intensity factor rises at first then decay with increasing frequency. For the actual crack length $2a' = 1.0$ cm. the peak occurs at frequency $\Omega' = 1.3$ rad/s and $\Omega' = 4.25$ rad/s for lead and copper respectively. The corresponding peak values for crack length $2a' = 2.0$ cm. are observed to take place at relatively lower frequency. However their corresponding peak values are observed to remain constant for the same materials. It is also noted that as $\Omega' \to 0$ all the

curves approach zero value. This implies that the stress-intensity factor vanishes under static thermal loading. The impact of the coupling term in heat conduction equation can be examined by setting $g=\varepsilon=0$ in the numerical process and the corresponding results are shown by dashed lines in Fig. 3 for both materials. It is noted that the coupling effect is negligibly small.

A similar behaviour is also observed when a plane elastic wave accompanied by thermal wave impinging upon a crack. The variation of $|k_1'|/\sigma\sqrt{a'}$, the ratio of max. dynamic stress-intensity factor over static value, with frequency $\Omega = \omega'/w^*$ shown graphically on semi-log scale in Fig. 4 shows that the maximum dynamic stress-intensity factor is about 42% and 31% higher than the corresponding static value for the given materials, lead and copper respectively. As $\omega' \to 0$ all the curves degenerate to unity and consequently the dynamic stress-intensity factor approaches static value $\sigma\sqrt{a'}$. For lead with crack length $2a' = 1.0$ cm. the peak in $|k_1'|$ occurs at frequency $\omega' = 11\times10^4$ rad/s while for copper it takes place at higher frequency $\omega' = 3.3\times10^5$ rad/s . When the crack length becomes twice, $2a' = 2.0$ cm., the corresponding peak is observed to

occur at lower frequency about half of the previous value. As frequency increases the stress-intensity factor decreases drastically for both materials. Similar to the previous case, the coupling effect is brought out by letting $g=\varepsilon=0$ in the numerical process and the results are shown in Fig. 4 by dashed lines. It is in excellent agreement with the analogous results for isotropic materials [6,21] . The coupling effect is found to be minimal. Therefore, it is justifiable to apply uncoupled theory (elastodynamic theory) when dealing with crack problems under harmonically time varying elastic P-wave.

Shown in Figs. 5 to 13 are the variation of the stress-intensity factors k_1' associated with the transient problem versus the dimensionless time $t = c_1^2 t'/\kappa$ for a crack of length $2a' = 2\kappa/c_1$. The results for non-dimensional surface conductivity $h = 1\times10^{-3}$, 1×10^{-4} and 1×10^{-5} are shown separately in Figs. 8 to 13. In order to find out the influence of the coupling term in the heat conduction equation on the response, another set of numerical computation was carried out with the coupling constant $\varepsilon = 0$ and the results were exhibited on the same curves by dotted

lines. Upon examining the results, it is seen that all the curves exhibit the same feature; that is the dynamic stress-intensity factor rises quickly with time, reaching a peak and then decreases in magnitude and approaches steady-state for sufficiently long time. The dynamic stress-intensity factors for Ex. 1, normal stress acting on the crack surfaces, are shown in Fig. 5. For lead, the rise in stress-intensity factor is about 25% and occurs at an elapsed time of $t'=5x10^{-9}$ sec. For the remaining material, copper, the peak is a little lower, about 21% above the steady-state value and occurs at shorter time $t'=3x10^{-9}$ sec.. The influence of the mechanical coupling term (coupling effect) is observed to be very small, about 0.1%, for both materials. In Ex. 2, flux specified inside the crack surfaces, the overshoot in stress-intensity factor is about 30% for lead and 11% for copper as shown in Figs. 6,7. The elapsed time is approximately the same for both materials taking place at $t'=3.5x10^{-9}$ sec.. The coupled theory seems to yield lower value in stress-intensity factor for both materials approximately less than 2.5%. Finally, Figs. 8 to 13 display the variation of the stress-intensity factor associated

with sudden variation of thermal radiation boundary condition on crack surfaces, Ex. 3, versus dimensionless time $t = c_1^2 t'/\kappa$ for a crack of length $2a' = 2\kappa/c_1$ and dimensionless surface conductivities $h = 1\times10^{-3}$, 1×10^{-4} and 1×10^{-5}. The peak in stress intensity factor k_1' is moderately high in lead, about 30%, and relatively low in copper, about 15% above the steady-state value. The elapsed time needed for k_1' to reach its maximum value is estimated to be approximately 3.3×10^{-9} sec. and 3.0×10^{-9} sec. for lead and copper respectively. Similar conclusion can be made concerning the influence of the mechanical coupling term as in the previous examples.

6.2 Conclusion and Suggestions for Future Researchs

The application of coupled thermoelasticity theory to 2-dimensional plane-strain crack problems is presented first time in this dissertation. Despite the complexity of the theory, coupled thermoelasticity theory allows one to examine the effects of thermal waves (steady state and transient) upon the crack situated inside the structural components, whereas the conventional thermoelasticity (quasi-static theory) is not able to explain. Moreover, some insight as to the interaction effects of straining and temperature upon the stress-intensity factor is also made possible and becomes clear. Few examples concerning the scattering of plane harmonic thermal waves (and/or elastic waves) and transient problems have been formulated and solved successfully.

Many of the crack problems can usually be reduced to a set of dual integral equations. The solution of such equations usually presents a formidable task for engineers and physicists, Most of solutions (stress-intensity factors) have been achieved successfully if the weigth functions are constants [11] . In this research a method of finding the stress-

intensity factor from the solution of a set of dual integral equations having non-constant weigth function has been developed.

By incorporating a system of moving coordinates into the method presented in this research, another interesting problem concerning a crack of fixed length travelling with constant velocity in a medium of infinite extent may be solved. A more realistic problem is the problem of a moving crack having crack tips moving in opposite directions with constant velocities.

It is hoped that the successful application of theory of coupled thermoelasticity to the crack problem treated in this research may stimulate further investigations and researches to the more advanced problems encountered in the years to come, especially, in the area of high elevated temperature fracture mechanics in which non-linear theory of coupled thermoelasticity must be employed.

Table 1: Material properties (measured at $21^{o}C$)

Symbol	Property	Units	Copper	Lead
k	Thermal conductivity	$Cal/s.cm.^{o}K$	0.93	0.084
κ	Thermal diffusitivity	cm^2/s	1.14	0.25
α_T	Coeff. of thermal expansion	$cm/cm^{o}C$	$16.5x10^{-6}$	$29.3x10^{-6}$
ε	Coupling constant	-	0.017	0.0729
E	Young modulus	dyn/cm^2	$11.45x10^{11}$	$1.625x10^{11}$
c_1	Velocity of longitudinal wave	cm/s	$4.36x10^{5}$	$2.14x10^{5}$
ν	Poisson ratio	-	0.32	0.446
ρ	Density	gm/cm^3	8.93	11.34

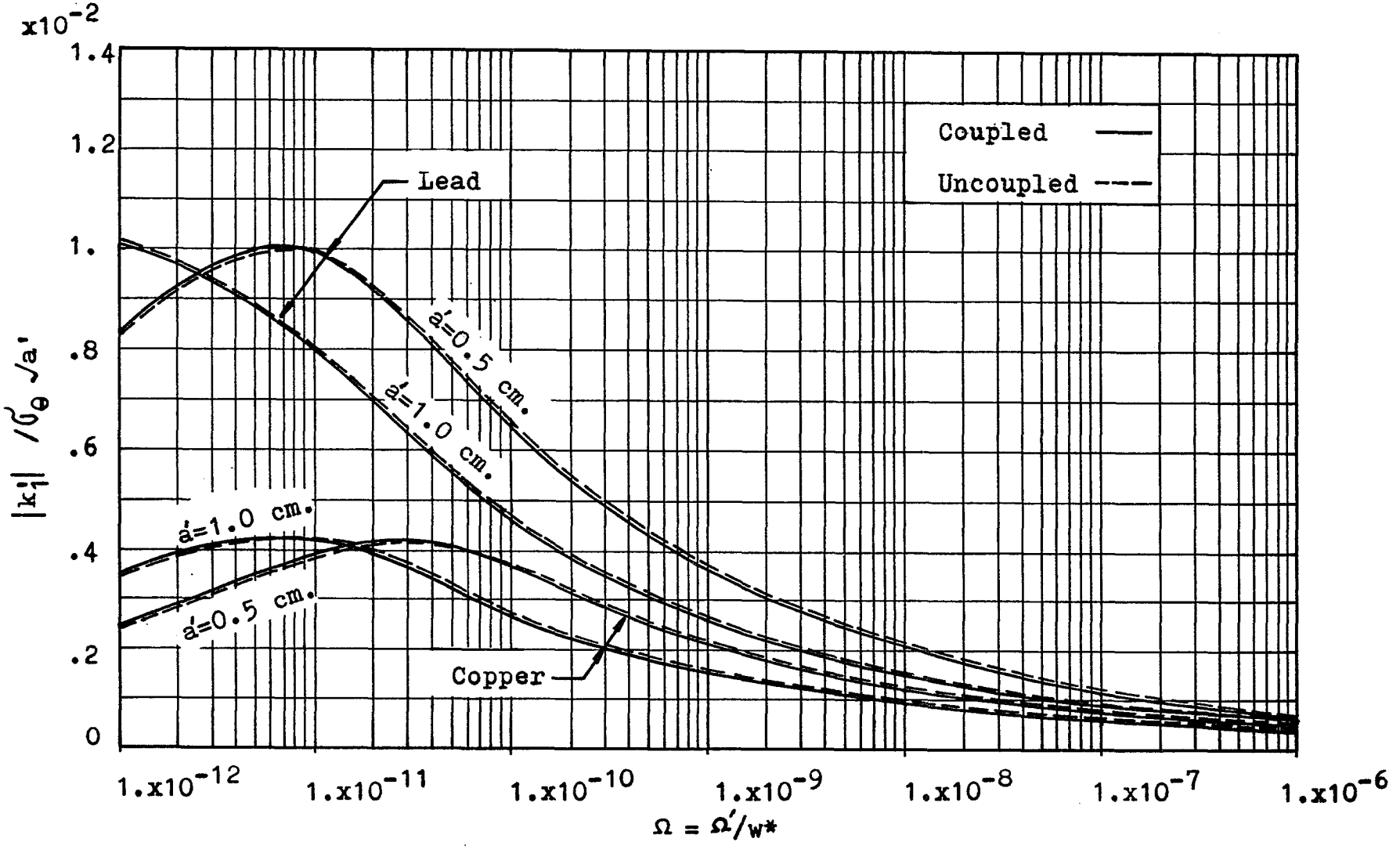

Figure 3 Variation of Stress-Intensity Factors with Frequency for Incident Thermal Wave Accompanied by Elastic Wave ($\bar{\phi} = 90^{o}$)

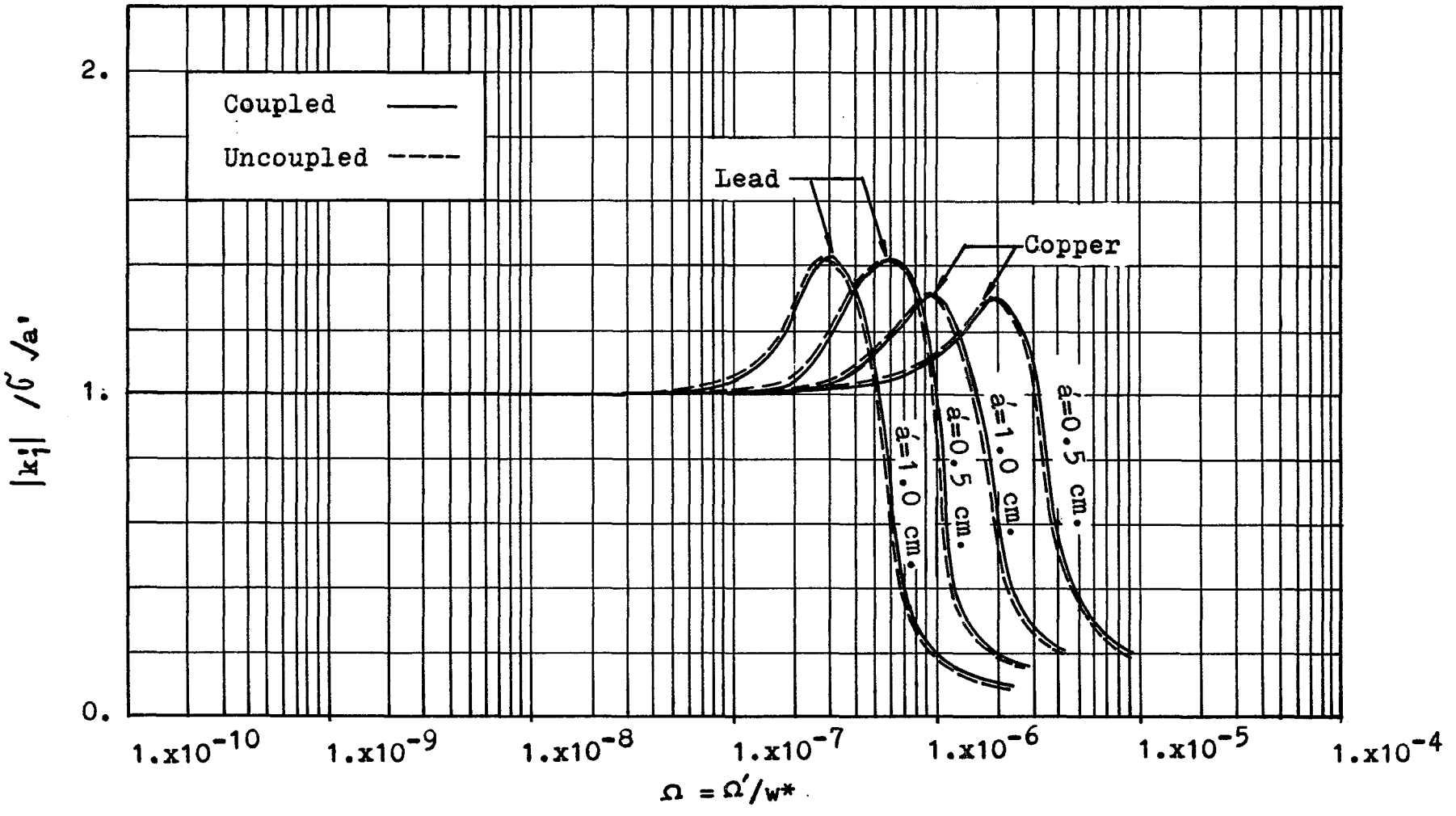

Figure 4 Variation of Stress-Intensity Factors with Frequency for Incident Elastic Wave Accompanied by Thermal Wave ($\bar{\beta} = 90^{o}$)

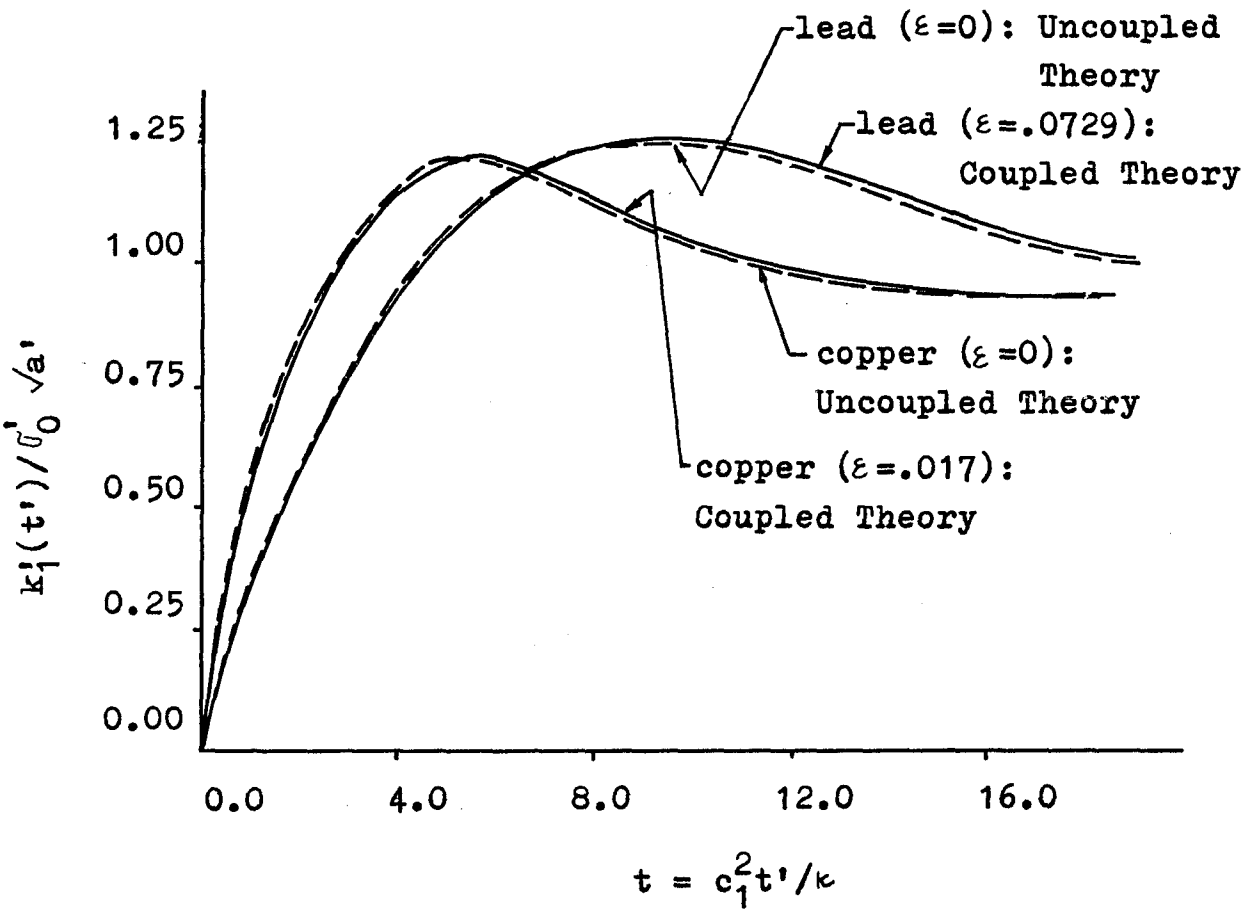

Figure 5 Variation of Stress-intensity Factors with Time for Lead and Copper Due to Sudden Application of Normal Stress on Crack Surfaces, (a = 1.0)

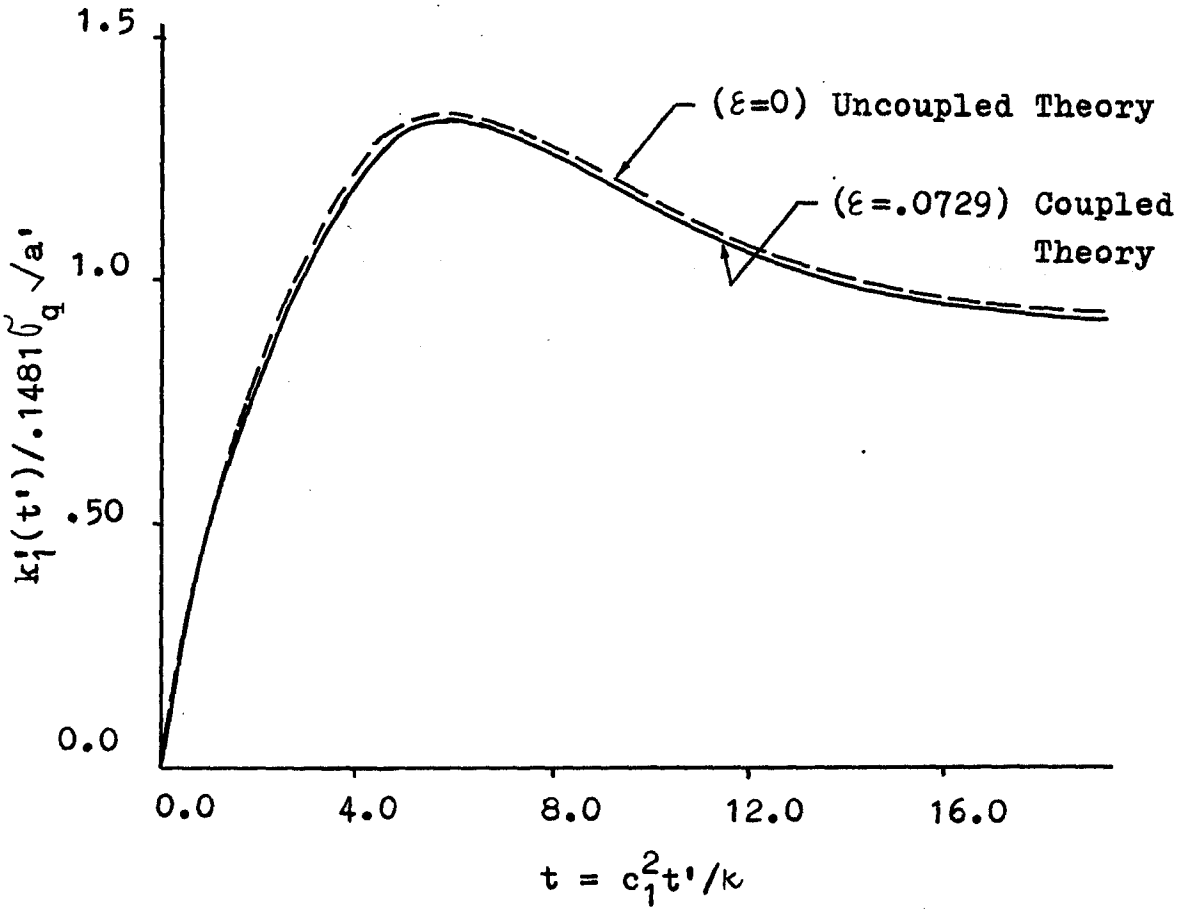

Figure 6 Variation of Stress-Intensity Factors with Time for Lead Due to Sudden Variation of Thermal Flux on Crack Surfaces, (a = 1.0)

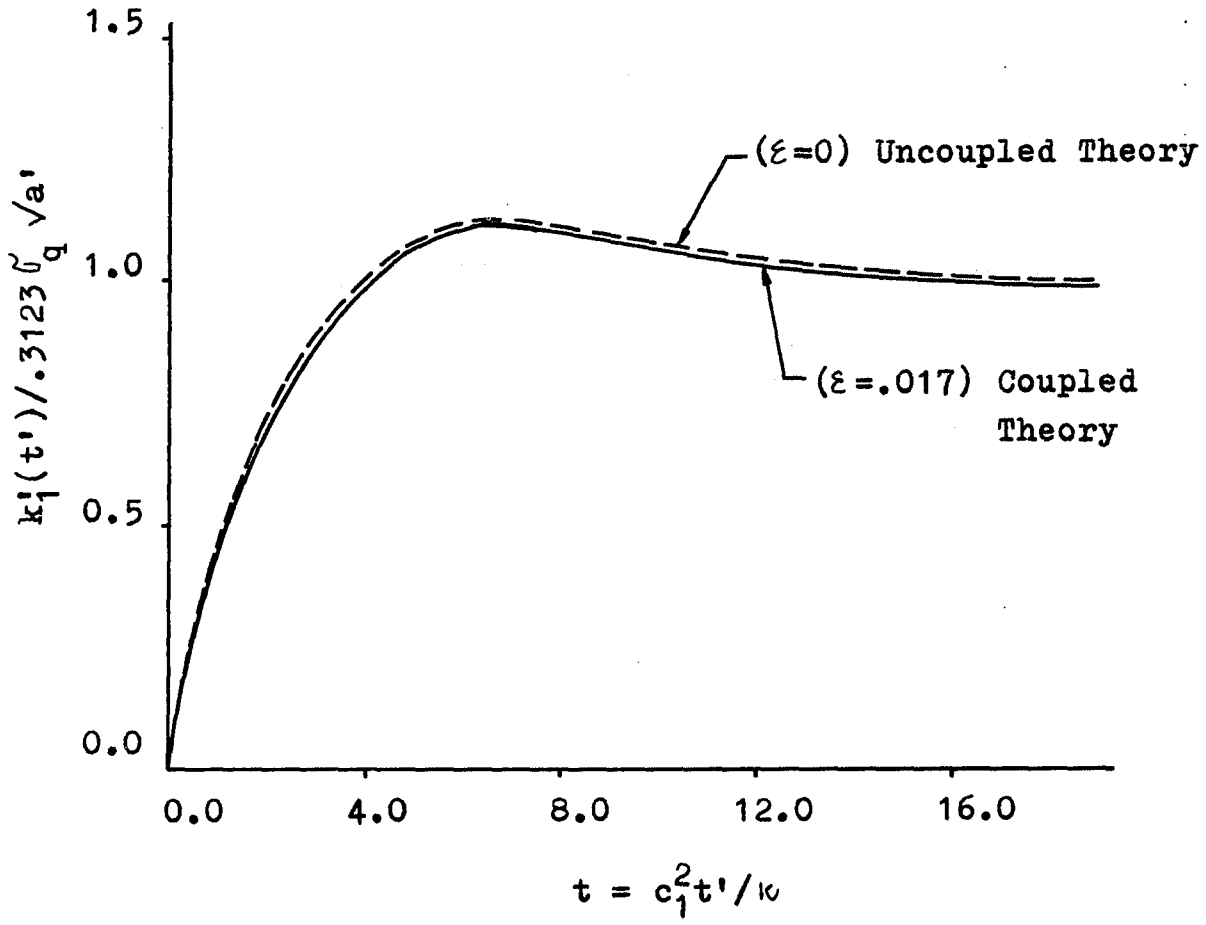

Figure 7 Variation of Stress-Intensity Factors with Time for Copper Due to Sudden Variation of Thermal Flux on Crack Surfaces, (a = 1.0)

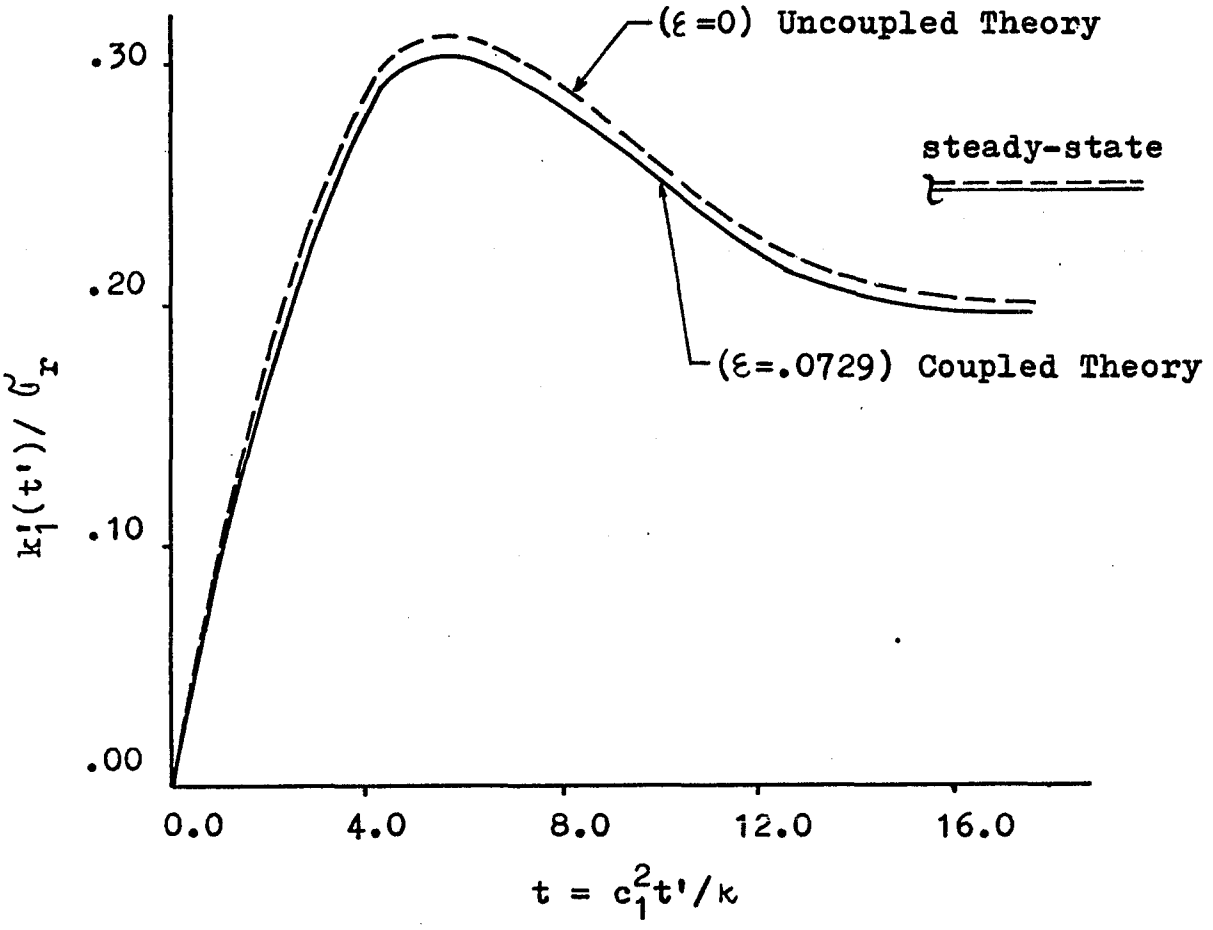

Figure 8 Variation of Stress-Intensity Factors with Time for Lead Due to Sudden Variation of Thermal Radiation on Crack Surfaces, ($a = 1.0$, $h = 1.0 \times 10^{-3}$)

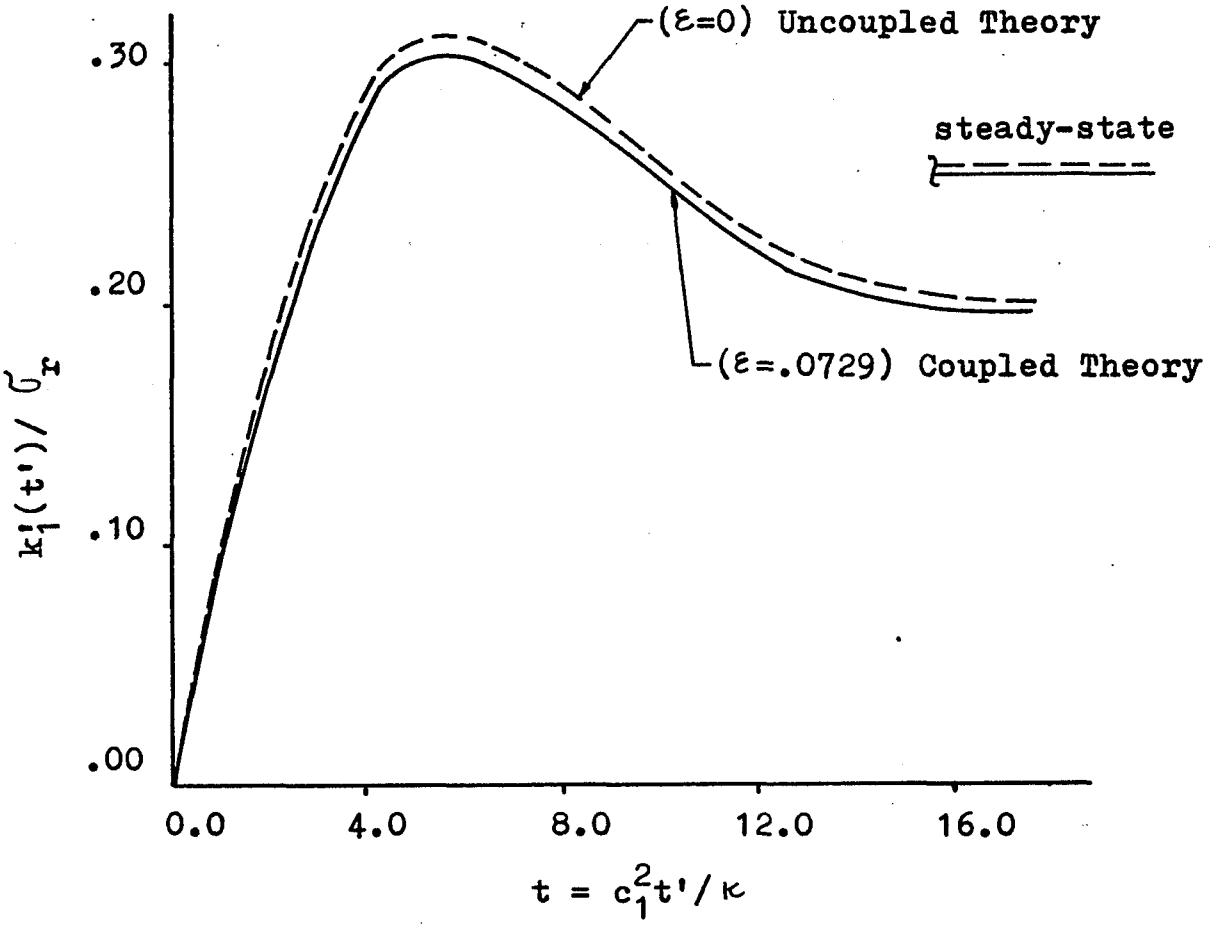

Figure 9 Variation of Stress-Intensity Factors with Time for Lead Due to Sudden Variation of Thermal Radiation on Crack Surfaces, ($a = 1.0$, $h = 1.0 \times 10^{-4}$)

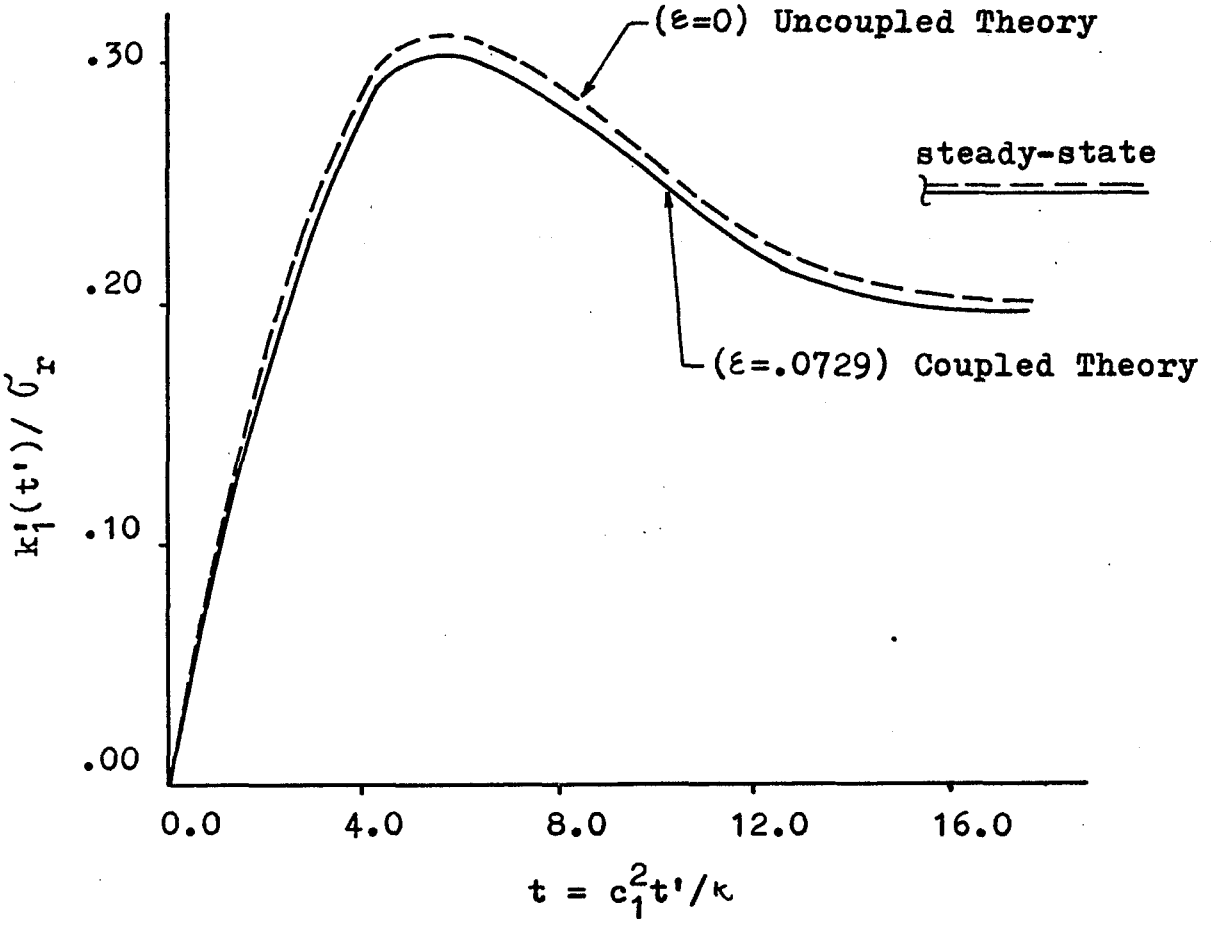

Figure 10 Variation of Stress-Intensity Factors with Time for Lead Due to Sudden Variation of Thermal Radiation on Crack Surfaces, ($a = 1.0$, $h = 1.0 \times 10^{-5}$)

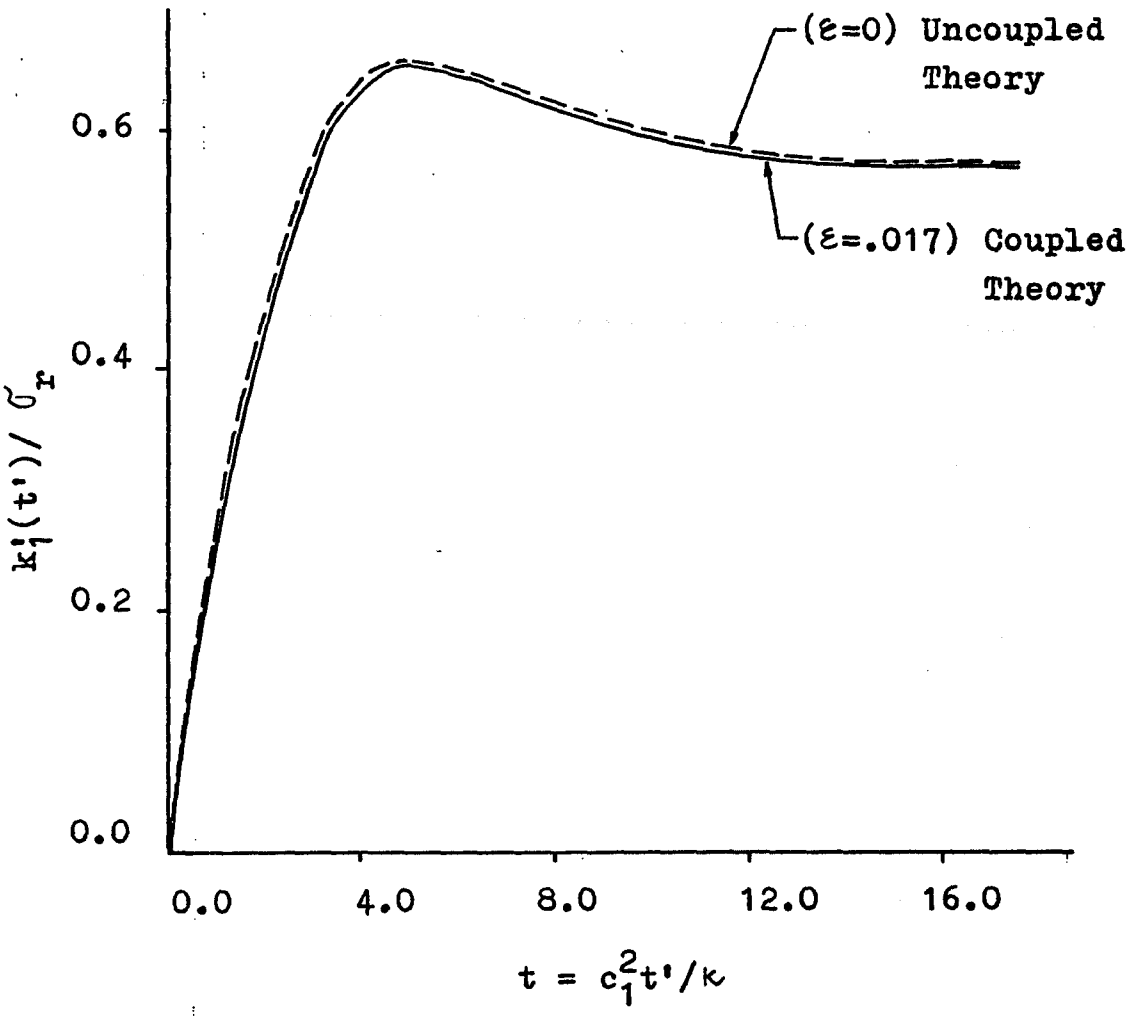

Figure 11 Variation of Stress-Intensity Factors with Time for Copper Due to Sudden Variation of Thermal Radiation on Crack Surfaces, ($a = 1.0$, $h = 1.0 \times 10^{-3}$)

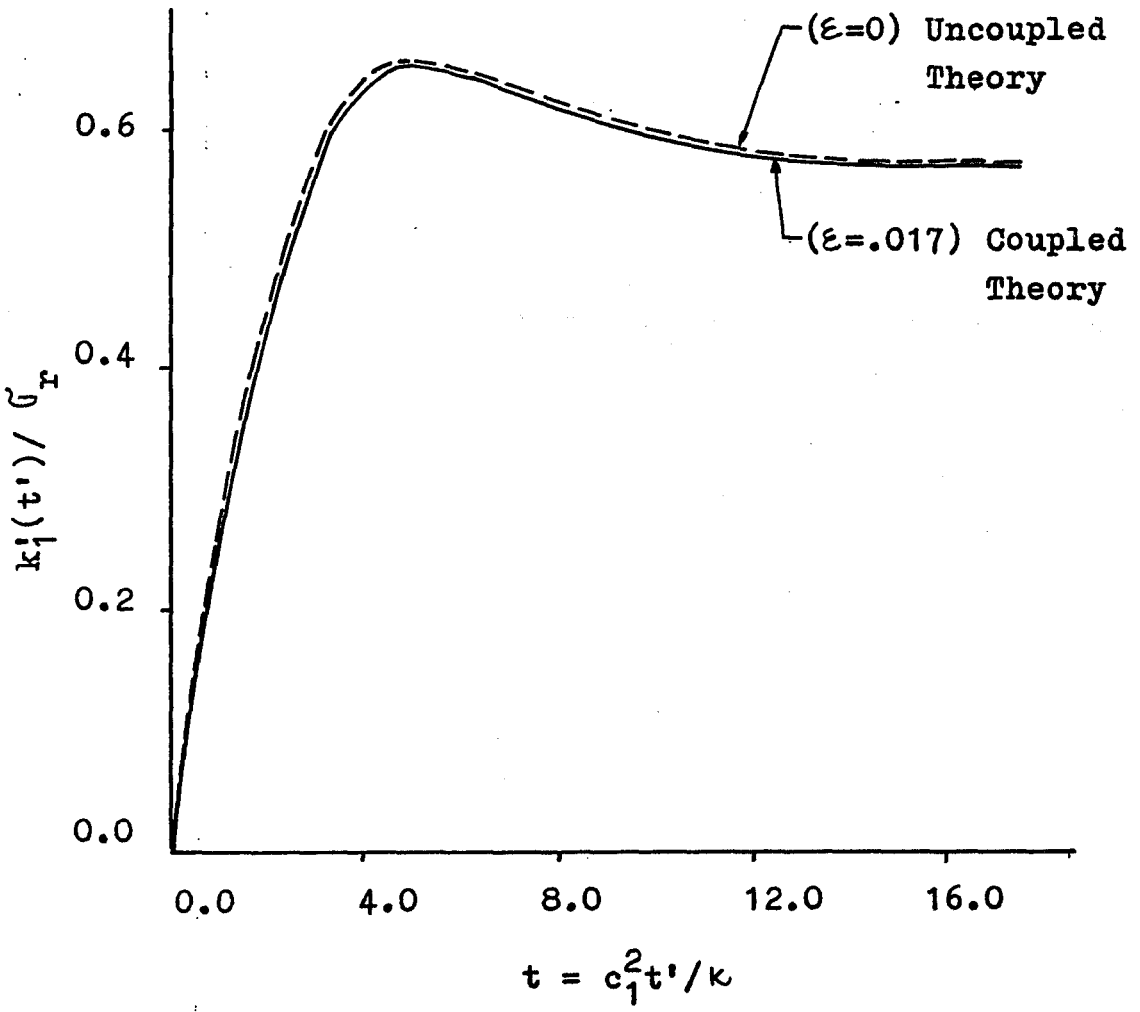

Figure 12 Variation of Stress-Intensity Factors with Time for Copper Due to Sudden Variation of Thermal Radiation on Crack Surfaces, ($a = 1.0$, $h = 1.0 \times 10^{-4}$)

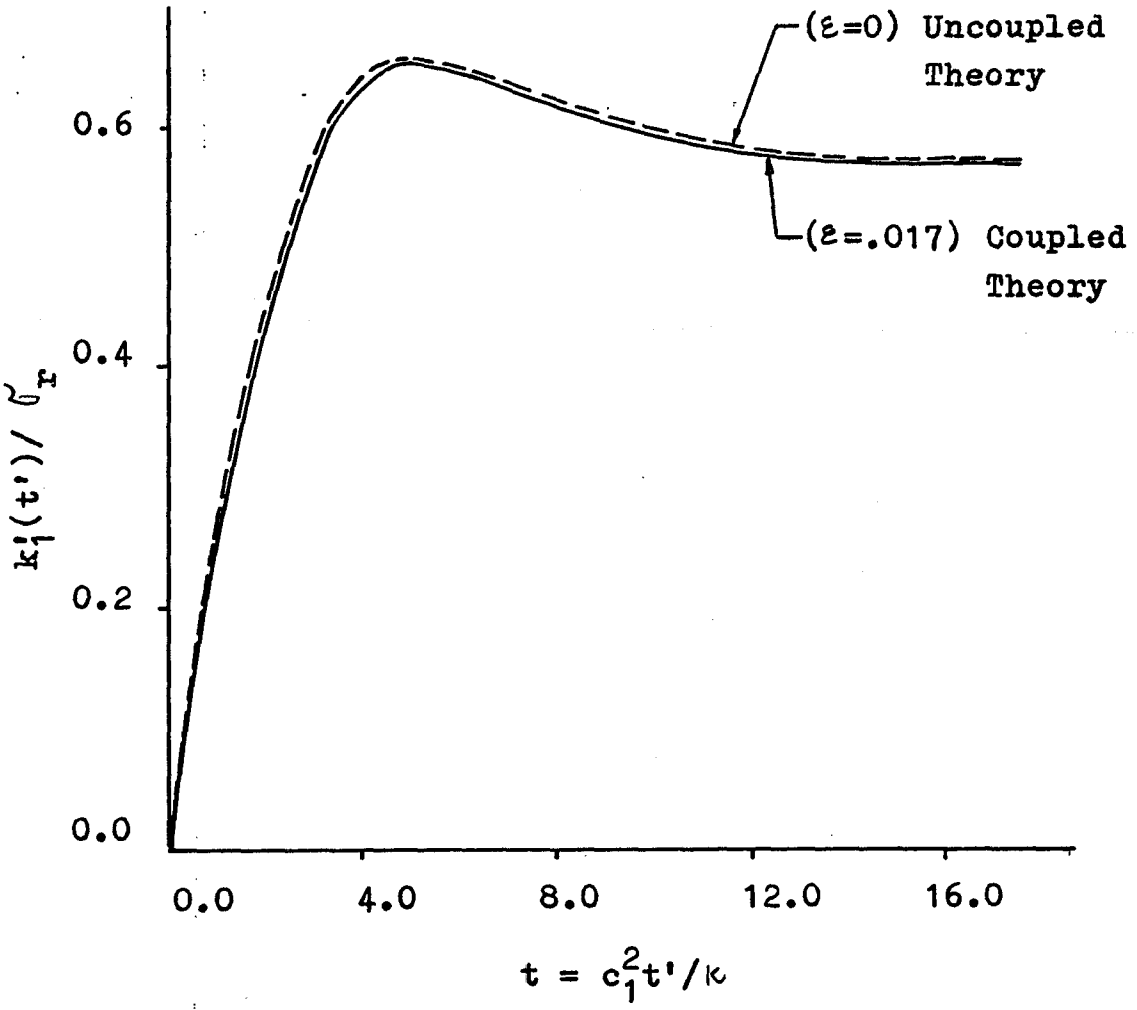

Figure 13 Variation of Stress-Intensity Factors with Time for Copper Due to Sudden Variation of Thermal Radiation on Crack Surfaces, ($a = 1.0$, $h = 1.0 \times 10^{-5}$)

APPENDIX A

Solution of a Pair of Dual Integral Equations

Consider a pair of dual integral equations of the form

$$\int_0^\infty sq(s)\Lambda(s)\cos(sx)ds = P(x), \quad 0<x<a \qquad (A.1a)$$

$$\int_0^\infty \Lambda(s)\cos(sx)ds = 0, \quad x>a \qquad (A.1b)$$

where $\Lambda(s)$ is unknown, $q(s)$ and $P(x)$ are the known functions.

Introducing

$$\bar{P}(x) = P(x) - \int_0^\infty s\left[q(s)-1\right]\Lambda(s)\cos(sx)ds \qquad (A.2)$$

into (A.1), then Eq. (A.1) may be written as

$$\int_0^\infty s\Lambda(s)\cos(sx)ds = \bar{P}(x), \quad 0<x<a \tag{A.3a}$$

$$\int_0^\infty \Lambda(s)\cos(sx)ds = 0, \quad x>a \tag{A.3b}$$

Defining

$$\Lambda(s) = \int_0^a Q(\eta)J_0(s\eta)d\eta \tag{A.4}$$

it can be seen that Eq. (A.3b) is automatically satisfied when use is made of the Bessel integral identity [10]

$$\int_0^\infty J_0(s\eta)\cos(sx)ds = 0, \quad x>a \tag{A.5}$$

Rewriting Eq. (A.3a) as

$$\frac{d}{dx}\int_0^{\infty} \Lambda(s)\sin(sx)ds \quad = \quad \bar{P}(x),\ 0 < x < a \qquad (A.6)$$

substituting for $\Lambda(s)$ from Eq. (A.4) and interchanging the order of integrations, thus

$$\frac{d}{dx}\int_0^{x} \frac{Q(\eta)d}{(x^2-\eta^2)^{\frac{1}{2}}} \quad = \quad \bar{P}(x),\ 0 < x < a\ . \qquad (A.7)$$

Eq. (A.7) is the equation of Abel's type the solution of which is [23] .

$$Q(\eta) \quad = \quad \frac{2}{\pi}\eta\int_0^{\eta} \frac{\bar{P}(x)dx}{(\eta^2-x^2)^{\frac{1}{2}}} \qquad (A.8)$$

Substituting for $\bar{P}(x)$ from Eq. (A.2) and making use of the integral identity [10]

$$\int_0^\infty \frac{\cos(sx)dx}{(\eta^2-x^2)^{\frac{1}{2}}} = \frac{\pi}{2} J_0(s\eta) \qquad (A.9)$$

Eq. (A.8) may be put in the form

$$Q(\eta) + \int_0^a Q(\xi)K(\xi,\eta)d\xi = \frac{2}{\pi}\eta \int_0^\infty \frac{P(x)dx}{(\eta^2-x^2)^{\frac{1}{2}}} \qquad (A.10)$$

$$0 < \eta < 1$$

If P(x) = constant = 1, then Eq. (A.10) becomes

$$Q(\eta) + \int_0^a Q(\xi)K(\xi,\eta)d\xi = \eta \ , \ 0 < \eta < a \qquad (A.11)$$

where the kernel $K(\xi,\eta)$ is defined as

$$K(\xi,\eta) = \eta \int_0^\infty s\left[q(s)-1\right] J_0(s\xi)J_0(s\eta)ds \qquad (A.12)$$

To normalize the quantities η and ξ and symmetrize the kernel K the following definitions will be used

$$\eta = a\beta \,, \quad \xi = a\tau \qquad (A.13)$$

$$Q(\eta) = a\sqrt{\beta}\,\bar{\Phi}(\beta) \qquad (A.14)$$

then Eq. (A.10) may be written as

$$\bar{\Phi}(\beta) + \int_0^1 \bar{\Phi}(\tau)K(\beta,\tau)d\tau = \sqrt{\beta} \,, \quad 0 < \beta < 1 \qquad (A.15)$$

where the symmetric kernel K is

$$K(\rho,\tau) = \sqrt{\rho\tau}\int_0^{\infty} s\left[q(s/a)-1\right] J_0(s\rho)J_0(s\tau)ds \quad (A.16)$$

Eq. (A.15) is the standard Fredholm integral equation of the second kind, J_0 is the Bessel function of zero order. The necessary conditions for the convergence of the kernel K have been discussed by Sneddon [23] .

APPENDIX B

Improvement of Convergence of Kernel, Eq. (4.35)

The constants c and n are to be determined from the condition that $F(s/a,p) \to 0$ when $s \to \infty$. Hence, asymtotic expansion of the right-hand side terms in Eq. (4.36) for large s and equating to zero leads to

$$\frac{a^2c}{s^2} - \frac{a^4cn^2}{s^4} + O(s^{-6}) = \frac{a^2}{s^2}M_1(p) + \frac{a^4}{s^4}M_2(p) + O(s^{-6}) \quad (B.1)$$

By identifying the like-power terms, the followings are obtained

$$c = M_1(p) \quad (B.2)$$

$$n^2 = -\frac{M_2(p)}{M_1(p)} \quad (B.3)$$

where

$$M_1(p) = \frac{\beta^2}{p^2(\beta^2-1)} \left[p^4 h_1 + p^2 h_2 + h_3 \right] \qquad \text{(B.4a)}$$

$$M_2(p) = \frac{\beta^2}{p^2(\beta^2-1)} \left[p^4 g_1 + p^2 g_2 + g_3 \right] \qquad \text{(B.4b)}$$

and

$$\begin{aligned}
h_1 &= -\tfrac{1}{2} \\
h_2 &= \frac{3}{4\beta^2}(\zeta_1^2+\zeta_2^2) + \frac{(\beta^2-1)}{2\beta^2}\zeta_3^2 \\
h_3 &= \frac{1}{4\beta^2}(\zeta_3^4 - 3\zeta_1^2\zeta_2^2) \\
g_1 &= \frac{1}{8}(3\zeta_1^2+3\zeta_2^2-2\zeta_3^2) \\
g_2 &= -\frac{3(\beta^2-2)}{8\beta^2}\zeta_1^2\zeta_2^2 - \frac{1}{8\beta^2}(5\zeta_1^4+5\zeta_2^4+11\zeta_2^2\zeta_1^2-3\zeta_2^2\zeta_3^2-3\zeta_1^2\zeta_3^2) \\
g_3 &= \frac{1}{8\beta^2}\left[\zeta_1^2\zeta_2^2(5\zeta_1^2+5\zeta_2^2-3\zeta_3^2) - \zeta_3^6 \right]
\end{aligned} \qquad \text{(B.5)}$$

APPENDIX C

Abbreviations

Some of the abbreviations which were used in this study are defined in this appendix.

$$a_{11}(s,p) = \frac{2s^2}{\beta^2} - \frac{4s^2\gamma_3\gamma_1}{\beta^2(2s^2+\zeta_3^2)} + p^2$$

$$a_{12}(s,p) = \frac{2s^2}{\beta^2} - \frac{4s^2\gamma_3\gamma_2}{\beta^2(2s^2+\zeta_3^2)} + p^2$$

$$a_{21}(s,p) = -(\zeta_1^2-p^2)(\gamma_1+h)$$

$$a_{22}(s,p) = -(\zeta_2^2-p^2)(\gamma_2+h)$$

$$b_{11}(s,p) = -\frac{2\gamma_1}{2s^2+\zeta_3^2}$$

$$b_{12}(s,p) = -\frac{2\gamma_2}{2s^2+\zeta_3^2}$$

$$b_{21}(s,p) = -(\zeta_1^2-p^2)\gamma_1$$

$$b_{22}(s,p) = -(\zeta_2^2 - p^2)\gamma_2$$

$$c_{11}(s,p) = \frac{-1}{\Delta(s,p)}\left[a_{11}b_{22} - a_{12}b_{21}\right]\frac{\beta^2}{p^2(\beta^2-1)}$$

$$c_{12}(s,p) = \frac{-1}{\Delta(s,p)}\left[-a_{11}b_{12} + a_{12}b_{11}\right]\frac{\beta^2}{p^2(\beta^2-1)}$$

$$c_{21}(s,p) = \frac{1}{\Delta(s,p)}\left[a_{21}b_{22} - a_{22}b_{21}\right]$$

$$c_{22}(s,p) = \frac{1}{\Delta(s,p)}\left[-a_{21}b_{12} + a_{22}b_{11}\right]$$

$$f_{11}(s) = 2s^2 - \xi_3^2 - \frac{4s^2\eta_1\eta_3}{2s^2 - \xi_3^2}$$

$$f_{12}(s) = 2s^2 - \xi_3^2 - \frac{4s^2\eta_2\eta_3}{2s^2 - \xi_3^2}$$

$$f_{21}(s) = (\Omega^2 - \xi_1^2)\eta_1$$

$$f_{22}(s) = (\Omega^2 - \xi_2^2)\eta_2$$

$$g_{11}(s) = \frac{2\xi_3^2\eta_1}{2s^2-\xi_3^2}$$

$$g_{12}(s) = \frac{2\xi_3^2\eta_2}{2s^2-\xi_3^2}$$

$$\Delta(s) = b_{11}b_{22}-b_{12}b_{21}$$

$$\Delta_1(s) = f_{21}g_{12}-f_{22}g_{11}$$

$$E_1(s) = \frac{\beta^2(p_5p_3+p_6p_4)}{2(\beta^2-1)\xi_3^2 s(p_5^2+p_6^2)}$$

$$E_2(s) = \frac{\beta^2(p_5p_4-p_6p_3)}{2(\beta^2-1)\xi_3^2 s(p_5^2+p_6^2)}$$

$$p_j = (2s^2-\xi_3^2)-4s^2(R_jR_3-I_jI_3), \quad j=1,2$$

$$p_3 = (\Omega^2-m_1)(p_2R_1-l_2I_1)+n_1(p_2I_1+l_2R_1) -$$
$$(\Omega^2-m_2)(p_1R_2-l_1I_2)-n_2(p_1I_2+l_1R_2)$$

$$p_4 = (\Omega^2-m_1)(p_2I_1+l_2R_1)-n_1(p_2R_1-l_2I_1) -$$
$$(\Omega^2-m_2)(p_1I_2+l_1R_2)+n_2(p_1R_2-l_1I_2)$$

$$p_5 = (m_2-m_1)(R_1R_2-I_1I_2) - (n_2-n_1)(R_1I_2+R_2I_1)$$

$$p_6 = (m_2-m_1)(R_1I_2+R_2I_1) + (n_2-n_1)(R_1R_2-I_1I_2)$$

$$l_j = -4s^2(R_jI_3+R_3I_j), \quad j=1,2$$

$$\bar{c} = \frac{1/4}{\Omega^2(\beta^2-1)}\left[\Omega^4\beta^2(3\beta^2-4)+3\Omega^2(m_1+m_2)-3(m_1m_2-n_1n_2)\right]$$

$$\bar{n}^2 = -\tfrac{1}{2}\Big\{\Omega^6\beta^4(\beta^2+2)-6\Omega^4\beta^2(m_1+m_2)+\Omega^2\big[5(m_2^2-n_2^2)+5(m_1^2-n_1^2)$$
$$+(6\beta^2+5)(m_1m_2-n_1n_2)\big] - 5\big[(m_1m_2-n_1n_2)(m_1+m_2)-$$
$$-(m_1n_2+m_2n_1)(n_1+n_2)\big]\Big\} / \Big[\Omega^4\beta^2(3\beta^2-4)+3\Omega^2(m_1+m_2)-$$
$$-3(m_1m_2-n_1n_2)\Big]$$

In formulating the diffraction of thermal waves by a stationary crack the following abbreviations are employed.

$$\sigma^t = \mathrm{Re}[\sigma^t] + i\,\mathrm{Im}[\sigma^t]$$

$$\mathrm{Re}[\sigma^t] = \theta^0 \Bigg(\Big\{ (\beta^2 - 2\cos^2\bar{\beta}) \Big[\Omega_{\phi r}\Big(q_2^2 - \frac{\Omega^2}{v_2^2}\Big) + \Omega_{\phi i} 2 \frac{\Omega}{v_2} q_2 \Big] - b \Big\}$$

$$\cosh(q_2 x\cos\bar{\beta})\cos\Big(\frac{\Omega}{v_2} x\cos\bar{\beta}\Big) - (\beta^2 - 2\cos^2\bar{\beta}).$$

$$\Big[-\Omega_{\phi i}\Big(q_2^2 - \frac{\Omega^2}{v_2^2}\Big) + \Omega_{\phi r} 2 \frac{\Omega}{v_2} q_2 \Big] \sinh(q_2 x\cos\bar{\beta}).$$

$$\sin\Big(\frac{\Omega}{v_2} x\cos\bar{\beta}\Big) \Bigg)$$

$$\mathrm{Im}[\sigma^t] = -\theta^0 \Bigg(\Big\{ (\beta^2 - 2\cos^2\bar{\beta}) \Big[\Omega_{\phi r}\Big(q_2^2 - \frac{\Omega^2}{v_2^2}\Big) + \Omega_{\phi i} 2 \frac{\Omega}{v_2} q_2 \Big] - b \Big\}$$

$$\sinh(q_2 x\cos\bar{\beta})\sin\Big(\frac{\Omega}{v_2} x\cos\bar{\beta}\Big) + (\beta^2 - 2\cos^2\bar{\beta})$$

$$\Big[-\Omega_{\phi i}\Big(q_2^2 - \frac{\Omega^2}{v_2^2}\Big) + \Omega_{\phi r} 2 \frac{\Omega}{v_2} q_2 \Big] \cosh(q_2 x\cos\bar{\beta})\cos\Big(\frac{\Omega}{v_2} x\cos\bar{\beta}\Big) \Bigg)$$

$$\tau^t = \mathrm{Re}\left[\tau^t\right] + i\,\mathrm{Im}\left[\tau^t\right]$$

$$\mathrm{Re}\left[\tau^t\right] = \theta^0 \sin\bar{\beta}\left[q_2 \cosh(q_2 x\cos\bar{\beta})\cos\left(\frac{\Omega}{v_2} x\cos\bar{\beta}\right) - \frac{\Omega}{v_2}\sinh(q_2 x\cos\bar{\beta})\sin\left(\frac{\Omega}{v_2} x\cos\bar{\beta}\right)\right]$$

$$\mathrm{Im}\left[\tau^t\right] = -\theta^0 \sin\bar{\beta}\left[q_2 \sinh(q_2 x\cos\bar{\beta})\sin\left(\frac{\Omega}{v_2} x\cos\bar{\beta}\right) + \frac{\Omega}{v_2}\cosh(q_2 x\cos\bar{\beta})\cos\left(\frac{\Omega}{v_2} x\cos\bar{\beta}\right)\right]$$

$$Z_1(x) = \frac{\beta^2}{(\beta^2-1)} \int_0^\infty \left\{ Y_1(s)\frac{b}{\beta^2} \int_0^a \mathrm{Re}\left[\tau^t\right] \cos(s\xi)\,d\xi - Y_2(s)\frac{b}{\beta^2} \int_0^a \mathrm{Im}\left[\tau^t\right] \cos(s\xi)\,d\xi \right\} \cos(sx)\,ds$$

$$- \frac{\beta^2 \pi}{2(\beta^2-1)} \mathrm{Re}\left[\tau^t\right]$$

$$Z_2(x) = \frac{\beta^2}{(\beta^2-1)} \int_0^{\infty} \left\{ Y_1(s) \frac{b}{\beta^2} \int_0^{a} \mathrm{Im}\left[\tau^t\right] \cos(s\xi)\,d\xi + \right.$$

$$\left. Y_2(s) \frac{b}{\beta^2} \int_0^{a} \mathrm{Re}\left[\tau^t\right] \cos(s\xi)\,d\xi \right\} \cos(sx)\,ds$$

$$- \frac{\beta^2 \pi}{2(\beta^2-1)} \mathrm{Im}\left[\sigma^t\right]$$

where Y_1 and Y_2 are the real and imaginary parts of $\left[f_{12}g_{11} - f_{11}g_{12} \right] / \Delta_1(s)$

$$Y_1(s) = (2s^2 - \xi_3^2) \left[(R_1-R_2)p_5 + (I_1-I_2)p_6 \right] / (p_5^2+p_6^2)$$

$$Y_2(s) = (2s^2 - \xi_3^2) \left[(I_1-I_2)p_5 - (R_1-R_2)p_6 \right] / (p_5^2+p_6^2)$$

For the diffraction of elastic wave, the following abbreviations are employed.

$$\sigma^{e} = \mathrm{Re}\left[\sigma^{e}\right] + i\,\mathrm{Im}\left[\sigma^{e}\right]$$

$$\mathrm{Re}\left[\sigma^{e}\right] = \phi^{0}\left\{\left[(\beta^{2}-2\cos^{2}\bar{\beta})(q_{1}^{2}-\frac{\Omega^{2}}{v_{1}^{2}}) - b\,\Omega_{Tr}\right]\right.$$

$$\cosh(q_{1}x\cos\bar{\beta})\cos(\frac{\Omega}{v_{1}}x\cos\bar{\beta}) - \left[(\bar{\beta}^{2}-2\cos^{2}\bar{\beta})\right.$$

$$\left.\left.2\frac{\Omega}{v_{1}}q_{1}+b\,\Omega_{Ti}\right]\sinh(q_{1}x\cos\bar{\beta})\sin(\frac{\Omega}{v_{1}}x\cos\bar{\beta})\right.$$

$$\mathrm{Im}\left[\sigma^{e}\right] = -\phi^{0}\left\{\left[(\beta^{2}-2\cos^{2}\bar{\beta})(q_{1}^{2}-\frac{\Omega^{2}}{v_{1}^{2}})-b\,\Omega_{Tr}\right]\sinh(q_{1}x\cos\bar{\beta})\right.$$

$$\sin(\frac{\Omega}{v_{1}}x\cos\bar{\beta}) + \left[(\beta^{2}-2\cos^{2}\bar{\beta})2\frac{\Omega}{v_{1}}q_{1}+b\,\Omega_{Ti}\right]$$

$$\left.\cosh(q_{1}x\cos\bar{\beta})\cos(\frac{\Omega}{v_{1}}x\cos\bar{\beta})\right\}$$

$$\tau^e = \mathrm{Re}[\tau^e] + i\,\mathrm{Im}[\tau^e]$$

$$\mathrm{Re}[\tau^e] = \phi^0 \left\{ \left(q_1 \Omega_{Tr} + \frac{\Omega}{v_1} \Omega_{Ti}\right) \cosh(q_1 x \cos\bar{\beta}) \cos\left(\frac{\Omega}{v_1} x \cos\bar{\beta}\right) \right.$$

$$\left. + \left(q_1 \Omega_{Ti} - \frac{\Omega}{v_1} \Omega_{Tr}\right) \sinh(q_1 x \cos\bar{\beta}) \sin\left(\frac{\Omega}{v_1} x \cos\bar{\beta}\right) \right\} \cdot$$

$$\cdot \sin\bar{\beta}$$

$$\mathrm{Im}[\tau^e] = \phi^0 \left\{ -\left(q_1 \Omega_{Tr} + \frac{\Omega}{v_1} \Omega_{Ti}\right) \sinh(q_1 x \cos\bar{\beta}) \sin\left(\frac{\Omega}{v_1} x \cos\bar{\beta}\right) \right.$$

$$\left. + \left(q_1 \Omega_{Ti} - \frac{\Omega}{v_1} \Omega_{Tr}\right) \cosh(q_1 x \cos\bar{\beta}) \cos\left(\frac{\Omega}{v_1} x \cos\bar{\beta}\right) \right\} \cdot$$

$$\cdot \sin\bar{\beta}$$

APPENDIX D

Derivation of Expressions in Eq. (4.66)

Consider

$$I_i = \int_0^1 h_i(x,p)x^{\mu_i+1}(1-x^2)^{\beta_i-1}\mathcal{J}_k(\mu_i+\beta_i,\mu_i+1,x^2)dx \qquad k=0,1,2,.... \qquad (D.1)$$

where $\mathcal{J}_k$ is the Jacobi polynomial.
Supposing

$$h_i(x,p) = x^{\mu_i}, \qquad (D.2)$$

then Eq. (D.1) may be written as

$$I_i = \int_0^1 x^{2\mu_i+1}(1-x^2)^{\beta_i-1}\mathcal{J}_k(\mu_i+\beta_i,\mu_i+1,x^2)dx. \qquad k=0,1,2,.... \qquad (D.3)$$

Now let

$$\begin{aligned} \mu_i+\beta_i &= \alpha \\ \mu_i+1 &= \gamma \\ x^2 &= \eta \end{aligned} \qquad \text{(D.4)}$$

Thus Eq. (D.3) becomes

$$I_i = \frac{1}{2}\int_0^1 \eta^{\gamma-1}(1-\eta)^{\alpha-\gamma}\, \mathcal{F}_k(\alpha,\gamma,\eta)\,d\eta\,. \qquad \text{(D.5)}$$

Because of the following property [16]

$$\mathcal{F}_0(\alpha,\gamma,\eta) = 1\,, \qquad \text{(D.6)}$$

the Eq. (D.5) may be written as

$$I_i = \frac{1}{2}\int_0^1 \eta^{\gamma-1}(1-\eta)^{\alpha-\gamma}\, \mathcal{F}_0(\alpha,\gamma,\eta)\, \mathcal{F}_k(\alpha,\gamma,\eta)\,d\eta \qquad \text{(D.7)}$$

Making use of the orthogonality property [16]

$$\int_0^1 \eta^{\gamma-1} (1-\eta)^{\alpha-\gamma} \mathcal{F}_m(\alpha,\gamma,\eta)\, \mathcal{F}_n(\alpha,\gamma,\eta)\, d\eta = 0 \qquad \text{(D.8)}$$

when $m \neq n$, Eq. (D.7) becomes

$$I_i = 0 \qquad \text{for } k > 0$$

and

$$I_i = \frac{1}{2}\int_0^1 \eta^{\gamma-1} (1-\eta)^{(\alpha-\gamma+1)-1}\, d\eta \quad \text{for } k=0 \qquad \text{(D.9)}$$

Noticing that the Beta function of γ and $(\alpha-\gamma+1)$ is defined by the integral [13]

$$B(\gamma,\alpha-\gamma+1) = \int_0^1 \eta^{\gamma-1} (1-\eta)^{(\alpha-\gamma+1)-1}\, d\eta$$

$$= \frac{\Gamma(\gamma)\,\Gamma(\alpha-\gamma+1)}{\Gamma(\alpha+1)} \qquad \text{(D.10)}$$

$$(\gamma,\alpha-\gamma+1) > 0$$

making use of Eq. (D.4), Eq. (D.9) is reduced to

$$I_i = \begin{cases} 0 & \text{for } k > 0 \\ \\ \frac{1}{2} \dfrac{\Gamma(\mu_i+1)\,\Gamma(\beta_i)}{\Gamma(\mu_i+\beta_i+1)} & \text{for } k = 0 \end{cases} \qquad \text{(D.11)}$$

For particular case, $\mu_i = -1/2$, $\beta_i = 1$

$$I_i = \int_0^1 \mathcal{F}_k\left(\tfrac{1}{2},\tfrac{1}{2},x^2\right)dx$$

$$= \begin{cases} 0 & \text{for } k > 0 \\ \\ 1 & \text{for } k = 0 \end{cases} \qquad \text{(D.12)}$$

APPENDIX E

Stress-Intensity Factors

Derivation of Stress-Intensity Factor, Eq. (4.41):

For the mere purpose of finding the dynamic stress-intensity factor, only $\sigma_y(x,0,t)$ will be considered here. Thus, with the help of Eq. (4.20) and the Laplace transform theorem Eqs. (4.17), Eq. (4.8a) becomes

$$\sigma_y^*(x,0,t) = \frac{2}{\pi}\int_0^\infty \left[a_{11}(s,p)A(s,p)+a_{12}(s,p)B(s,p)\right]\cos(sx)ds \tag{E.1}$$

where $a_{11}(s,p)$ and $a_{12}(s,p)$ are given in Appendix C.

Making use of Eqs. (4.29), (4.31) and Appendix C, Eq. (E.1) may be written as

$$\sigma_y^*(x,0,p) = -\frac{2p^2}{\pi\beta^2}(\beta^2-1)\int_0^\infty s\,\Lambda_1(s,p)\cos(sx)ds -$$

$$-\frac{2p^2}{\pi\beta^2}(\beta^2-1)\left[s\,F(s,p)-1\right]\Lambda_1(s,p)\cos(sx)ds \qquad (E.2)$$

Substitution for $\Lambda_1(s,p)$ from Eq. (4.33) and integrating the first term by parts, leads to

$$\sigma_y^*(x,0,p) = -\frac{\sigma_0 a}{p}\,\Phi_1(1,p)\int_0^\infty J_1(sa)\cos(sx)ds +$$

$$+\frac{\sigma_0 a}{p}\int_0^\infty \cos(sx)\int_0^\infty \beta J_1(sa\beta)\frac{d}{d\beta}\left[\Phi_1(\beta,p)/\sqrt{\beta}\right]d\beta\,ds$$

$$-\frac{2p^2}{\pi\beta^2}(\beta^2-1)\int_0^\infty s\left[F(s,p)-1\right]\Lambda_1(s,p)\cos(sx)ds \qquad (E.3)$$

It is not difficult to see that only the first term in Eq. (E.3) contains a singularity at $x = \pm a$.

Making use of the Bessel integral identity [10]

$$\lim_{x \to a^+} \int_0^\infty J_1(sa)\cos(sx)ds = 1/a - 1/(2ar_1)^{\frac{1}{2}} \qquad (E.4)$$

where $x=r_1+a$ for $\bar{\theta}_1=0$, and inversion of the Laplace transform theorem, the closed elementary form of σ_y near the crack tip on the y=0 plane is obtained.

$$\sigma_y = \frac{k_1(t)}{(2r_1)^{\frac{1}{2}}} + O(r_1^0) \quad \text{as } r_1 \to 0^+ \qquad (E.5)$$

where $k_1(t)$, the dynamic stress-intensity factor in dimensionless units is given by

$$k_1(t) = \mathcal{L}^{-1}\{k_1(p)\} = \sigma_0 \sqrt{a}\, \mathcal{L}^{-1}\{\Phi_1(1,p)/p\} \qquad (E.6)$$

Making use of Eqs. (4.4), (4.13) and

$$a = c_1 a'/\kappa \quad , \quad r_1 = c_1 r_1'/\kappa \tag{E.7}$$

the dynamic stress-intensity factor in conventional units is obtained

$$k_1'(t') = \sigma_0' \sqrt{a'}\, \mathcal{L}^{-1}\left\{\Phi_1(1,p)/p\right\} \tag{E.8}$$

Derivation of Stress-Intensity Factor, Eq. (4.69):

To obtain the dynamic stress-intensity factor, it is only necessary to consider the singular stress σ_y near the crack tips on the y=0 plane. Thus, upon applying the Laplace transform theorem Eqs. (4.17) to Eq. (4.8a) and making use of Eqs. (4.20), the following result is obtained.

$$\sigma_y^*(x,0,p) = \frac{2}{\pi}\int_0^\infty \left[a_{11}(s,p)A(s,p)+a_{12}(s,p)B(s,p)\right]\cos(sx)ds \tag{E.9}$$

Substituting for V_1 and V_2 from Eqs. (4.61) into Eqs. (4.58), then substituting the resulting expressions for A(s,p) and B(s,p) into Eq. (E.9) yields

$$\sigma_y^*(x,0,p) = -\sqrt{\frac{2}{\pi}}\frac{h\theta_0}{p\beta^2}(\beta^2-1)\int_0^\infty\left[\sum_{m=0}^{\infty}{}' \chi_{1,1}(p)J(s)_{1+2m}\right]\cos(sx)ds$$

$$-\sqrt{\frac{2}{\pi}}\frac{h\theta_0}{\rho^3}\int_0^\infty\left\{S_1(s,p)-\frac{p^2}{\beta^2}(\beta^2-1)\right\}\left[\sum_{m=0}^{\infty}{}' \chi_{1,1}(p)J(s)_{1+2m}\right]$$

$$\cos(sx)ds - \sqrt{\frac{2}{\pi}}\frac{h\theta_0}{p^3}\int_0^\infty S_2(s,p)s^{\frac{1}{2}}\left[\sum_{m=0}^{\infty}{}' \chi_{2,1}(p)J(s)_{\frac{1}{2}+2m}\right]\cos(sx)ds \tag{E.10}$$

where

$$S_1(s,p) = F(s,p)p^2(\beta^2-1)/\beta^2 \tag{E.11}$$

$$S_2(s,p) = \frac{a_{11}(s,p)}{(\zeta_2^2-\zeta_1^2)s\gamma_1} + \frac{a_{12}(s,p)}{(\zeta_2^2-\zeta_1^2)s\delta_2} \tag{E.12}$$

in which $F(s,p)$ is given by Eq. (4.32) and $a_{ij},(j=1,2)$ are given in Appendix C.

It can be seen that only the first term contains singularity at $x=1^+$. Thus upon interchanging the order of integration and summation, and using the following recurrence formular [16]

$$J_{n+1}(s) = \frac{2n}{s} J_n(s) - J_{n-1}(s) \tag{E.13}$$

Eq. (E.10) may be written as

$$\sigma_y^*(x,0,p) = -\sqrt{\frac{2}{\pi}}\,\frac{h\theta_0}{p\beta^2}\,(\beta^2-1)\Phi_3(p)\int_0^\infty J_1(s)\cos(sx)\,ds +$$

$$+ \text{Non-Singular Terms} \qquad \text{(E.14)}$$

in which

$$\Phi_3(p) = \sum_{m=1}^{\infty}(-1)^{m+1}\chi_{1,2m-1}(p) \qquad \text{(E.15)}$$

Passing the limit as $x \to 1^+$ to Eq. (E.14) and making use of the identity Eq. (E.4), the closed elementary form of σ_y is obtained

$$\lim_{x\to 1^+}\sigma_y(x,0,t) = \frac{k_1(t)}{(2r_1')^{\frac{1}{2}}} + O(r_1^0) \qquad \text{(E.16)}$$

where $k_1(t)$, the dynamic stress-intensity factor in

dimensionless units, is

$$k_1(t) = \sqrt{\frac{2}{\pi}}\, h\theta_0 \frac{(\beta^2-1)}{\beta^2}\, \mathcal{L}^{-1}\left\{\Phi_3(p)/p\right\} \qquad (E.17)$$

The stress-intensity factor $k_1(t)$ is then converted to conventional units through Eqs. (E.7) and (4.4). Thus

$$k_1'(t') = \sigma_r \mathcal{L}^{-1}\left\{\Phi_3(p)/p\right\} \qquad (E.19)$$

in which $k_1'(t')$ is the required dynamic stress-intensity factor and

$$\sigma_r = \sqrt{\frac{2}{\pi}}\, h\theta_0'(\beta^2-1)/\beta^2 \qquad (E.20)$$

APPENDIX F

A Note on the Isolation of Weak Singularities of Improper Integral

In certain case, the usual numerical evaluation of an improper integral of the type $I = \int_a^b f(x)dx$ leads to difficulties. This situation occurs whenever $f(x)$ or one of its derivatives is infinite at any point within or near the ends of the range of integration. In such a case $f(x)$ is said to possess a singularity at that point. A useful technique in calculating the approximate value of this type of integral is to take out of the integrand $f(x)$ a certain function $g(x)$ having the same singularities as $f(x)$, which is integrable in elementary terms on the given interval $[a,b]$ and is such that the difference $f(x)-g(x)$ has a necessary number of derivatives.

Write the integral in the form

$$I = \int_a^b f(x)dx = \int_a^b g(x)dx + \int_a^b \left[f(x)-g(x)\right] dx.$$

The first integral can be evaluated analytically, and the second integral is readily evaluated by standard quadrature formulas.

Consider the integral function of the form

$$f(x) = (x-c)^p \varphi(x), \quad a \leq c \leq b$$

where $-1 < p < 0$, and $\varphi(x)$ is continuous and has a sufficient number of derivatives on the interval $[a,b]$. Then $f(x)$ can be written in the form

$$f(x) = \left[\varphi(c)(x-c)^p + \frac{\varphi(c)}{1!}(x-c)^{p+1} + \cdots\cdots + \frac{\varphi^{(k)}(c)(x-c)^{p+k}}{k!}\right.$$
$$\left. + (x-c)^p\left[\varphi(x) - \varphi(c) - \frac{\varphi(c)}{1!}(x-c) - \frac{\varphi(c)}{2!}(x-c)^2 \cdots\cdots - \frac{\varphi^{(k)}(c)}{k!}(x-c)^k\right]\right.$$

The first square bracket contains a power function which can integrated directly. The expression in the second square bracket vanishes at x=c together with its derivatives up to order k. The product of this expression by the factor $(x-c)^{p}$ is a continuous function. Therefore, the integral of this function can be evaluated by one of the standard quadrature formulas.

REFERENCES

1. Achenbach, J. D., "Dynamic Effects in Brittle Fracture," Chapter 1 of S. Nemat-Nasser, Mechanics Today, Vol. 1, Pergamon Press Inc., Oxford, 1972.
2. Biot, M. A., "Thermoelasticity and Irreversible Thermodynamics," J. Appl. Phys., Vol. 27, 1956, pp. 240-253.
3. Boley, B. A. and Weiner, J. H., Theory of Thermal Stresses, John Wiley & Sons, Inc., New York, 1960.
4. Carslaw, H. S. and Jaeger, J. C., Conduction of Heat in Solids, Oxford, 1959.
5. Chadwich, P., "Thermo-Elasticity, the Dynamical Theory," Chapter 6 of I. N. Sneddon and R. Hill, Progress in Solid Mechanics, Vol. 1, North-Holland Publishing Co., Amsterdam, Holland, 1960, pp. 264-328.
6. Chen, E. P. and Sih, G. C., Elastodynamic Crack Problems, Noordhoff International Publishing, Leyden, The Netherlands, 1977.
7. Cherepanov, G. P., Mechanics of Brittle Fractures, Mc Graw-Hill Inc., New York, 1979.

8. Dhaliwal, R. S. and Shanker, M. U., "Coupled Thermoelastic Problem for an Infinite Medium with a Cylindrical Hole," Arch. Mech. Stos., Vol. 5, No. 22, 1970.

9. Duhamel, J. M. C., "Second Me'moire sur les Phe'nomenes Thermomecaniques," J. L'Ecole Polytech., Vol. 15, 1837, pp, 1-57.

10. Erdelyi, A., Editor, Table of Integral Transforms, Vol. 2, Mc Graw-Hill Book Co. Inc., New York, 1954.

11. Erdogan, F. and Bahar, L. Y., "On the Solution of Simultaneous Dual Integral Equations," J. Soc. Indust. Appl. Math., Vol. 12, No. 3, 1964.

12. Freund, L. B., "The Analysis of Elastodynamic Crack Tip Stress Field," Chapter 2 of S. Nemat-Nasser, Mechanics Today, Vol. 3, Pergamon Press Inc., Oxford, 1976.

13. Hildebrand, F. B., Advanced Calculus for Applications, Second Edition, Prentice-Hall Inc., Englewood Cliffs, New Jersey, 1976.

14. Kantorovich, L. V. and Krylov, V. I., Approximate Methods of Higher Analysis, Interscience Publishers, New York, 1958.

15. Kassir, M. K. and Sih, G. C., Three-Dimensional Crack Problems, Noordhoff International Publishing, Leyden, The Netherlands, 1975.

16. Magnus, W. and Oberhettinger, F., Formulas and Theorems for the Functions of Mathematical Physics, Chelsea Publishing Co., New York, 1949.

17. Miller, M. K. and Guy, W. T., "Numerical Inversion of the Laplace Transform by Use of Jacobi Polynomials," SIAM, J. of Numerical Analysis, Vol. 3, pp. 624-635.

18. Neumann, F. E., "Vorlesungen uber die Theorie der Elastizitat der festen Korper und des Lichtathers," Teuber, Leipzig, 1885, pp. 107-120.

19. Noble, B., Methods Based on the Weiner-Hopf Technique, Pergamon Press Inc., New York, 1958.

20. Nowacki, W., Thermoelasticity, PWN-Polish Scientific Publishers, Warsaw, 1962.

21. Sih, G. C. and Loeber, J. F., "Wave Propagation in an Elastic Solid with a Line of Discontinuity or Finite Crack," Quarterly of Appl. Math., Vol. 27, No. 2, pp. 193-213, 1969.

22. Sneddon, I. N. and Lowengrub, M., Crack Problems in the Classical Theory of Elasticity, John Wiley and Sons, Inc., New York, 1969.

23. Sneddon, I. N., Mixed-Boundary Value Problems in Potential Theory, North-Holland Publishing Co., Amsterdam, John Wiley & Sons, Inc., New York, 1966.

24. Tranter, C. J., Integral Transforms in Mathematical Physics, John Wiley & Sons, Inc., New York, 1956.